The Dissertation Committee for Miri Jwa
certifies that this is the approved version of the following dissertation:

The Regulation of Chromosome Segregation by Aurora Kinase, Protein Phosphatase 1 and Nucleolar Protein Utp7

Committee

Clarence S.M. Chan, Supervisor

Kevin N. Dalby

Arturo De Lozanne

Arlen W. Johnson

John C. Sisson

The Regulation of Chromosome Segregation by Aurora Kinase, Protein Phosphatase 1 and Nucleolar Protein Utp7

by

Miri Jwa, B.S.; M.S.

Dissertation

Presented to the Faculty of the Graduate School of

the University of Texas at Austin

in Partial Fulfillment

of the Requirements

for the Degree of

Doctor of Philosophy

The University of Texas at Austin

August 2007

Dedication

To my parents

Acknowledgements

I wish to thank my advisor, Clarence Chan, for the contagious enthusiasm that he has had for projects that I have been involved in. He does not hesitate to study completely unknown matters and finds his joy by unraveling them. I have been working with him with a strange mixture of gratitude (for his detailed attention and thoroughness) and jealousy (why didn't I think of that?). I have learned from him about how science is done and I am certain that it will take me a long way in my career. It is rich reward for my stay at UT.

I would like to thank the members of my thesis committee, Kevin Dalby, Arturo De Lozanne, Arlen Johnson and John Sisson for their helpful inputs. I acknowledge the past and present members of the Johnson laboratory, in particular, George Kallstrom, Matt West and Kai-Yin Lo for analyzing polysomes for my research, and for teaching me how to do it. I also thank members of the Paul, Jayaram, Tucker and Molineux laboratories.

I am fortunate to have dear friends, Mikyoung Park and Jihoon Lee, with whom I have shared highs and lows through my life.

Finally, I sincerely express my gratitude to God and my family for all their love.

The Regulation of Chromosome Segregation by Aurora Kinase, Protein Phosphatase 1 and Nucleolar Protein Utp7

Publication No. _____

Miri Jwa, Ph.D.
The University of Texas at Austin, 2007

Supervisor: Clarence S.M. Chan

The Sli15-Ipl1-Bir1 chromosomal passenger complex is essential for proper kinetochore-microtubule attachment and spindle stability in the budding yeast *Saccharomyces cerevisiae*. Subcellular localization of this complex during anaphase is regulated by the Cdc14 protein phosphatase, which is kept inactive in the nucleolus until anaphase onset. I show here that the predominantly nucleolar ribosome biogenesis protein Utp7 is also present at kinetochores and is required for normal organization of kinetochore proteins and proper chromosome segregation. Utp7 associates with and regulates the localization of Sli15 and Cdc14. It prevents the abnormal localization of Sli15 on cytoplasmic microtubules, the premature concentration of Sli15 on the pre-anaphase spindle, and the premature nucleolar release of Cdc14 before anaphase onset. Utp7 regulates Sli15 localization not entirely through its effect on Cdc14. Furthermore, the mitotic exit block caused by Cdc14 inactivation is relieved partially by the simultaneous inactivation of Utp7. Thus, Utp7 is a multifunctional protein that plays essential roles in the vital cellular processes of ribosome biogenesis, chromosome segregation and cell cycle control.

Protein phosphatase 1, Glc7 opposes *in vivo* functions of the Ipl1-Sli15-Bir1 kinase complex in budding yeast. I show here Scd5- a targeting subunit of Glc7 that regulates endocytosis/cortical actin organization and undergoes nuclear-cytoplasmic

shuttling- is present at kinetochores. Ipl1 associates with both Glc7 and Scd5. The *scd5-PP1Δ2* mutation, which disrupts the association between Glc7 and Scd5, also disrupts the association between Ipl1 and Scd5-Glc7 without affecting the kinetochore localization of these proteins. Genetic studies suggest that Scd5 may positively regulate both Glc7 phosphatase and the Ipl1 kinase complex. In accordance, Scd5 stimulates *in vitro* kinase activity of Ipl1.

scd5-PP1Δ2 cells missegregate chromosomes severely due to several defects: i) at least one of sister kinetochores appears not attached to microtubule. ii) sister chromatids are persistently cohesed through anaphase. iii) Sli15 is hyperphosphorylated and less abundant on the anaphase spindle resulting in unstable mitotic spindle. These results together suggest that Scd5 functions in diverse processes that are essential for faithful chromosome segregation. How Scd5 coordinately regulates two apparently antagonistic enzymatic activities of Ipl1 and Glc7 remains to be determined.

Table of Contents

List of Figures

List of Tables

CHAPTER ONE

Introduction

Since Sutton's historic paper that clearly demonstrated "the chromosome theory of heredity" and that fully acknowledged "the abnormalities in mitosis increase with the degree of sterility" (Sutton, 1903), it has been well established that genomic instability and aneuploidy are the cause of tumorigenesis. A human being consists of approximately 10^{14} cells, all of which originate from one fertilized egg. In addition, an adult human carries out cell division about 25 million times every second. Thus, the precise transmission of a complete set of chromosomes to each progeny from mother in every cell division is the basis of heredity and continuity of life. The cell cycle is the process by which cells duplicate themselves and divide. The basic mechanisms underlying cell cycle events and controls have been unraveled and shown to be highly conserved in eukaryotes. The simplest form of cell cycle as highlightened in embryonic cell cycle consists of S phase and mitosis. During S phase, chromosomal DNA duplicates so that one complete copy is made available for each progeny cell. Mitosis is the process by which the replicated chromosomes are equally segregated into the two progeny cells. Faithful duplication of a cell relies not only on the accuracy of each cell cycle event but also on the correct sequence of the events. The major engines that drives cell cycle are the cyclin-dependent kinases (CDKs), each of which is a binary complex of protein kinase and a regulatory subunit known as cyclin. The abundance of cyclin protein fluctuates during the cell cycle and thereby accounts for fluctuations in CDK activity through the cell cycle. For a cell to divide into two, the activity of CDKs must be coordinated so that the drop in activity of one (e.g., M-CDK) is coordinated in the rise in activity of another CDK (e.g., G1-CDK).

In the following chapter, I discuss key cell cycle events in mitosis that are related to my research topics and I also discuss how they are regulated in a timely manner.

1.1. Kinetochore assembly

1.1.1 Centromere

Kinetochore is a proteinaceous structure that assembles on centromeric DNA. It provides sites for spindle microtubule (MT) attachment during mitosis and meiosis. Centromeres of eukaryotic cells vary to a great extent in size and DNA sequence. Centromere of the budding yeast *Saccharomyces cerevisiae* is simple and spans only 125 bp. It consists of three distinct DNA elements (CDE I, II, and III), two of which provide sequence-specific binding of kinetochore proteins. Point mutations in these DNA elements abolish kinetochore activity (Hegemann et al., 1988), suggesting that the DNA sequence alone can direct kinetochore assembly in yeast. In contrast, metazoan centromeres extend over megabases. Although these centromeres contain arrays of certain tandem repeats (e.g. α-satellite of 171 bp in human centromere), the formation of kinetochore is determined by an epigenetic mechanism than solely by the DNA sequence-specific binding of kinetochore proteins.

1.1.2. Molecular mechanisms of kinetochore-MT connection

Over 60 proteins are known to associate with a budding yeast kinetochore and they are organized into multiple complexes (Fig. 1; reviewed in Westermann et al., 2007). Furthermore, these complexes are assembled hierarchically on centromeric DNA, with the inner complexes associating directly with DNA, the outer complexes associating with MT, and the central complexes bridging the other complexes. Despite the differences in the kinetochores of yeast and metazoa (e.g., positioning mechanism and the number of spindle MT that attaches to a kinetochore), the majority of yeast kinetochore proteins are conserved in mammals and kinetochore architectures of different organisms show striking resemblance.

The CBF3 complex of the budding yeast binds directly to the CDE III element shortly after centromeric DNA replication. The presence of this complex at centromere is essential for the localization of every kinetochore protein that is tested so far, and is

therefore required for the assembly of a functional kinetochore. Mutations in CBF3 components disrupt kinetochore-MT attachment *in vivo* as well as *in vitro* (Lechner et al., 1991; Goh et al., 1993; Sorger et al., 1994). The Dam1 (DASH or DDD) complex provides an interface to kinetochore for MT attachment and plays a key role in mediating kinetochore-MT connection (Cheeseman et al., 2001; Jones et al., 2001; Kang et al., 2001; Janke et al., 2002; Li et al., 2002; Cheeseman et al., 2002). the Ndc80, Mtw1 (MIND), and Ctf19 (COMA) complexes bridge the centromere-bound CBF3 complex to the MT-associated Dam1 complex (Oritz et al., 1999; Wigge et al., 2001; Janke et al., 2001; Measday et al., 2002; De Wulf et al., 2003; Nekrasov et al., 2003; Westermann et al., 2003; Pinsky et al., 2003). Additional kinetochore factors include Cse4 and Mif2. Cse4 (Cenp-A in metazoa) is a centromere-specific histone H3 varient. The chromatin assembly factors Cac1 and Hir1, and the centromere-silencing factor Spt4 restrict Cse4 localization to centromeric nucleosome (Sharp et al., 2002; Crotti et al., 2004). In fission yeast and human cells, histon deacetylation by the histon deacetylases Mis16 and Mis18 is required for Cenp-A loading onto centromere (Hayashi et al., 2004). Mif2 (Cenp-C in metazoa) associates with centromeric DNA as well as centromeric nucleosome components in Cse4-dependent manner (Meluh et al., 1995 and 1997). The hierachical assembly of some kinetochore complexes assemble is shown in Fig. 1.2.

In addition to structural kinetochore complexes, the Ipl1-Sli15-Bir1 complex (Aurora B-INCENP-Survivin complex in metazoa) also localizes to kinetochores and ensures bi-orientation of sister kinetochores (Chan et al., 1993; Kim et al., 1999; Biggins et al., 1999 and 2001; Kang et al., 2001; He et al., 2001; Tanaka et al., 2002). Four microtubule plus-end-tracking proteins (+TIPs; Bim1, Bik1, Stu1, and Stu2 in budding yeast; Mal3, Tip1, MAST and Dis1 in fission yeast; EB1, CLIP170, CLASP, and ch-TOG in metazoa) are found at kinetochores and regulate microtubule dynamics (Wang et al., 1997; Tirnauer et al., 1999; Severin et al., 2001; Kosco et al., 2001; Yin et al., 2002; van Breugel et al., 2003; Carvalho et al., 2004).

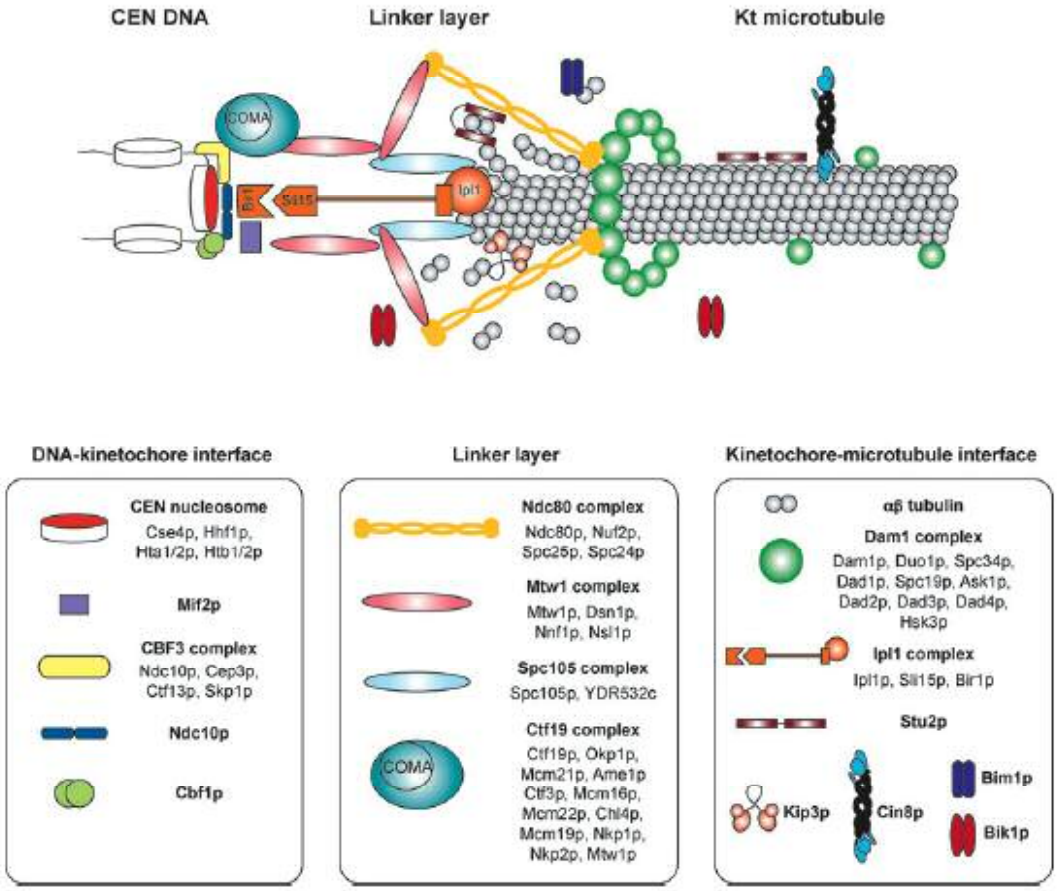

Source: Westermann et al., 2007.

Figure1.1. Overview of the budding yeast kinetochore.
The illustration goups protein complexes according to theis relative position in the DNA-microtubule linkage. If known, structures of kinetochore complexes are taken into consideration. For clarity reason, some kinetochore proteins such as Sgo1, Slk19, Mps1, Glc7 or Kip1 have been omitted from the illustration. CEN: centromere; COMA: kinetochore complex consisting of Ctf19, Okp1, Mcm21 and Ame1. kt: kinetochore.

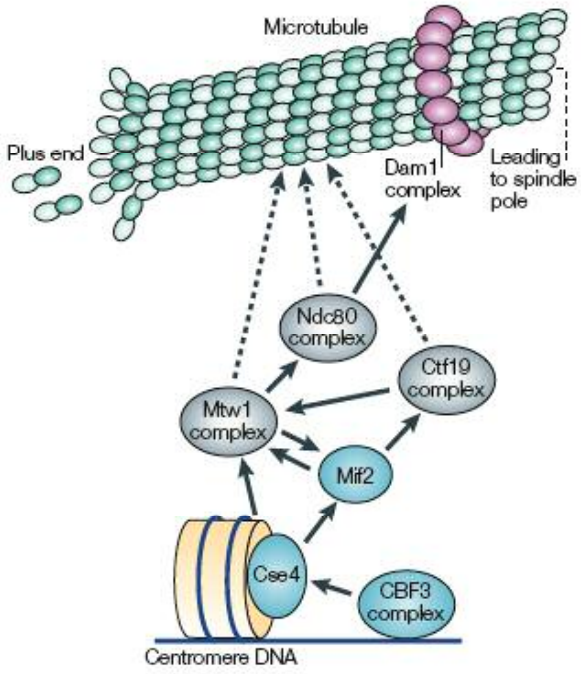

Source: Tanaka et al., 2005c

Figure1.2. Hierarchical organization of kinetochorore in the budding yeast.
Continuous arrows show the order of assembly of the different kinetochore components. The component at the start of each continuous arrow is required for the association of the component to which it points. For example, CBF3 complex is required for the kinetochore association of Cse4. Initial kinetochore capture by the microtubules is dependent on Mtw1, Ndc80, and Ctf19 complexes as shown by dotted arrows. After kinetochores are captured by microtubules, the Dam1 ring complex is loaded onto kinetochores in a Ndc80-dependent manner. The absence of continuous arrows does not necessarily mean that the association of the relevant components occurs independently.

1.1.3. M phase in budding yeast from a chromosomal point of view

The stages of M (mitosis) phase in metazoan cells are defined in part by the timing of M-Cdk activation, nuclear envelope breakdown (NEBD; open mitosis), chromosome condensation. In contrast, NEBD clearly does not occur in budding yeast (closed mitosis) and chromosome condensation is less dramatic (Guacci et al., 1994) and is readily visible. Furthermore, M-Cdk is activated earlier. Thus, I briefly describe M phase in budding yeast with emphases on its unique features (Fig. 1.3).

Spindle pole body (SPB). SPB is the microtubule-organizing center (MTOC) in budding yeast and its counterpart in metazoa is the centrosome. Since budding yeast experiences closed mitosis, SPB is embedded in the nuclear envelope. Kinetochores are tethered to SPBs through MTs for most of the cell cycle (Jin et al., 2000). The old SPB inherited from the previous cell cycle is functional from the beginning of the G1 while the new SPB formed during S phase is initially unable to nucleate MTs. Later during S phase it becomes mature (Adams et al., 2000; Winey et al., 2001). In metazoa, it is only after NEBD that kinetochores can capture MTs since the centrosome is located outside the nucleus.

Pre-anaphase. Centromere of budding yeast is duplicated earlier than most of the rest of chromosome (McCarroll, et al., 1988) and at the time the new SPB is not fully functional. Recent studies showed that centromeres transiently detach from MTs while centromeric DNA is being replicated (Tanaka et al., 2005a) and kinetochore capture by MTs occurs only in S phase in an unperturbed cell cycle (Tanaka. et al., 2005b). In support, the centromeric histone H3 varient Cse4 is turned over at kinetochores only during S phase. Little, if any, turnover occurs during other cell cycle phases (Pearson et al., 2004). These results suggest that kinetochores transiently disassemble (possibly due to Cse4 turn-over) during centromere replication, and reassemble soon afterwards, and the sister kinetochores are recaptured by MTs from old SPB (leading to syntelic attachment) since the new SPB is still immature at that time. It also suggests that there is no distinction between old and new sister kinetochores after reassembled. During late S

phase, the new SPB becomes functional and starts to nucleate MTs while it separates from the old SPB. When old and new SPBs are fully separated, they allow formation of bipolar spindle (Lim et al., 1996). Bi-orientation occurs when one of the sister kinetochores detaches from a MT and subsequently attaches to a MT from the new SPB. Unlike metazoa, budding yeast seems not have a true metaphase since bi-oriented yeast kinetochores do not all move to the middle of the bipolar spindle.

Anaphase. Loss of cohesion between sister chromatids allows poleward movement of sister chromatids along kinetochore MT (anaphase A). Anti-parallel non-kinetochore MTs from opposite SPBs slide against each other to push the two SPBs apart, resulting in spindle elogation (anaphase B).

Telophase. This is the last stage of M phase. The spindle starts to disassemble. A checkpoint mechanism ensures that no chromosome is present at the cell equator before nuclear division occurs (Norden et al, 2006). Cytokinesis finishes the cell cyle.

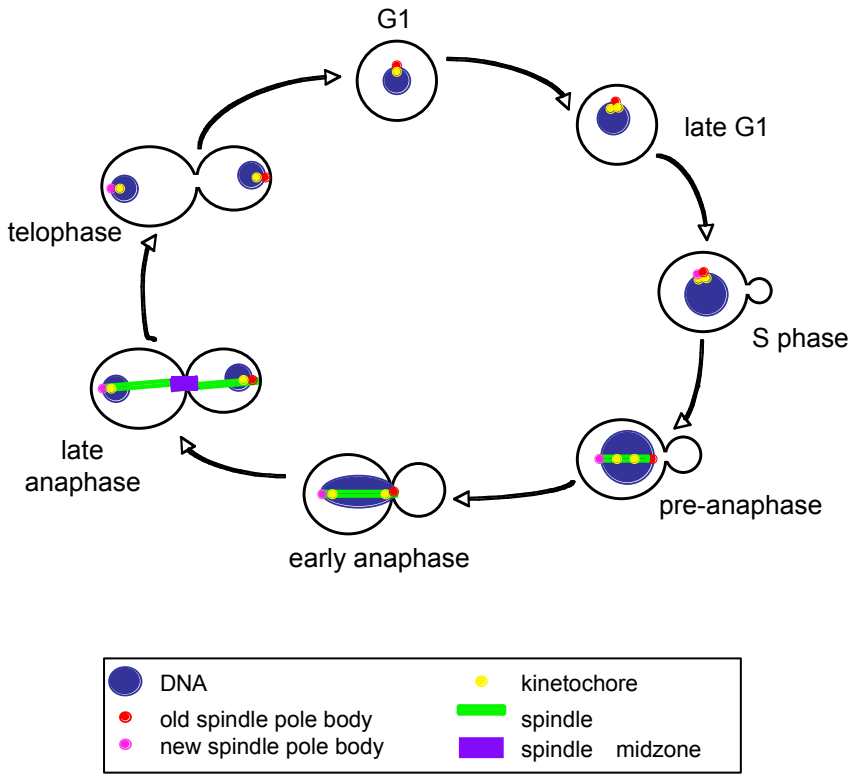

Figure 1.3. The budding yeast cell cycle from a chromosomal point of view. Cytoplasmic microtubules are not shown in this cartoon. See text for details.

1.1.4. Initial kinetochore capture by Microtubule

In metazoa, the initial kinetochore capture by MTs occur rapidly after NEBD (Reider et al., 1990; Hayden et al., 1990). In budding yeast, once kinetochores have assembled, they attach immediately to MTs (see above), with each kinetochore attaching to a single MT. What facilitates the efficiency of kinetochore captures by MTs? *Xenopus* egg extract studies have shown that MTs extend preferentially towards kinetochores from the centrosome, which appears to be dependent on the gradient of Ran-GTP (Carazo-Salas, et al., 2003). Other studies have shown that decrease in the Ran-GTP gradient by increasing the antagonizer, Ran-GAP, is correlated to decrease in the directional growth of centrosomal MTs, and importantly decrease in kinetochore capture (Caudron et al., 2005). These results suggest that the spatial gradient of Ran-GTP orients centrosomal MT growth to kinetochores. Indeed, Ran-GTP gradient regulates MT dynamics by facilitating MT rescue in *Xenopus* egg extract (Carazo-Salas et al., 2001; Wilde et al., 2001).

In budding yeast, although overexpression of Ran-GTP promotes MT growth from spindle pole (Tanaka et al., 2005b), a Ran-GTP gradient seems largely dispensable probably due to the small size of the yeast nucleus and the nature of closed mitosis (Ran-GTP is predominantly cytoplasmic). Instead, +TIPs (Bim1, Bik1 and Stu2) that localize to the plus end of kinetochore MT facilitate MT growth. Among kinetochore complexes mentioned above, the CBF3, Ndc80, Mtw1, and Ctf19 complexes, but importantly not the Ipl1 and Dam1 complexe, are necessary for the initial kinetochore capture. Mutations in these kinetochore components result in unattached kinetochores.

1.1.5. Kinetochore transport along microtubule

Once kinetochores are captured by MTs, they are transported along the MTs towards the minus end of MTs (i.e., towards spindle poles). The detection of ATP-driven motor proteins at kinetochores by chromatin immunoprecipitation assay has made it reasonable to suspect their roles in poleward movement of chromosomes. Budding yeast have six kinesin-related motors (Cin8, Kar3, Kip1, Kip2, Kip3, and Smy1) and a single dynein heavy-chain Dyn1 (reviewed in Hildebrandt and Heiter, 2000). Only four of these

motors (Cin8, Kip1, Kip3, and Kar3) localize to kinetochores and other MT-related nuclear structures (Fig. 1.4; Tytell and Sorger, 2006). Kip3 (Kinesin-8, -13/Kin1 family), Cin8 and Kip1 (both kinesin-5/BimC family) are plus-end-directed motors that stay mainly at kinetochores and they remain kinetochrore-bound upon MT depolymerization. In deletion mutants of *cin8* and (to less extent) of *kip1*, distinctive bi-lobed kinetochore clusters are disrupted without significant dis-organization of spindle or drastic increase in detached kinetochores, suggesting that Cin8 and Kip1, like other kinesin-5 family members (Gordon and Roof, 1999), function in cross-linking kinetochore MTs from non-sister chromatids (Tytell and Sorger, 2006). The clustering of kinetochores by Cin8 and Kip1 may create a multi-stranded kinetochore fiber that is, to some degree, similar to the bundling of multiple MTs (~ 20 MTs) in a kinetochore fiber of metazoan cells. In this model, multiple MTs attached to multiple kinetochores are cross-linked in yeast, whereas multiple MTs attached to a single kinetochore are cross-linked in metazoan cells. The physiological significance of kinetochore clustering may be reflected by cytological defects of *cin8* deletion mutant- the presence of some unattached kinetochores and slightly increased rate of chromosome loss. Alternatively, the presence of unattached kinetochores might disrupt kinetochore clustering and bi-lobed structures since unattached kinetochores are subject to diffusion. *kip3* deletion mutant cells shows different defects in chromosome behaviors such as lagging chromosome and hyper-stretching of peri-centromeric region, suggesting that Kip3 plays a role in synchronizing chromosome movement during anaphase (Tytell and Sorger, 2006).

Kar3 (kinesin-14 family) is the sole minus end-directed motor amongst other nuclear motors that localize to kinetochores. For this reason, it has been suspected for poleward (i.e., towards minus end of MT) movement of chromosomes. The majority of *kar3* deletion mutant cells is able to transport chromosomes along MTs during anaphase with wild-type kinetics (Tanaka et al., 2005b), although cells expressing "rigour" mutant *kar3* that binds to but cannot move along MTs due to ATP-hydrolysis defect (Meluh and Rose, 1990; Maddox et al., 2003) delay kinetochore movement considerably (Tanaka et al., 2005b). In addition, Kar3 is primarily SPB-bound, with only a low level being at

kinetochores during early mitosis. It is highly recruited to detached kinetochores upon MT depolymerization (Tytell and Sorger, 2006). In an unperturbed cell cycle, kinetochores are not detached from MTs except during a very short period in early S-phase (see above). So, Kar3 may play a role in *de novo* MT capture when kinetochores are detached naturally for centromere replication or detached by defects in kinetochores or MTs. In addition, if Kar3 is involved in poleward kinetochore transport during anaphase, it may act redundantly with unknown factors since the majority of *kar3* deletion mutant cells are not defective in this process.

1.2. Bi-orientation of sister kinetochores

The exact number of MT that attaches to a kinetochore varies between model organisms and cell cycle stages in mitosis. In budding yeast, only one spindle MT binds to a kinetochore, and kinetochores hardly detach from spindle MT throughout the mitotic cell cycle. In metazoa, a bundle of about 20 microtubules (K-MTs), called a kinetochore fiber can associate with a kinetochore in pro-metaphase (McEwen et al., 1997). In late-metaphase, kinetochores have more K-MTs and kinetochores gain additional K-MTs as they progress through anaphase (McEwen et al., 1997; King et al., 2000).

Following DNA replication, sister kinetochores need to establish amphitelic/bipolar attachment to MTs that emanate from opposite spindle poles. Inappropriate and presumably unstable attachment can occur. Sister kinetochores can be attached to MTs that all emanate from one spindle pole (syntelic/monopolar attachment). In metazoan cells, kinetochores can simultaneously bind to MTs that emanate from two both poles (merotelic attachment). In budding yeast, syntelic attachment occurs in a normal mitosis and precedes amphitelic attachment. Because spindle pole bodies are embedded in the nuclear envelope, nuclear MTs have acess to kinetochores throughout the cell cycle. Therefore, yeast kinetochores are attached to MTs throughout the cell cycle. In early S phase, centromeric DNA is duplicated early and sister kinetochores both attach to MTs

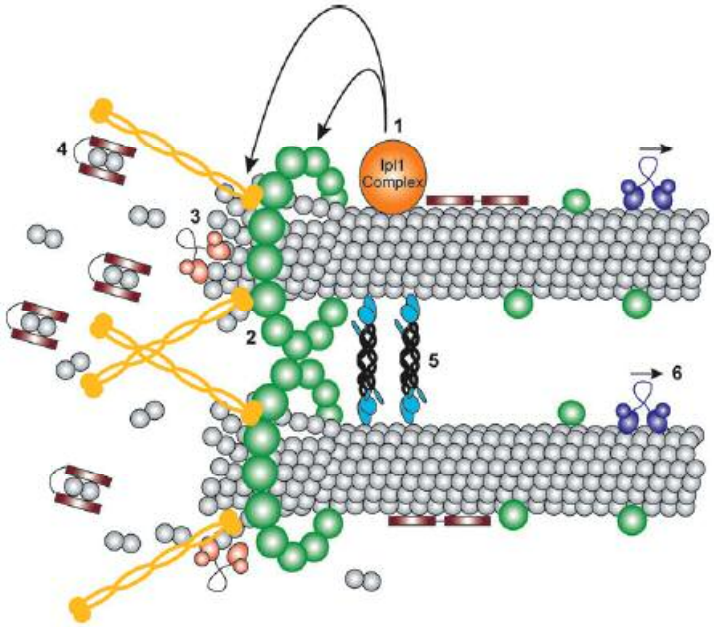

Source: Westermann et al., 2007.

Figure 1.4. Different functions for microtubule-associated proteins (MAPs) at budding yeast kinetochores.
Multiple MAPs and motors cooperate to connect microtubules to kinetochores.
1. Ipl complex: phosphoregulation of attachments, tension-sensing mechanism.
2. Dam1 complex: dynamic end-on attachments, force generation and control of dynamics, possible microtubule cross-linking function.
3. Kip3:orchestration of coordinated anaphase movements, depolymerizing kinesin.
4. Stu2: control of kinetochore microtubule dynamics, contribution to force generation.
5. Kinesins Cin8/Kip1: organization of kinetochores, cross-links to cluster centromeres.
6. Kinesin Kar3: minus-end directed transport of captured kinetochores.

from the old SPB since the new SPB is not functional to nucleate MTs at the time. This syntelic attachment must be corrected later before the onset of anaphase.

I discuss below what factors contribute to bi-orientation of sister kinetochores, and how cells correct mal-orientation to prevent chromosome segregation errors.

1.2.1. Geometry of sister kinetochores and centrosomes

Because sister kinetochores are held together due to sister chromatid cohesion, this back-to-back geometric arrangement would theoretically facilitate bi-orientation by the following mechanism. If one kinetochore (a) is captured by MT(s) from a spindle pole and thus becomes oriented towards this spindle pole, it would position its sister kinetochore (b) towards the other spindle pole and therefore increases chance of its capture by the second pole. It also simultaneously decreases the chance for kinetochore a and b to attach to MTs from the second and first poles, respectively. Similarly, centrosomes that are positioned on opposite sides of sister kinetochores would promote bi-orientation of sister kinetohcores by facilitating the assembly of bipolar spindle.

Live cell imaging in cultured human cells has shown that about 30% of pro-metaphase cells has one or two merotelic kinetochores and the number is drastically decreased to 1% as cells enter anaphase, thus suggesting that there is an error-correction mechanism that generates amphitelic kinetochores before anaphase onset (Cimini et al., 2003). When pro-metaphase cells are treated with the MT polymerizing drug nocodazole, the two centrosomes become positioned next to each other. Upon removal of nocodazole, over 90% of pro-metaphase cells have merotelic orientation (vs. 30% in untreated cells) and 80% of such cells in anaphase have corrected the error by anaphase (Cimini et al., 2003). These data suggest that spindle bipolarity made possible by opposite position of centrosomes contributes significantly to kinetochore bi-orientation and that inappropriate attachment of kinetochores can be corrected before anaphase onset.

In budding yeast, since sister kinetochores are initially in syntelic configuration, geometric arrangement of sister kinetochores obviously does not prevent this form of kinetochore attachment. Nonetheless, especially engineered unreplicated minichromosome (i.e., no sister chromatids) that carries two centromeres (i.e., two kinetochores) becomes efficiently bi-oriented, with the two kinetochores attached to MTs from opposite poles (Dewar et al., 2004). This result indicates i) that it is the connection between sister kinetochore that promotes bi-orientation, possibly by resisting opposing pulling forces that are exerted by MTs; and ii) that tension between sister kinetochores is sufficient for bi-orientation.

However, these data do not exclude the geometry-dependent mechanism as a bi-orientation factor. It certainly is a contributing factor for kinetochores that are captured by multiple MTs and are therefore subjected to merotelic attachment (e.g., in fission yeast and metazoa.

1.2.2. Tension hypothesis: Ipl1/Aurora B kinase

How do cells know if their kinetochores are bi-oriented? Sister kinetochores that are bi-oriented experience tension caused by the opposing poleward forces exerted at these kinetochores. Other forms of kinetochore-MT attachment generate reduced or no tension. Thus, cells may monitor tension at kinetochores. The idea of tension is mainly based on imaging of live cells from many organisms (Skibbens et al., 1993; Goshima and Yanagida, 2000; Tanaka et al., 2000; He, et al., 2001). When kinetochores are bi-oriented, their centromeres (and the peri-centromeric regions) are visibly stretched out. The most plausible interpretation of this phenomenon is that bipolar attachment of MT(s) to sister kinetochores exerts pulling forces towards opposite spindle poles while sister chromatids are held together by cohesin complex along the chromosome arms. Therefore, bi-orientation creates tension at sister kinetochores, resulting in visible stretching of peri-centromeric chromatin.

Initial studies on the Ipl1-Sli15-Bir1 complex in budding yeast showed that both *ipl1* and *sli15* temperature sensitive mutant cells mis-segregate chromosomes frequently without noticeable spindle defects (Chan et al., 1993; Kim et al., 1999). Subsequent studies showed that in both mutant cells, chromosome mis-segregation is non random. Both sister chromatids most often segregate to the old pole and they are syntelically attached to MTs from the old pole (Biggins et al., 1999; He et al., 2001; Tanaka et al., 2002), suggesting that syntelic attachment cannot be corrected in these mutant cells. The Ipl1-Sli15 complex corrects syntelic attachment possibly by acting as a tension-sensor that also destabilizes kinetochore-MT connection at kinetochores that are not under tension. The Ipl1-Sli15-Bir1 complex is conserved in other eukaryotic cells, with the metazoan complex containing Aurora B, INCENP, Survivin and Borealin. These

complexes perform similar function from yeast to humans. For example, Aurora B kinase inhibitor hesperadin causes syntelic attachment for pro-metaphase human kinetochores (Hauf et al., 2003). Destabilization of syntelic or merotelic MT attachment by the Ipl1/Aurora B kinase would lead to generation of unattached kinetochores, which will activate the spindle checkpoint and halt cell cycle progression.

The Ipl1/Aurora B kinase destabilizes improper MT attachment by phosphorylating specific kinetochore proteins. Amongst the known targets of Ipl1 kinase are Ndc80, Dam1 and Sli15. Non-phosphorylatable mutant forms of the kinetochore proteins Ndc80 and Dam1 together phenocopy loss of function mutations of Ipl1 (unpublished data). Recent studies of mammalian Ndc80 (Hec1) revealed that the N-terminal domain of Hec1 is phosphorylated by Aurora B kinase *in vitro*. A mutant Hec1 that can no longer be phosphorylated by Aurora B kinase causes a significant increase in the frequency of merotelic kinetochores and defects in chrosmosome alignment at metaphase plate (DeLuca et al., 2006). At the same time, independent biochemical works showed that the N-terminus of Ndc80 from *C. elegans* binds MT and is phosphorylated by the budding yeast Ipl1 kinase *in vitro*. The *C. elegans* Ndc80 that has been phosphorylated by the budding yeast Ipl1 kinase displays reduced *in vitro* MT binding activity (Cheeseman et al., 2006). These results together suggest that in response to improper kinetochore-MT attachment, Ipl1/Aurora B phosphorylates Ndc80/Hec1 to reduce the affinity of kinetochores to MT.

The ability of "kinetochores" assembled *in vitro* with CEN DNA and wild-type yeast extract to bind MT is abolished by the addition of ATP to the extract (Biggins et al., 1999). However, these "kinetochores" can bind MT in the presence of ATP if the extract is prepared from *ipl1* mutant cells, thus suggesting that Ipl1 kinase activity inhibits kinetochore-MT interaction. The CBF3 binds directly to CEN DNA and is required for functional kinetochore assembly *in vivo* and *in vitro*. However, this complex alone is not sufficient to mediate CEN DNA-MT binding *in vitro* (Biggins et al., 1999; Sassoon et al., 1999), suggesting that additional factors mediate CEN DNA-MT interaction. Recent studies to identify such factors have revealed the Sli15-Bir1 complex (that does not

contain Ipl1) can mediate the *in vitro* binding of CBF3-bound CEN DNA to MT (Sandall et al., 2006). Other studies have also showned that two Sli15-Bir1 complexes exist, one containing Ipl1 and the other does not (Widlund et al., 2006). In accordance, the Sli15-Bir1 complex, but not Ipl1, is required for the *in vitro* assembly of kinetochore that can bind MT (Sandall et al., 2006). Taken together, Sli15-Bir1, but not Ipl1, is necessary and sufficient for the CBF3-bound CEN DNA to bind MT *in vitro*. However, these results seem not in agreement with the *in vivo* observation that sister kinetochores are syntelically attached when Sli15 or Ipl1 is inactivated (Tanaka et al., 2002; Sandall et al., 2006), which suggest that Sli15 is not required for kinetochore-MTattachment *in vivo*. A clue that may reconcile these apparent conflicts came from the observation that mutant Sli15 protein that lacks MT-binding domain also phenocopies the loss of Ipl1 and it can no longer mediate the *in vitro* binding of CBF3-bound CEN DNA to MT, suggesting that the Sli15-Bir1 complex and CBF3 complexes may sense tension at the kinetochores (Sandall et al., 2006). In this model, association of Ipl1 with Sli15-Bir1 causes disassociation of CBF-bound CEN DNA (i.e., "kinetochore") from MT. However, once bi-orientation is achieved, tension-induced configuration changes in the CBF3 land/or Sli15-Bir1 complexes would no longer activate Ipl1 kinase, therefore stabilizing bipolar attachment. It still remains to be elucidated how the Ipl1 complex reads out tension and translates it into signals that are transduced to the downstream targets.

1.3. Sister chromatids cohesion

1.3.1. Topological models of cohesin ring

Cohesin is highly conserved multi-protein complex from yeast to human that holds sister chromatids together until anaphase onset in which the complex is dissolved to separate and segregate sister chromatids to opposite spindle poles. Conhesin complex consists of a heterodimer of Smc1 and Smc3 (Structural Maintenance of Chromosomes) subunits, kleisin subunit, Scc1, and Scc3 (Fig. 1.5A). Biochemical experiments in budding yeast, crystallography and EM studies have shown that cohesin complex forms a ring like structure (Haering et al., 2002; Anderson et al., 2002); Smc1 and Smc3

separately folds into coiled coil rod-like structures and they together shapes a open V-shaped structure with a hinge at which two Smc rods make a contact with each other. Open end of this structure is closed by binding of ATPase-heads of two Scc1 that are later subject to cleavage at anaphase onset leading to opening of the ring to liberate sister chromatids (Uhlmann et al., 1999). Scc1 in turn binds to Scc3. This topological arrangement into a ring structure has raised a possibility that cohesin complex traps two sister chromatids within its ring (Gruber et al., 2003; Fig. 1.5B). Consistent with the embrace of DNA, circular mini-chromosome was co-purified with yeast cohesin complex and cleavage of Scc1 subunit or circular mini-chromosome destroyed the DNA-cohesin complex ineraction (Ivanov and Nasmyth, 2005). A topological alternative, the snap model (Fig. 1.5C; Huang et al., 2005), proposes that each cohesin ring binds to each sister chromatids and tethering is achieved by dimerization of two cohesin rings at their hinges. This model has been favored by recent studies on genome-wide mapping of cohesin binding sites has shown that cohesions are found enriched at specific loci of chromosomes (Glynn et al., 2004; Weber et al., 2004). This model also seems to reconcile with cohesin establishment factors that interact with replication machinery especially at replication fork. To date, current methodology seems not easily distinguish the proposed models although evidences support one over the other. Mechanism of cohesion remains still challenged and further technical advances will distinguish models.

Evidence has been accumulating that cohesin complex plays roles more than simply sister chromatids tethering at different loci on chromosomes. Its key roles at centromere are discussed below.

1.3.2. Cohesin at centromeres

Chromatin immunoprecipitation (ChIP) analysis of budding yeast chromosomes has shown that cohesin subunits- Scc1 and Smc- are highly enriched within 20-50kb region of the conserved 120-bp centromeric DNA (Blat and Kleckner, 1999; Weber et al., 2004). Ectopic centromere was also able to recruit high amount of cohesin within similar range of ectopic centromere, suggesting that functional kinetochores enhance pericentromeric

enrichment of cohesin complex (Weber et al., 2004). At peri-centromeric region, the cohesin-enriched domain acts beyond the region (<20 kb of centromere) that is stretched out by bipolar attachment of MT. Interestingly, yeast kinetochore mutants that are known to cause alteration in MT attachment or reduction in tension displayed higher magnitude of cohesin binding at pericentromeric region (Eckert et al., 2007). In accordance, depolymerization of MT by drug such as nocodazole recruited the highest amount of cohesin at pericentromeric region (Eckert et al., 2007). These results strongly suggest that the level of cohesin binding reflects the degree of tension between sister kinetochores. Combined with the observation that reduction in cohesin binding in pericentromeric region, not on chromosome arms led to chromosome instability (Eckert et al., 2007), In support, elimination of cohesin from centromere increased syntelic attachment (Tanaka et al., 2000), suggesting that cohesin facilitate bi-orientation probably by facing sister kinetochores in opposite directions. Thus, Cohesin complex at centromeres significantly contributes to high-fidelity of chromosome segregation probably i) by constraining sister kinetochores towards opposite spindle poles, which would increase a chance of bi-orientation, ii) by resisting poleward force of MT until bipolar attachment is established, and iii) by reading out of tension across sister kinetochores.

Immufluorescence microscopy in metazoan revealed that cohesins are also highly enriched at peri-centromeric heterochromatin while cohesins at chromosome arms are dissociated earlier during prophase. However, mechanisms of peri-centromeric recruitment of cohesin are poorly understood. Due to lack of conserved centromeric sequence in metazoan centromere, the repetitive heterochromatin has been suspected for

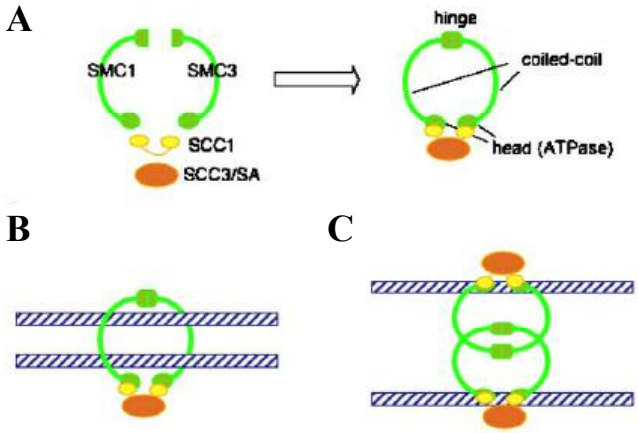

Source: Losada, 2007

Figure 1.5. Models of cohesin-mediated cohesion.

(A) Subunit composition of the cohesin complex and arrangement of the subunits in the shape of a ring. (B)-(C) Models proposed to explain how cohesin interacts with DNA to perform its function. (B) A cohesin ring entraps the two sister DNA molecules. (C) Two cohesin rings interact with each other and bind to each to a sister DNA molecule.

this role. In fact, studies in fission yeast and mammalian cells have tied homologs of HP1 (Heterochromatin Protein 1) that binds to the repetitive sequence to recruitment of pericentromeric cohesin (Bernard et al., 2001; Nonaka et al., 2001). However, the requirement of HP1 seems loose because neocentromeres in human lack of repetitive heterochromatin- i.e. no HP1, and because HP1 depletion from centromere that is relieved from silencing caused by Dicer-deficiency did not decrease cohesin binding at centromeres, suggesting that other mechanism(s) independent of HP1 exists.

The existence of so called protector at metazoan centromere that keeps centromeric cohesin from dissociation during prophase had long been postulated until recent genetic screens in yeast identified meiotic cohesin protector, shugoshin (Sgo; Japanese for " guardian spirit"; Kitajima et al., 2004). At anaphase onset during meiosis I, cohesins on chromosome arms are phosphorylated by Polo kinase, which is in turn cleaved by separase. Centomeric cohesions, however, are dephosphorylated by PP2A, a Ser/Thr phosphatase 2A, that are recruited to centromere by Sgo1 and protected from

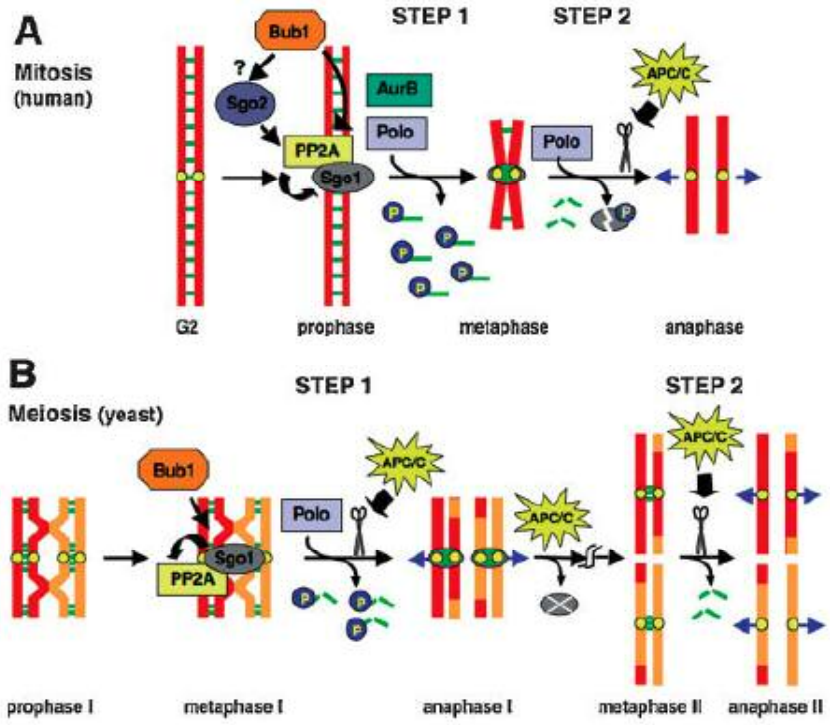

Source: Rivera and Losada, 2006

Figure 1.6. Roles of Sgo and PP2A in regulation of cohesin in mitosis and meiosis.

Two-step release of cohesin in metazoan mitosis (A) and in yeast meiosis. (B). During prophase (A) and meiotic anaphase I (B), cohesins on chromosome arms (green bars) are phosphorylated by Polo kinase (A and B) and Aurora B kinase (only in A) and cleaved by separase (represented as a pair of scissor; STEP 1) while centromeric cohesions (yellow circles) are protected by Sgo-PP2A from separase action. The remaining centromeric cohesions are cleaved by separase at the onset of anaphase (A) and at the onset of anaphase II (B).

separase action (Kitajima et al., 2006; Riedel et al., 2006; Tang et al., 2006; Fig. 1.6B). Similary, human hmologs, hSgo1 and hSgo2, along with human PP2A antagonize Polo kinase (and Aurora B kinase) and protect centromeric cohesin from separase during prophase (Salic et al., 2004; Tang et al., 2004; Kitajima et al., 2005; McGuinness et al., 2005; Fig. 1.6A). These survived centromeric cohesins of yeast cells in meiotic anaphase I and of human cells in mitotic prophase are later cleaved by separase at onset of meiotic anaphase II and mitotic anaphase, respectively.

1.3.3. Loading and establishment of cohesin

Cohesin is loaded onto chromatin at the end of M phase in fission yeast and mammalian cells, and in late G1 in budding yeast. This process requires highly conserved loading factors, Scc2 (Mis4 in fission yeast and Nipped-B in mammal) and Scc4 that are, however, not essential for cohesin maintenance (Ciosk et al., 2000; Tomonaga et al., 2000). Although how Scc2/4 complex promotes cohesin loading onto chromatin is largely unknown, biochemically engineered Smc1 and Smc3 mutant proteins provided some clues to speculate a model (Arumugam et al., 2003; Weitzer et al., 2003); i) Mutation on Smc1 but not on Smc3 that prevents ATP binding to their head domain abolished association of Scc1 with Smc1/Smc3 heterodimer, suggesting that ATP binding is required for cohesin ring formation. ii) Other mutations on either Smc1 or Smc3 that block ATP hydrolysis did not disable Scc1 to associate with Smc proteins but abolish cohesin ring complex association with chromatin, suggesting that ATP hydrolysis, but not ATP binding, is essential for cohesin loading onto chromatin. The latter observation is similar to that in mutaions in loading factors, Scc2 and Scc4 in which cohesin complex was assembled into a ring structure but was not loaded on chromatin. Thus, Scc2/4 may regulate ATP hydrolysis activity of Smc1 of opened V-shaped Smc1/3 complex to engage it with Scc1 that may be already on chromatin, which leads to closing the cohesin ring. In *Xenopus* egg extract, recruitment of Scc2 onto chromatin requires the presence of Mcm2-7 complex on replication origin where Mcm2-7 complex liscenses DNA replication only once per cell cycle (Gillespie et al., 20044; Takahashi et al., 2004), suggesting that in *Xenopus*, cohesin loading is tightly linked to liscensing of DNA replication. However, in budding yeast, cohesin loading is independent of pre-replicative complex and Mcm2-7 complex. Besides, cohesin can be loaded from G1 to late anaphase in which DNA replication has completed (Uhlmann et al., 1998; Haering et al., 2004). This post-replication loading of cohesin may not contribute to tethering of sister chromatids. As mentioned above, cohesin association has been mapped preferentially to peri-centromeric region and sites between transcription units (Lengronne et al., 2004). It is unknown if transcription machinery recruits Scc2/4 complex to chromatin.

Alternatively, transcription activation itself, independently of Scc2/4 complex, may load cohesin complex on chromatin or once cohesin is loaded by Scc2/4 complex, transcription machinery redistributes cohesin to other places on chromatin.

How do cells pair only sister chromatids and not non-sister chromatids which otherwise would be catastrophic? It is conceivable that cohesion may occur during DNA replication because newly synthesized sister is in proximity of old sister as it emerges from replication machinery. A yeast genetic screen that was designed to identify genes (ctf) that are potentially implicated in chromosome transmission fidelity (Spencer et al., 1990) identified the third class of cohesion factors- establishment factors. These factors are distinct from structural cohesins in that their functions are exclusively required during S phase when pairing of sister chromatids is established but not during G2 or M phase when cohesion is maintained. Establishment factors are also unique from loading factors, Scc2 and Scc4, in that cohesins stay bound to chromatin in loss of function mutants of establishment factors. Although a molecular mechanism by which cohesion is established is largely unknown, growing body of potential establishment factors identified through genetic and physical interactions indicates that cohesion establishment is intimately linked to DNA replication. The first clue came from the genetic interaction between Ctf7/Eco1 (Skibbons et al., 1999; Toth et al., 1999), Pol30 (PCNA; proliferating cell nuclear antigen) and Ctf18/Chl12 (a RFC: a replication factor). PCNA, a sliding clamp, associates with DNA polymerases and provides processivity. RFC complexes hydrolyze ATP and load processivity factor such as PCNA onto double-stranded DNA. Second, Ctf7/Eco1 associates with four other clamp loading RFC complexes (Kenna and Skibbens, 2003) each of which is comprised of four small subunits (Rfc2-5) and one of four large subunits (Rfc1, Rad24, Ctf18, or Elg1) with identity of large subunit determining their roles in many facets of DNA replication/repair/checkpoint (Majka and Burgers, 2004). Interestingly, mutations in either small (Rfc2, Rfc4, and Rfc5) or a large subunit (Ctf18) result in precocious sister separation with cohesin bound to chromatin, suggesting that these mutations failed to establish cohesion (Skibbens et al., 1999; Mayer et al., 2001; Hanna et al., 2001; Krause et al., 2001; Kenna and Skibbens, 2003;

Petronczki et al., 2004). Although still remained to be elucidated is if RFC complexes recruit Ctf7/Eco1 to replication fork, a possible model is that Ctf7 helps replication machinery progress through cohesin ring at replication fork- this model assumes that cohesin ring is huge enough for the passage of replication machinery and for this reason among others it favors less the brace model (Fig. 1.5B). Alternatively, cohesin ring transiently dissociates as replication fork passes and rebinds behind replication fork to sister chromatids. Ctf7 may keep dissociated cohesin close to replication machinery or facilitate rebinding of cohesin behind replication fork by a mechanism that is distinct from cohesin loading complex, Scc2/4. Third, mutations in diverse DNA replication factors causes cohesion defect with S-phase specific lethality, the hallmark of establishment factor; i) Trf4 (DNA polymerase kappa; Wang et al., 2000) and Pol2 (DNA polymerase epsilon; Edwards et al., 2003); ii) RFC-associated factors, Dcc1 and Ctf8 (Petronczki, 2004); iii) DNA polymerase alpha binding protein, Ctf4 (Warren et al., 2004); iv) S phase replication/repair checkpoint protein (Mre11, Xrs2, Mrc1, Tof1, and Csm??) identified by their synthetic genetic relationship with *ctf4* knock out mutation (Warren et al., 2004; Xu et al., 2004).

Intriguingly, recent synthetic genetic array (SGA) analysis using *ctf8* knock out mutation revealed new potential implication of factors in spindle integrity and positioning (Chl1, Csm3, Bim1, Kar3, Tof1 and Vik1; Mayer et al., 2004). Since first identified from the genetic chromosome loss screen (Haber et al., 1974), Chl1, a DNA helicase, has been repeatedly isolated from such similar genetic screens. *chl1* knock out mutation caused lethality when combined with spindle checkpoint mutation but, unexpectedly from its biochemical function, not with DNA damage checkpoint mutation (Li and Murray 1991). How a DNA helicase might function in chromosome segregation has been unresolved until recent genetic analysis identified Chl1 as a cohesin establishment factor as mentioned above (Mayer et al., 2004). Cohesion defects reduce tension at sister kinetochores, which in turn activates spindle checkpoint and subsequently delays/ arrests cell cycle at metaphase. Thus, *chl1* knock out mutation, for example, arrests cell cycle at metaphase through spindle checkpoint and upon concomitant inactivation of spindle

checkpoint, *chl1* knock out mutant missegregate chmosomes severely, causing lethality. BACH1, a human ortholog of yeast Chl1, is of clinical significance. It associates with BRCA1, breast cancer tumor suppressor, and this association is required for BRCA1-dependent double strand break repair (Cantor et al., 2001). Individuals that harbor loss of function mutation in BACH1 is more susceptible to tumorigenesis and importantly, cells from such individuals displayed gaps between sister chromatids– i.e. precocious separation (Cantor et al., 2004). Taken together, Chl1, an establishment factor, provides links between cohesion defects, aneuploidy, and tumorigenesis. Growing list of DNA helicases that also function as establishment factors suggests that cohesion establishment may occur even before DNA replication initiation.

1.4. Anaphase onset and anaphase-promoting complex (APC)

The critical cell cycle transition that controls the decision to physically separate sister chromatids is termed metaphase-to-anaphase transition. This decision to proceed anaphase is based on the criterion: All kinetochores must have established amphitelic attachment. Rapid separation of sister chromatids is dependent on protease activity of separase, a cystein protease (Esp1 in budding yeast, Cut1 in fission yeast). Separase, once activated, cleaves Scc1 subunit of cohesin complex in a site-specific manner, which consequently opens up cohesin ring complex and allows disjunction of sister chromatids (Guacci et al., 1997; Uhlmann et al., 1999). The nature of irreversibility of this process puts separase function under the tight control. Until anaphase onset, separase is kept inactive by following mechanisms: first by its association with the inhibitor, securin [Pds1 in budding yeast, Cut2 in fission yeast, PTTG (pituitary tumor transforming gene) in human] (Uhlmann et al., 1997; Ciosk et al., 1998) and second due to its phosphorylation by the M-Cdk (Cdk1/cyclin B) protein kinase. Separase becomes active when Pds1 and cyclin B are simultaneously destructed at the hands of the 26S proteosome, which is preceded by ubiquitination at the hands of a huge multi-subunit ubiquitin protein ligase called anaphase-promoting complex or cyclosome (APC/C). The activity of APC/C is regulated by two mechanisms (Peters, 2002): First by its M-Cdk –

dependent phosphorylation, and second by its association with accessory proteins- Cdc20 or Cdh1/Hct1. The accessory proteins have duel functions. They provide substrate specificity to APC/C by recognizing and recruiting substrates. They also provide means to regulate APC/C activity in cell cycle-dependent manner.

Cdc20 is expressed in peak at G2/M phase and critical for APC functioning at metaphase-to-anaphase transition. It is subject to inhibition when preceeding cell cycle events has not completed- e.g. kinetochore biorientation. In addition, budding yeast APC^{Cdc20} plays additional role in mitotic exit.

Cdh1/Hct1 plays a major role in late mitosis events-e.g. destruction of residual mitotic cyclin and resequestration of Cdc14, a key to mitotic exit, at the end of mitosis although it is not essential for cell viability. Cdh1 is constitutively expressed throughout the cell cycle but kept inactive by M-Cdk-dependent phosphorylation. In late anaphase, Cdc14 dephosphorylates and thereby activates Cdh1, which eventually results in inactivation of Cdc14, forming a negative feedback loop.

1.5. Mitotic exit

The simplest scheme of mitosis is that it is initiated by M-Cdk and is finished by a phosphatase- e.g. Cdc14 to reverse M-Cdk action as well as to inactivate it. If the first part of mitosis concerns ultimately establishing chromosome biorientation, the second part of mitosis ensures equal division of genetic material and subsequent cell division. Cell cycle events in the second part are timely controlled by sequential action of APC^{Cdc20} and Cdc14 phosphatase. APC^{Cdc20} triggers chromosome segregation by cleaving Scc1 and starts inactivating M-Cdk, which in turn signals FEAR (Cdc fourteen early anaphase release) network to activate transiently Cdc14 phosphatase to finish up chromosome segregation. In addition, Cdc14 that is released by FEAR activates MEN (mitotic exit network) to further and fully release itself (positive feedback), which leads to mainly two consequences: First, complete M-Cdk inhibition that initiates cytokinesis and second, inactivation of itself- i.e. negative feedback.

The critical cell cycle decision that is made to undergo cytokinesis, a physical cell division to two genetically identical cells, termed mitotic exit. It is named such way because cytokinesis occurs with interphase version of Cdk. Therefore, the hallmark of mitotic exit is inactivation of mitotic Cdk. The criterion to make this cell cycle transition based upon is that chromosomes must be fully segregated along an axis- i.e. spindle axis- that must be perpendicular to plane of cell division. Budding yeast, like metazoan that undergo asymmetric cytokinesis, check if the criterion has met by spatially and asymmetrical organized decision-making factors/sensors. They ensure i) that mitotic spindle is properly aligned and positioned because further elongation of such mitotic spindle in anaphase will likely inherit genetic material equally to two sides of cell division plane- i.e. bud and mother in budding yeast, and ii) that chromosome segregation precedes cytokinesis, and iii) that chromosome segregation has completed by confirming the absence of chromosome at cell division plane, bud neck in budding yeast.

1.5.1. Mitotic cyclin degredation

In budding yeast, mitotic cyclin, Clb2, degradation occurs in a biphasic way (Yeong et al., 2000): APC^{Cdc20} is responsible for first phasic proteolysis of Clb2. The resulting reduced mitotic Cdk activity tips the balance in favor of Cdc14 phosphatase that dephosphorylates targets that have been phosphorylated by M-Cdk and thereby reverses M-Cdk actions (Visintin et al., 1998). For example, M-Cdk phosphorylates and prevents Cdh1 from activating APC/C and at the end of anaphase, Cdc14 dephosphorylates and activates Cdh1 (Jasperson et al., 1999). Consequent activation of APC^{Cdh1} triggers the second phasic proteolysis of Clb2. The first phasic proteolysis of Clb2 is sufficient to exit mitosis even in the absence of Cdh1 and Sic1, a Cdk inhibitor (Wasch et al., 2002). The main role of the second phasic proteolysis mediated by APC^{Cdh1} is thus to keep M-Cdk activity low as in interphase level.

1.5.2. FEAR (Cdc Fourteen early anaphase release) release of Cdc14

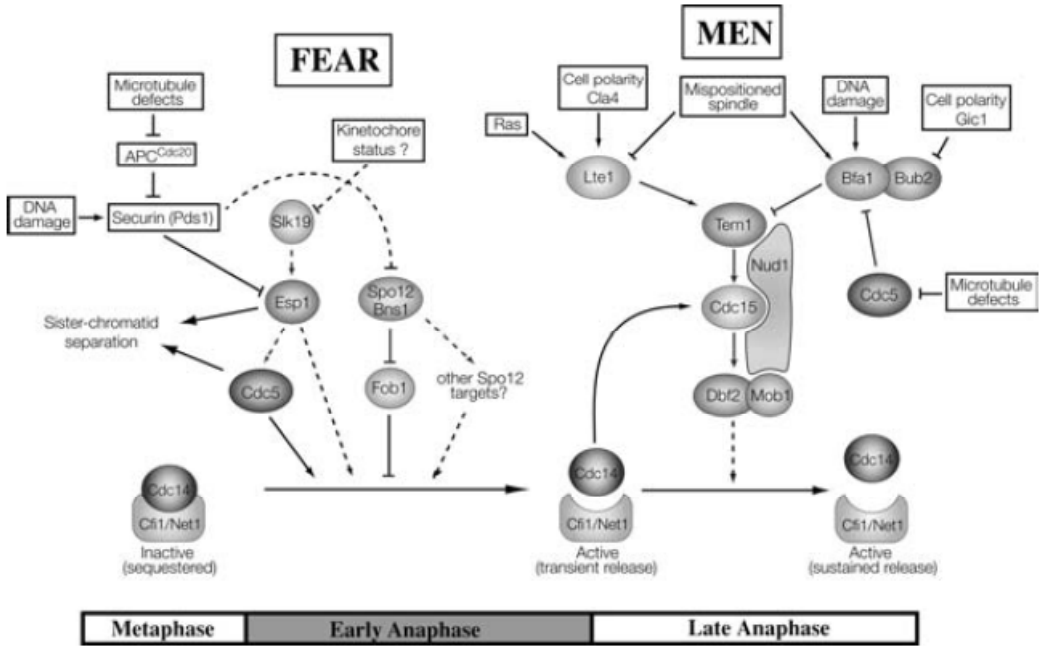

Source: Stegmeier and Amon, 2004

Figure 1. 7. Components of the FEAR network and the MEN and signals controlling these pathways.
The release of Cdc14 from its inhibitor Cfi1/Net1 is initiated during early anaphase by the FEAR network. During later stage of anaphase, the MEN promotes and sustains the release of the phosphatase. The signals and proteins regulating the activation of these two pathways are shown. Solid arrows indicate reasonably well-established interactions; dashed arrows indicate more speculative interactions.

Cdc14 is kept inactive in nucleolus by its association with the inhibitor, Net1 bound to its catalytic center during the most of cell cycle until anaphase onset. The release of Cdc14 from Net1 is controlled by two pathways: FEAR network releases only small fraction of Cdc14 at the anaphase onset and MEN that is activated by FEAR-released Cdc14 promotes and maintains full release of Cdc14 at late anaphase (Fig. 1.7 and 1.8).

Components of FEAR network. To date, five proteins function in FEAR network in positive manner and epistasis analyses have revealed three parallel branches in the network; i) polo-like kinase, Cdc5, ii) separase (Esp1)-the kinetochore protein Slk19, iii) Spo12 and it close homologue, Bns1. Two negative regulators are securin (Pds1) and the

replication fork block protein, Fob1. Although how these factors function mechanistically is not clear, some interactions have been reported; i) the initial release by FEAR requires Cdc5- (and M-Cdk-) dependent phosphorylation on both Cdc14 and Net1, which is believed to reduce the affinity between these two proteins, ii) Slk19 translocates to spindle mid-zone from kinetochores at the anaphase onset, which in turn recruits separase. Surprisingly, their presence at spindle midzone is rather important for Cdc14 release than proteolytic activity of separase or anaphase-specific cleavage of Slk16 by separase, iii) Unlike other components, Spo12, Bns1, and Fob1 are present in the nucleolus throughout the cell cycle. Spo12-Bns1 complex binds to Net1 through Spo12 and acts positively. Fob1 also physically interacts with Net1 as well as Spo12 but serving a negative regulator. It has been proposed that anaphase-specific phosphorylation of Spo12 (by unidentified kinase) may induce a conformational change in Fob1 that would, in turn, reduce the affinity between Net1 and Cdc14 and thereby release Cdc14. In this scenario, at the beginning of anaphase, Spo12 (and Bns1) acts as a positive regulator of Cdc14 release by antagonizing inhibitory Fob1 function, iv) Securin (Pds1) is well known for its inhibitory role against proteolytic separase function in sister chromatid separation. Interestingly, securin also inhibits non-proteolytic function of separase and therefore FEAR release of Cdc14. This might coordinate timely chromosome segregation and the beginning of mitotic exit and serve surveillance mechanism that blocks both the onsets of sister chromatid separation and FEAR by delaying Pds1 degradation when chromosomes have not attained amphitelic attachment.

Molecular mechanism of dissociation of Cdc14 from Net1. Although Cdc14 is clearly released from Net1 and therefore, from the nucleolus during anaphase by FEAR and MEN, how Net1-Cdc14 complex is disassembled is poorly understood. The observation that phosphorylation status of Net1 and Cdc14 is temporally correlated with timing of Cdc14 release raised the possibility that phosphorylation underlies the

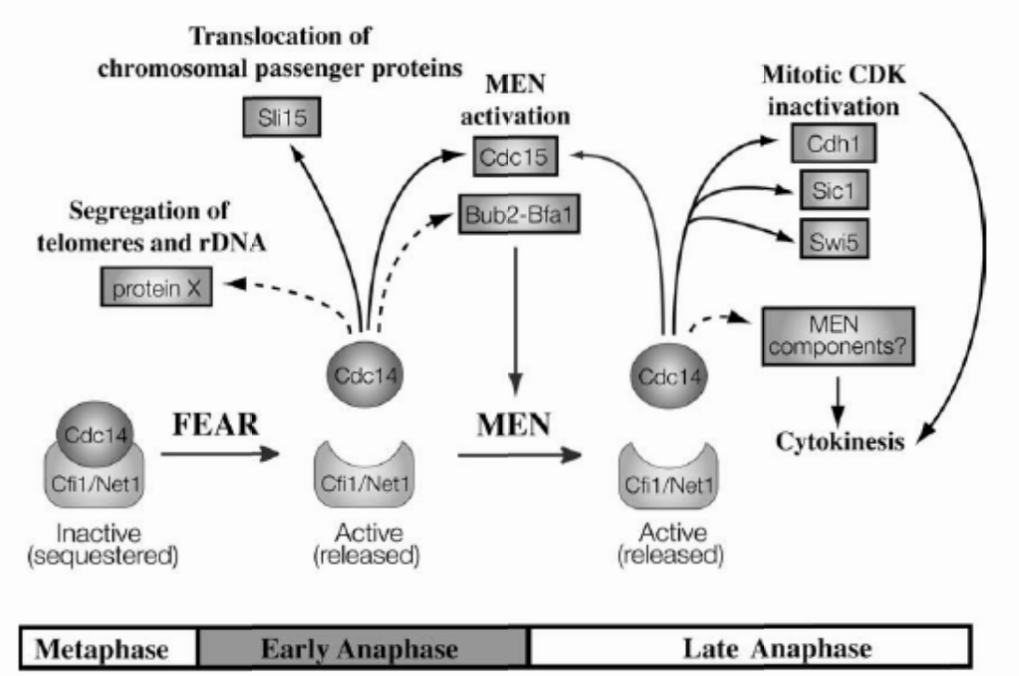

Source: Stegmeier and Amon, 2004

Figure 1.8. Substrates and functions of Cdc14 during mitosis.

Cdc14 releasesd by the FEAR and the MEN regulates many mitotic processes. The FEAR network-activated Cdc14 promotes the segregation of telomeres and rDNA, the translocation of chromosomal passenger proteins, and activation of the MEN. Cdc14 activated by the MEN promotes the inactivation of mitotic CDKs and cytokinesis. The known targets of Cdc14 in the regulation of these processes are shown in the gray boxes. Solid arrows indicate reasonably well-established Cdc14 targets; dashed arrows indicate more speculative ones.

disruption of Net1-Cdc14 complex. Several lines of evidences implicated that Cdc5 and M-Cdk are likely potential candidate kinases. They phosphorylate Cdc14 and Net1 both *in vitro* and *in vivo* (Shou et al., 2002; Azzam et al., 2004). Overexpression of either kinase leads to increase in phosphorylation in Net1 and ectopic release of Cdc14. With the notion of the caveat that both Cdc5 and M-Cdk are involved in many other cellular processes and overexpression data should be carefully interpreted, these results suggest that they are sufficient to disassemble the complex. Furthermore, nonphosphorylable Net1 mutant displayed higher affinity for Cdc14 even in the presence of either kinase *in vitro*, suggesting that they likely abolish the interaction between Net1 and Cdc14 by phosphorylating Net1 (Shou et al., 2002; Azzam et al., 2004). Net1 mutant that cannot be

phosphorylated by M-Cdk displayed defect in Cdc14 release, that is a reminiscent of FEAR loss of function mutants (Azzam et al., 2004). Despite Cdc5 can disassemble Net1 and Cdc14 interaction *in vitro*, it has little, if any, effect *in vivo*. Cells carrying nonphosphorylable Net1 mutant by Cdc5 exhibited almost identical kinetics of Cdc14 release to that in wild-type (Shou et al., 2002) and loss of function mutation of Cdc5 does not impair Cdc14 release. These observations can be explained that Cdc5 is activated earlier than M-Cdk and acts upstream of M-Cdk and positively regulates Cdc14 release mainly through M-Cdk at the anaphase onset when Cdc14 is released by FEAR- i.e. MEN-independently. However, it is unclear that how cells can release Cdc14 in M-Cdk-dependent way as M-Cdk activity starts declined.

Temporal Coordination of Chromosome segregation and onset of mitotic exit. The onset of chromosome segregation is triggered by a universal protease, separase that cleaves Scc1 subunit of cohesin ring. Another universal kinase, Cdc5 assists separase function by phosphorylating Scc1 subunit (Alexandru et al., 2001; Sumara et al., 2002). Budding yeast ensure that mitotic exit does not occur before chromosome segregation by engaging same proteins for both processes. Separase and polo kinase both trigger sister chromatid separation and FEAR-driven Cdc14 release. Although what Slk19 does at kinetochores is little known, it is tempting to speculate that status of kinetochores is ensured by Slk19 before mitotic exit starts, which might in turn activate FEAR network.

Segregation of rDNA. The observation that loss/reduction of function mutation of FEAR network components failed to dissolve rDNA whereas this mutation had no effect on segregation of the rest of genome (Sullivan et al., 2004; D'Armours et al., 2004; Machin et al., 2005) has first revealed that repetitive DNA sequences such as rDNA and telomeres require cohesin-independent cohesion mechanism. Recent studies have shown that FEAR-activated Cdc14 activity is required for efficient segregation of repetitive sequences but not for early-segregating region.

Anaphase spindle stability. The middle region of spindle is thought to be fragile particularly during anaphase. The rapid elongation of spindle during this phase reduces the overlap between pole-to-pole MTs to a critically small region of the spindle (spindle

midzone; Winey et al., 1995). The spindle midzone is reinforced by the population of MT (+) end binding proteins Bim1 and Bik1 (Berlin et al., 1990; Schwartz et al., 1997); the Ipl1-Sli15-Bir1 complex (Pereira et al., 2003); Ase1 (Schuyler et al., 2003); Cin8 and Kip3 kinesin-like motor proteins (Saunders and Hoyt, 1992; DeZwaan et al., 1997); the CLIP-associating protein–like protein Stu1 (Yin et al., 2002); the separase Esp1-kinetochore protein Slk19 (Sullivan and Uhlmann, 2003). FEAR-released Cdc14 regulates spindle midzone assembly in two independent pathways, Sli15-Ipl1 complex and Ase1. Cdc14 dephosphorylates at least Sli15 of the Ipl1-Sli15-Bir1 complex and translocates the complex to the spindle midzone, which in turn recruits the Esp1-Slk19 complex there (Pereira et al., 2003). Unlike these components, others localize to spindle earlier during pre-anaphase spindle and become restricted to spindle midzone during late-anaphase in Ase1-dependent manner. Recent study has shown that ectopic overexpression of Cdc14 dephosphorylates Ase1 that has been phosphorylated by Cdk1-Clb5 at the end of S phase, and an Ase1 mutant protein that mimics constituitive phosphorylation either could not be concentrated on the spindle midzone or occupied a part of anaphase spindle that was shifted toward one of the two spindle poles, which nonetheless mislocalized all other Ase1-dependent components (Khmelinskii et al., 2007). Interestingly, *td-cdc14* mutation that rapidly degrades Cdc14 upon temperature-shift, enriched the latter mislocalization phenotype of Ase1, implying that unknown phosphatase may regulate Ase1 in Cdc14-dependent way.

1.5.3. MEN (Mitotic exit network)

The MEN is essential for mitotic exit as MEN mutants in budding yeast arrest in telophase with high mitotic Cdk activity. In contrast, FEAR network is not essential. Cells lacking FEAR network activity delay but eventually exit mitosis by MEN. FEAR-released Cdc14 is short-lived and not maintained without following MEN activation mainly due to two mechanisms. First, Cdc14 dephosphorylates itself and Net1, and regains its ability to interact with Net1, leading to resequestration of itself into nucleolus (Jasperson and Morgan, 2000). Second, FEAR network releases only small amounts of

Cdc14, which appears not enough to direct itself to cytoplasm where some of critical substrates to trigger mitotic exit such as Cdh1 and Swi5 are located.

MEN signaling resembles Ras-like GTPase signaling cascade. It employs Tem1 GTPase, the putative GEF (guanine nucleotide exchange factor) Lte1, the hetero-dimeric GAP (GTPase activating protein) Bub2-Bfa1 and downstream protein kinase cascade of Cdc15, Dbf2 that is in a complex with Mob1, and Dbf20. Polo-like Cdc5 kinase is also a MEN component and acts at multiple steps (Fig. 1.7). Most of MEN components, Tem1, Bub2-Bfa1, Cdc15, Dbf2-Mob1, and Dbf20 associate with SPB in cytoplasmic side through scaffold protein Nud1 that is a core SPB component and their SPB association is cell cycle regulated. During the most of cell cycle, Tem1 associates asymmetrically with the SPB that enters the bud- i.e. old SPB- in a manner dependent on its two-component GAP Bub2-Bfa1. As the old pole enters the bud at late anaphase, Cdc5 phosphorylates and inhibits the GAP complex, freeing Tem1 from its inhibition and also making it accessible to the GEF Lte1 that is restricted to the cell cortex in the bud. Active GTP-bound Tem1 then recruits Cdc15 to the old pole where it is also dephosphorylated by FEAR-driven Cdc14 and becomes activated. Activated Cdc15 in turn phosphorylates and activates downstream kinase complex Dbf2-Mob1, ultimately leading to full release of Cdc14 from Net1 and nucleolus. Cdc5 also contributes to the full activation of the Dbf2-Mob1 complex. Once set free as a result of MEN activation, Cdc14 carries out critical dephosphorylation events to trigger mitotic exit (Fig. 1.8): i) it activates Cdh1/Hct1, leading to second phase of Clb2 proteolysis. ii) it stabilizes the Cdk inhibitor, Sic1. iii) it recruits Swi5, the transcription factor of Sic1, to the nucleus, leading to accumulation of Sic1. These altogether cause the inactivation of M-Cdk.

1.6. Spindle checkpoint

Checkpoints engage an error-monitoring/detecting mechanism, a signaling pathway, and effectors that stall cell cycle progression to give time for error correction. One of such is spindle checkpoint (SCP). Improper attachment of MT to kinetochores would unevenly sort genome content to daughter cells, leading to changes in ploidy– i.e.

aneuploidy. The SCP becomes activated when errors arise in kinetochore-MT attachment and transmits the inhibitory signal to cell cycle machinery of metaphase-anaphase transition and much later event, mitotic exit. In doing so, cells can ensure that it is not until chromosomes are properly attached to MT to segregate chromosomes and to enter next cell cycle.

1.6.1. The SPC components and cell cycle arrest at the metaphase-anaphase transition

The major players of the SCP were identified in budding yeast as mutants that failed to arrest in mitosis when MTs were damaged. These are Mad (mitotic arrest defective)1, Mad2, and Mad3 (Li and Murray, 1991); Bub (bud uninhibited by benomyl)1, Bud2, and Bub3 (Hoyt et al., 1991). Mps1 and Ipl1 also play roles in the SCP signaling (Weiss and Winey, 1996; Biggins and Murray, 2001). These proteins are highly conserved in other organisms.

Studies in mammalian cells have shown that the presence of single unattached kinetochores could stop the mitotic progression and the SCP signaling proteins are enriched at unattached kinetochore (Taylor and McKeon, 1997; Taylor et al., 2001). In addition, when that unattached kinetochore is destroyed by laser, arrest in anaphase is relieved, suggesting that unattached kinetochore creats inhibitory signal to halt cell cycle (Reider et al., 1994).

Mps1 and Bub1 are dependent on each other for their kinetochore localization. Upon spindle damage, the SCP kinases Mps1 and Bub1 recruit subcomplexes of SCP proteins (Mad1-Mad2, Mad3-Bub3) to unattached kinetochores in part by phosphorylating them (Fig. 1.9). Ipl1/Aurora kinase is also implicated in mitotic arrest that are induced by Mps1 overexpression in budding yeast (Biggins and Murray, 2001) and inactivation of Aurora B kinase by its antibodies overrides nocodazole-induced mitotic arrest in *Xenopus* egg extract (Kallio et al., 2002), suggesting its direct role in the SCP activation. Moreover, Aurora B kinase recruits Mps1 and Bub1 kinase to the

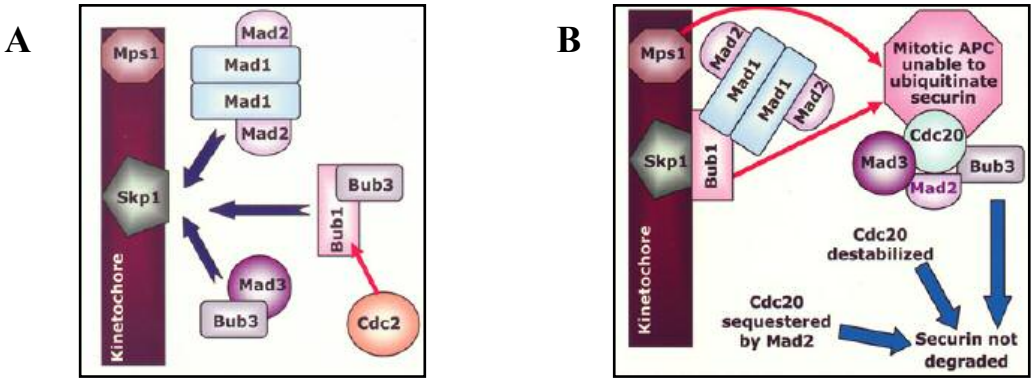

Source: Tan et al., 2005

Figure 1.9. The "anaphase arm" of the SCP.

A. Recruitment: Upon SCP engagement, subcomplexes of checkpoints are recruited to the kinetochore. Cdc2-dependent Bub1 phosphorylation is required to activate the SCP after spindle damage. Recruitment of SCP complexes presumably occurs via their direct or indirect interaction with kinetochore components (e.g., Skp1) and other checkpoint proteins. B. Inhibition of anaphase: Targeting of substrates (e.g., securin) by APC^{Cdc20} inhibited independently and collaboratively by the various Mad-Bub complexes.

kinetochores, which in turn recruit Mad1-Mad2 complex. Therefore, at least in *Xenopus* egg extract system, Aurora B kinase acts at the most upstream of the SCP signaling. Once recruited to the kinetochores, Mad2 is modified to an inhibitory form, released from the kinetochores and transferred to Cdc20 that is already associated with Bub3 and Mad3 (mammalian BubR1), which then renders APC^{Cdc20} incapable of ubquitinating securin, Pds1, resulting in cell cycle arrest in metaphase-anaphase transition (Fig. 1.9; Fang et al., 1998). In addition to inhibition of Cdc20 and thereby APC^{Cdc20}, the SCP also destabilizes Cdc20 to inhibit completely APC^{Cdc20} (Pan and Chen, 2004).

1.6.2. Cell cycle block in mitotic exit by the SCP

Unlike other Mad and Bub proteins, Bub2 localizes to the SPB and negatively regulates, as a GAP complex, Tem1 GTPase and thereby MEN signaling. Bub2 does not block cell cycle progression by inhibiting APC^{Cdc20}-dependent Pds1 degredation (Fraschini et al., 1999; Alexandru et al., 1999). Instead, when spindle is damaged, the SCP activates the GAP activity through Bub2 (and its partner Bfa1), which in turn inactivates Tem1 and MEN, resulting in block in mitotic onset.

1.7. Protein phosphatase 1 and chromosome segregation

Ipl1/Aurora kinase family serves elemental cellular functions such as histone H3 phophorylation, kinetochore-microtubule attachment, mitotic spindle stability, rDNA condensation and subsequent complete segregation, and coordination of cytokinesis to clearance of chromosomes at future cell division site (Norden et al., 2006). Given its fundamental roles in cellular signaling through phosphorylation of subset of target proteins, it is not surprising that the activity of Ipl1/ Aurora kinase must be tightly regulated. Works of many research groups have shown that this is accomplished by auto-phosphorylation, interaction with its stimulator, Sli15/INCENP, and its cellular locations. Equally important is the role of protein phosphatase 1, Glc7/PP1c, which reverses Ipl1/Aurora kinase *in vivo* functions (Francisco et al., 1994) by removing phosphates from its substrates.

Glc7 is the catalytic subunit of Ser/Thr protein phosphatase (PP1c). PP1 is one of the most conserved eukaryotic proteins. Eukaryotic genomes contain PP1 gene somewhere between one (*Saccharomyces cerevisiae*; *GLC7*) to eight (*Arabidopsis thaliana*). Their catalytic center employs virtually identical three-dimensional structure and catalytic mechanism (Barford et al., 1998). Mammalian PP1 has four isoforms-PP1α, two alternatively spliced forms (PP1γ1 and PP1γ2), and PP1β/δ (reviewed in Cohen et al., 2002). The mammalian isoforms are ubiquitously expressed with the exception of PP1γ2 that is limited in testis. Mouse PP1 isoforms- α, β, and δ, when expressed at the basal level, were able to suppress *Schizosaccharomyces pombe* PP1 mutant *dis2* (Sangrador et al., 1998). Similarly, rabbit muscle PP1 fully suppressed all the phenotypes

that were associated with *Aspergillus* PP1 mutant *bimG11* (Doonan et al., 1991). These observations indicate that PP1 is conserved not only in sequence but also in functions.

1.7.1. Interactions of regulatory (R) subunits with PP1

PP1 regulates a variety of cellular processes (figure 1.10; reviewed in Ceulemans and Bollen, 2004) by dephosphorylating substrates. This multi-functionality is only understood in a context of diverse holo-enzyme complexes each of which contains different regulatory (R) subunit. R subunits dictate substrate specificity, alter enzymatic activity, and/or target to cellular locations. Over 50 bona fide or putative R subunits have been identified in mammalian cells and the list of R subunit has been expanded by PP1-interactors of which mammalian orthologs are not (yet) found (Cohen et al., 2002; for review, see Ceulemans et al., 2003 and Barford et al., 1998). It is perplexing in that a relatively small protein PP1 (35-38kD) can associate with a spectrum of R subunits that do not appear to have structural similarity and make different effects on PP1 functions.

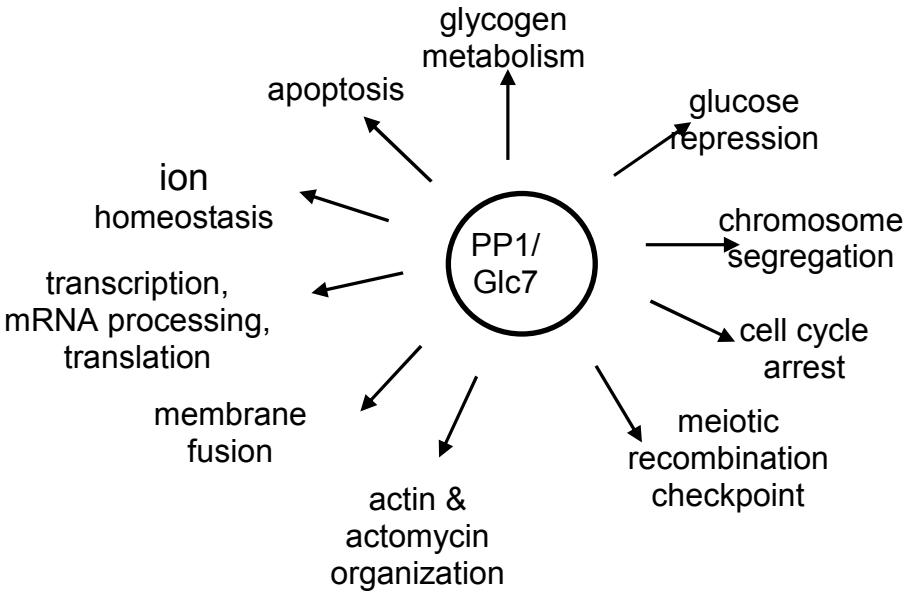

Figure 1.10. A subset of functions PP1c/Glc7

Researches such as mutational analysis, peptide inhibitor studies and crystallography have mapped the interaction sites on R subunits and PP1: First, many of R subunits contain a short degenerate motif, (R/K)(V/I)xF (x being any residue but proline) that is often preceded by basic amino acids (Egloff et al., 1997; Wakula et al., 2003). Co-crystallization of a peptide with these two features along with PP1 showed (i) that degenerate KVxF bound to a site on PP1 that is distant from catalytic site and (ii) that basic amino acids were stabilized by accommodating negatively charged amino acids on PP1. Mutation on valine or phenylalanine on this motif of many R subunits abolished or greatly weakened the interaction with PP1 (Chang et al., 2002). This suggests that KVxF motif primarily mediates the association with PP1. Second, almost all R subunits have multiple additional contact sites scattered over their DNA sequences in addition to the degenerate KVxF motif. One of such is the basic amino acid stretch that precedes the KVxF motif as mentioned above. Mutations on these contact sites were synergistically weakened and correlated to changes in PP1 functions (Schillace et al., 2001; Bollen et al., 2001). This suggests that additional contacts may reinforce the primary interaction via KVxF motif. In addition, it implies that second contacts may provide PP1 a way to distinguish different R subunits. Finally, R subunits can share interaction sites. A model of "combinatorial control " of PP1 has been proposed (Bollen, 2001). The model proposes that a PP1 has only limited number of R subunit binding sites and each R subunit occupies a combinatorial subset of binding sites, leading to assigning PP1 to distinct cellular functions.

1.7.2. Reversal of Ipl1/Aurora kinase

Since the Aurora kinase promotes kinetochore-microtubule turnover by phosphorylating subset of kinetochore target proteins until sister pairs of kinetochores are bioriented and thus under tension, Aurora kinase activity must be turned off and kinetochore proteins that have been phosphorylated by Aurora kinase must be dephosphorylated once bi-orientation has achieved at sister kinetochores to avoid futile cycles of kinetochore-microtubule turnover. The antagonistic relationship between

Aurora kinase and PP1 phosphatase was first proposed in the budding yeast homologs-Ipl1 kinase and Glc7 phosphatase (Francisco et al., 1994; Tung et al., 1995). Although similar relationship has been reported for metazoan Aurora kinase and PP1 (Giet et al., 2005), how PP1 opposes Aurora kinase is largely unknown. One possibility is that PP1 shares common set of substrates with Aurora kinase and removes phosphates from substrates that have been phosphorylated by Aurora kinase without affecting activity of Aurora kinase. Alternatively, PP1 negatively regulates Aurora kinase activity. These possibilities are not mutually exclusive. Studies in yeast have shown that histone H3 and Dam1 are likely common substrates of Ipl1 kinase and Glc7 phosphatase (Hsu et al., 2000; Pinsky et al., 2006).

Glc7 is found in the nucleus with high concentration in the nucleolus throughout the mitotic cell cycle. Shortly after anaphase onset, Glc7 also appears at kinetochores until cytokinesis (Bloecher and Tatchell, 2000). Since PP1 carries out its cellular functions by selectively binding to function-specific R subunits, it is important to identify nuclear-specific R subunits to elucidate molecular mechanism by which Glc7 is targeted to kinetochores where it antagonizes Ipl1. Although not well understood, some of proteins are known to regulate nuclear function of Glc7. The budding yeast PP1 inhibitor-2 Glc8 regulates chromosome segregation by functioning as both an *in vivo* activator and inhibitor of Glc7 depending on its dosage (Tung et al., 1995). The Ypi1-Sds22 regulatory complex targets in part Glc7 into the nucleus (Pedelini et al., 2007) and requires to complete mitosis. Interestingly, earlier biochemical studies have observed that Glc8/I-2 and mammalian Sds22 largely reduces phosphorylase phosphatase activity of Glc7/mammalian PP1 (Tung et al., 1995; Dinischiotu et al., 1997). However, this does not necessarily imply that I-2 and Sds22 function only as negative regulators of PP1 *in vivo*. The effects of R subunits on PP1 activity would be well understood in the context of substrates as the combinatorial model proposes. Alternatively, R subunits may act as both *in vivo* positive and negative regulator depending on their dosage as Glc8/I-2 does (Tung et al., 1995).

CHAPTER TWO

Materials and methods

2.1. Strains, media, and genetic techniques

The yeast strains that were used in this study are listed in Tables 2.1 and 2.2. Media and genetic techniques were performed as described by Rose et al (1990). Yeast cells were grown at 26°C unless otherwise specified. Yeast transformation was performed by a lithium acetate procedure and yeast transformants were selected as essentially described in Rose et al (1990) with an exception of G418-resistant transformants that were screened as described previously (Wach et al., 1994; Wach 1996). G418 (US Biological) was used at 200 μg/ml, and 5-fluoroorotic acid (5-FOA; US Biological) at 1 mg/ml for incubation at 26°C or at 0.5 mg/ml for incubation at 37°C.

2.2. DNA manipulation

The plasmids used in this study are listed in Table 2.3. DNA fragments were eluted from TAE (40 mM Tris-acetate, 1 mM EDTA [pH8.0]) agarose gel using Geneclean kit II as recommended by the manufacturer (BIO101 Inc.). PCR was performed in standard 30-cycle reaction using high fidelity *pfx* polymerase (Promega) or *Taq* DNA polymerase (NEB).

2.2.1. Epitope tagging of chromosomal genes

Epitopes such as 3x HA, 13x Myc and 1x GFP (S65T) were fused in frame at the C-terminus of target genes by homologous recombination technique as described by Longtine et al (1998). PCR template modules were amplified by a standard 30-cycle PCR reaction using high fidelity *pfx* polymerase and target gene-specific forward and reverse primers. Resulting PCR fragments contained DNA sequences that are homologous to 44 bp upstream and downstream of stop codon of a target gene as well as an epitope tag and a yeast selection marker. PCR fragments purified from TAE agarose gel were

Table 2.1. Yeast strains used in this study.

Name	Features
CCY715-19D	**a** *ade2 ade3-130 his3-Δ200 leu2-3,112 ura3-52 ipl1-2 utp7-1* [*ADE3*, *URA3*, *IPL1*] (i.e., pCC476)
CCY766-9D	**a** *his3-Δ200 leu2-3,112 lys2-801 trp1-1 ura3-52*
CCY1060-1D-1	**a** *ade2 his3-Δ200 leu2-3,112 ura3-52 sli15-3*
CCY1060-1D-1-1	**a** *ade2 his3-Δ200 leu2-3,112 ura3-52 sli15-3-13xMYC::HIS3*
CCY1299-8D	**a** *his3-Δ200 leu2-3,112 lys2-801 trp1-1 ura3-52 UTP7-3xHA::TRP1*
CCY1304-2C	**a** *his3-Δ200 leu2-3,112 lys2-801 trp1-1 ura3-52 UTP7-3xHA::TRP1 ipl1-2*
CCY1305-6D	**a** *ade2 his3-Δ200 leu2-3,112 lys2Δ101::HIS3::lys2Δ102 ura3-52 UTP7-3xHA::TRP1 sli15-3*
CCY1341-1C	**a** *his3-Δ200 leu2-3,112 trp1-1 ura3-52 SLI15-13xMYC::KanMX6*
CCY1365-3D	**a** *his3 leu2-3, 112 lys2-801 trp1-1 ura3-52 UTP7-3xHA::TRP1 ndc10-1*
CCY1398-11B	**a** *his3Δ1 leu2Δ0 lys2Δ0 ura3Δ0 utp7Δ::KanMX6* [*URA3, UTP7*] (i.e., with pCC1000)
CCY1398-12B	**a** *his3Δ1 leu2Δ0 lys2Δ0 ura3Δ0 utp7Δ::KanMX6* [*URA3, UTP7*] (i.e., with pCC1000)
CCY1404-12B	**a** *his3-Δ200 leu2-3,112 lys2-801 trp1-1 ura3-52 bir1Δ::LEU2::HA-BIR1::HIS3*
CCY1473-5B	**a** *his3-Δ200 leu2-3,112 trp1-1 ura3-52 UTP7-3xHA::TRP1 IPL1-13xMYC::HIS3*
CCY1476-19C	**a** *his3-Δ200 leu2-3,112 trp1-1 ura3-52 UTP7-3xHA::TRP1 SLI15-13xMYC::KanMX6*
CCY1739-9A	**a** *his3 leu2 trp1-1 ura3 SLI15-13xMYC::KanMX6 utp7Δ::KanMX6::2x utp7-26::HIS3::LEU2*
CCY1790-6C	**a** *his3 leu2 ura3 utp7Δ::KanMX6::2x utp7-26::HIS3::LEU2*
CCY1804-7C	**a** *his3 leu2 ura3 cdc14-3*
CCY1811-3B	**a** *ade2 his3 leu2 trp1 ura3 SLI15-13xMYC::KanMX6 cdc14-3 utp7Δ::KanMX6::2x utp7-26::HIS3::LEU2*

CCY1811-8A	**a** *his3 leu2 trp1 ura3 SLI15-13xMYC::KanMX6*
CCY1813-3B-1	**a** *his3 leu2 lys2 trp1-1 ura3 CDC14-13xMYC::KanMX6 utp7Δ::KanMX6::2x utp7-26-3xHA::TRP1::HIS3::LEU2*
CCY1821-10D	**a** *his3 leu2 lys2 trp1-1 ura3 bir1Δ::LEU2::HA-BIR1::HIS3 utp7Δ::KanMX6::2x utp7-26::HIS3::LEU2*
CCY1825-2D	**a** *his3 leu2 lys2 ura3 KIP1::URA3::3xMYC-KIP1*
CCY1825-6B	**a** *his3 leu2 lys2 trp1-1 ura3 KIP1::URA3::3xMYC-KIP1 utp7Δ::KanMX6::2x utp7-26::HIS3::LEU2*
CCY1828-6D	**a** *his3 leu2 ura3 CDC14-13xMYC::KanMX6 UTP7-3xHA::TRP1*
CCY1829-18D	**a** *his3 leu2 lys2 trp1 ura3 NOP1-3xHA::KanMX6 CDC14-13xMYC::KanMX6*
CCY1829-34A	**a** *his3 leu2 lys2 trp1 ura3 NOP1-3xHA::KanMX6 CDC14-13xMYC::KanMX6 utp7Δ::KanMX6::2x utp7-26::HIS3::LEU2*
CCY1830-3B	**a** *his3 leu2 trp1-1 ura3 UTP7-3xHA::TRP1*
CCY1830-3D	**a** *ade2-1 his3 leu2 trp1-1 ura3 UTP7-3xHA::TRP1 NET1-TEV-9xMYC::HIS3*
CCY1831-12B	**a** *his3 leu2 trp1-1 ura3 utp7Δ::KanMX6::2X utp7-26-3xHA::TRP1::HIS3::LEU2*
CCY1834-1C	**a** *his3 leu2 lys2 ura3 trp1 CTF19-HA::KanMX*
CCY1834-4B	**a** *his3 leu2 ura3 CTF19-HA::KanMX utp7Δ::KanMX6::2x utp7-26::HIS3::LEU2*
CCY1836-1B	**a** *his3 leu2 ura3 KIP1::URA3::3xMYC-KIP1 sli15-3*
CCY1841-3D	**a** *his3 leu2 lys2 trp1 ura3 NOP1-3xHA::KanMX6 NET1-TEV-9xMYC::HIS3 utp7Δ::KanMX6::2x utp7-26::HIS3::LEU2*
CCY1841-5B	**a** *his3 leu2 trp1 ura3 NET1-TEV-9xMYC::HIS3*
CCY1841-10A	**a** *his3 leu2 trp1 ura3 NET1-TEV-9xMYC::HIS3 utp7Δ::KanMX6::2x utp7-26::HIS3::LEU2*
CCY1841-12A	**a** *his3 leu2 lys2 trp1 ura3 NOP1-3xHA::KanMX6 NET1-TEV-9xMYC::HIS3*
CCY1841-16A	**a** *his3 leu2 trp1 ura3*

CCY1841-21D	**a** *his3 leu2 trp1 ura3 utp7Δ::KanMX6::2x utp7-26::HIS3::LEU2*
CCY1844-4C	**a** *his3 ura3 leu2::TetR-GFP::LEU2 SPC110-RFP::KanMX6 1.4kb left of CEN5::TetO 2x112::HIS3*
CCY1844-9C	**a** *his3 ura3 leu2::TetR-GFP::LEU2 SPC110-RFP::KanMX6 1.4kb left of CEN5::TetO 2x112::HIS3 utp7Δ::KanMX6::2x utp7-26::HIS3::LEU2*
CCY1847-2B	**a** *his3 leu2 ura3*
CCY1847-2D	**a** *his3 leu2 ura3 cdc14-3 utp7Δ::KanMX6::2x utp7-26::HIS3::LEU2*
CCY1848-2D	**a** *ade2 his3 leu2 ura3 CTF19-HA::KanMX sli15-3*

Most of the strains were constructed specifically for this study with the following exceptions:
Strains CCY715-19D, CCY766-9D, CCY1060-1D-1 and CCY1404-12B are from C. Chan's laboratory collection.

Table 2.2. Yeast strains that contain Ts$^-$ *utp7* alleles.

Name	Features
CCY1398-11B with pCC863	**a** *his3Δ1 leu2Δ0 ura3Δ0 lys2Δ0 utp7Δ*:: *KanMX6* containing pCC863 [*UTP7, LEU2, CEN*]
CCY1398-11B with pCC1751	Same as 1398-11B but with pCC1751 [*utp7-10, LEU2, CEN*]
CCY1398-11B with pCC1752	Same as 1398-11B but with pCC1752 [*utp7-11, LEU2, CEN*]
CCY1398-11B with pCC1753	Same as 1398-11B but with pCC1753 [*utp7-12, LEU2, CEN*]
CCY1398-11B with pCC1754	Same as 1398-11B but with pCC1754 [*utp7-13, LEU2, CEN*]
CCY1398-11B with pCC1755	Same as 1398-11B but with pCC1755 [*utp7-14, LEU2, CEN*]
CCY1398-11B with pCC1756	Same as 1398-11B but with pCC1756 [*utp7-15, LEU2, CEN*]
CCY1398-11B with pCC1757	Same as 1398-11B but with pCC1757 [*utp7-16, LEU2, CEN*]
CCY1398-11B with pCC1758	Same as 1398-11B but with pCC1758 [*utp7-17, LEU2, CEN*]
CCY1398-11B with pCC1759	Same as 1398-11B but with pCC1759 [*utp7-18, LEU2, CEN*]
CCY1398-11B with pCC1760	Same as 1398-11B but with pCC1760 [*utp7-19, LEU2, CEN*]
CCY1398-11B with pCC1761	Same as 1398-11B but with pCC1761 [*utp7-20, LEU2, CEN*]
CCY1398-11B with pCC1762	Same as 1398-11B but with pCC1762 [*utp7-21, LEU2, CEN*]
CCY1398-11B with pCC1763	Same as 1398-11B but with pCC1763 [*utp7-22, LEU2, CEN*]
CCY1398-11B with pCC1764	Same as 1398-11B but with pCC1764 [*utp7-23, LEU2, CEN*]
CCY1398-11B with pCC1765	Same as 1398-11B but with pCC1765 [*utp7-24, LEU2, CEN*]
CCY1398-11B with pCC1766	Same as 1398-11B but with pCC1766 [*utp7-25, LEU2, CEN*]
CCY1398-11B with pCC1767	Same as 1398-11B but with pCC1767 [*utp7-26, LEU2, CEN*]
CCY1398-11B with pCC1768	Same as 1398-11B but with pCC1768 [*utp7-27, LEU2, CEN*]
CCY1398-11B with pCC1769	Same as 1398-11B but with pCC1769 [*utp7-28, LEU2, CEN*]
CCY1398-11B with pCC1770	Same as 1398-11B but with pCC1770 [*utp7-29, LEU2, CEN*]
CCY1398-11B with pCC1771	Same as 1398-11B but with pCC1771 [*utp7-30, LEU2, CEN*]

CCY1398-11B with pCC1772	Same as 1398-11B but with pCC1772 [*utp7-31, LEU2, CEN*]
CCY1398-11B with pCC1773	Same as 1398-11B but with pCC1773 [*utp7-32, LEU2, CEN*]
CCY1398-11B with pCC1774	Same as 1398-11B but with pCC1774 [*utp7-33, LEU2, CEN*]
CCY1398-11B with pCC1775	Same as 1398-11B but with pCC1775 [*utp7-34, LEU2, CEN*]
CCY1398-12B-1	α *his3Δ1 leu2Δ0 ura3Δ0 lys2Δ0 utp7Δ::Kan^r::utp7-10::LEU2*
CCY1398-12B-2	α *his3Δ1 leu2Δ0 ura3Δ0 lys2Δ0 utp7Δ::Kan^r::utp7-11::LEU2*
CCY1398-12B-3	α *his3Δ1 leu2Δ0 ura3Δ0 lys2Δ0 utp7Δ::Kan^r::utp7-12::LEU2*
CCY1398-12B-4	α *his3Δ1 leu2Δ0 ura3Δ0 lys2Δ0 utp7Δ::Kan^r::utp7-13::LEU2*
CCY1398-12B-5	α *his3Δ1 leu2Δ0 ura3Δ0 lys2Δ0 utp7Δ::Kan^r::utp7-14::LEU2*
CCY1398-12B-6	α *his3Δ1 leu2Δ0 ura3Δ0 lys2Δ0 utp7Δ::Kan^r::utp7-15::LEU2*
CCY1398-12B-7	α *his3Δ1 leu2Δ0 ura3Δ0 lys2Δ0 utp7Δ::Kan^r::utp7-16::LEU2*
CCY1398-12B-8	α *his3Δ1 leu2Δ0 ura3Δ0 lys2Δ0 utp7Δ::Kan^r::utp7-17::LEU2*
CCY1398-12B-9	α *his3Δ1 leu2Δ0 ura3Δ0 lys2Δ0 utp7Δ::Kan^r::utp7-18::LEU2*
CCY1398-12B-10	α *his3Δ1 leu2Δ0 ura3Δ0 lys2Δ0 utp7Δ::Kan^r::utp7-19::LEU2*
CCY1398-12B-11	α *his3Δ1 leu2Δ0 ura3Δ0 lys2Δ0 utp7Δ::Kan^r::utp7-20::LEU2*
CCY1398-12B-12	α *his3Δ1 leu2Δ0 ura3Δ0 lys2Δ0 utp7Δ::Kan^r::utp7-21::LEU2*
CCY1398-12B-13	α *his3Δ1 leu2Δ0 ura3Δ0 lys2Δ0 utp7Δ::Kan^r::utp7-22::LEU2*
CCY1398-12B-14	α *his3Δ1 leu2Δ0 ura3Δ0 lys2Δ0 utp7Δ::Kan^r::utp7-23::LEU2*
CCY1398-12B-15	α *his3Δ1 leu2Δ0 ura3Δ0 lys2Δ0 utp7Δ::Kan^r::utp7-24::LEU2*
CCY1398-12B-16	α *his3Δ1 leu2Δ0 ura3Δ0 lys2Δ0 utp7Δ::Kan^r::utp7-25::LEU2*
CCY1398-12B-17	α *his3Δ1 leu2Δ0 ura3Δ0 lys2Δ0 utp7Δ::Kan^r::utp7-26::LEU2*
CCY1398-12B-18	α *his3Δ1 leu2Δ0 ura3Δ0 lys2Δ0 utp7Δ::Kan^r::utp7-27::LEU2*
CCY1398-12B-19	α *his3Δ1 leu2Δ0 ura3Δ0 lys2Δ0 utp7Δ::Kan^r::utp7-28::LEU2*

CCY1398-12B-20	α *his3Δ1 leu2Δ0 ura3Δ0 lys2Δ0 utp7Δ::Kan^r::utp7-29::LEU2*
CCY1398-12B-21	α *his3Δ1 leu2Δ0 ura3Δ0 lys2Δ0 utp7Δ::Kan^r::utp7-30::LEU2*
CCY1398-12B-22	α *his3Δ1 leu2Δ0 ura3Δ0 lys2Δ0 utp7Δ::Kan^r::utp7-31::LEU2*
CCY1398-12B-23	α *his3Δ1 leu2Δ0 ura3Δ0 lys2Δ0 utp7Δ::Kan^r::utp7-32::LEU2*
CCY1398-12B-24	α *his3Δ1 leu2Δ0 ura3Δ0 lys2Δ0 utp7Δ::Kan^r::utp7-33::LEU2*
CCY1398-12B-25	α *his3Δ1 leu2Δ0 ura3Δ0 lys2Δ0 utp7Δ::Kan^r::utp7-34::LEU2*
CCY1398-12B-26	α *his3Δ1 leu2Δ0 ura3Δ0 lys2Δ0 utp7Δ::Kan^r::UTP7::LEU2*
CCY1398-12B-27	α *his3Δ1 leu2Δ0 ura3Δ0 lys2Δ0 utp7Δ::Kan^r::UTP7::LEU2*
CCY1398-11B-1	**a** *his3Δ1::UTP7::HIS3 leu2Δ0 ura3Δ0 lys2Δ0 utp7Δ::Kan^r*
CCY1398-11B-2	**a** *his3Δ1::utp7-10:: HIS3 leu2Δ0 ura3Δ0 lys2Δ0 utp7Δ::Kan^r*
CCY1398-11B-3	**a** *his3Δ1::utp7-11::HIS3 leu2Δ0 ura3Δ0 lys2Δ0 utp7Δ::Kan^r*
CCY1398-11B-4	**a** *his3Δ1::utp7-13::HIS3 leu2Δ0 ura3Δ0 lys2Δ0 utp7Δ::Kan^r*
CCY1398-11B-5	**a** *his3Δ1::utp7-14::HIS3 leu2Δ0 ura3Δ0 lys2Δ0 utp7Δ::Kan^r*
CCY1398-11B-6	**a** *his3Δ1::utp7-15::HIS3 leu2Δ0 ura3Δ0 lys2Δ0 utp7Δ::Kan^r*
CCY1398-11B-7	**a** *his3Δ1::utp7-16::HIS3 leu2Δ0 ura3Δ0 lys2Δ0 utp7Δ::Kan^r*
CCY1398-11B-8	**a** *his3Δ1::utp7-17::HIS3 leu2Δ0 ura3Δ0 lys2Δ0 utp7Δ::Kan^r*
CCY1398-11B-9	**a** *his3Δ1::utp7-18::HIS3 leu2Δ0 ura3Δ0 lys2Δ0 utp7Δ::Kan^r*
CCY1398-11B-10	**a** *his3Δ1::utp7-20::HIS3 leu2Δ0 ura3Δ0 lys2Δ0 utp7Δ::Kan^r*
CCY1398-11B-11	**a** *his3Δ1::utp7-21::HIS3 leu2Δ0 ura3Δ0 lys2Δ0 utp7Δ::Kan^r*
CCY1398-11B-12	**a** *his3Δ1::utp7-22::HIS3 leu2Δ0 ura3Δ0 lys2Δ0 utp7Δ::Kan^r*
CCY1398-11B-13	**a** *his3Δ1::utp7-23::HIS3 leu2Δ0 ura3Δ0 lys2Δ0 utp7Δ::Kan^r*
CCY1398-11B-14	**a** *his3Δ1::utp7-24::HIS3 leu2Δ0 ura3Δ0 lys2Δ0 utp7Δ::Kan^r*
CCY1398-11B-15	**a** *his3Δ1::utp7-25::HIS3 leu2Δ0 ura3Δ0 lys2Δ0 utp7Δ::Kan^r*
CCY1398-11B-16	**a** *his3Δ1::utp7-26::HIS3 leu2Δ0 ura3Δ0 lys2Δ0 utp7Δ::Kan^r*

CCY1398-11B-17	**a** *his3Δ1::utp7-27::HIS3 leu2Δ0 ura3Δ0 lys2Δ0 utp7Δ::Kan^r*
CCY1398-11B-18	**a** *his3Δ1::utp7-29::HIS3 leu2Δ0 ura3Δ0 lys2Δ0 utp7Δ::Kan^r*
CCY1398-11B-19	**a** *his3Δ1::utp7-30::HIS3 leu2Δ0 ura3Δ0 lys2Δ0 utp7Δ::Kan^r*
CCY1398-11B-20	**a** *his3Δ1::utp7-31::HIS3 leu2Δ0 ura3Δ0 lys2Δ0 utp7Δ::Kan^r*
CCY1398-11B-21	**a** *his3Δ1::utp7-32::HIS3 leu2Δ0 ura3Δ0 lys2Δ0 utp7Δ::Kan^r*
CCY1398-11B-22	**a** *his3Δ1::utp7-33::HIS3 leu2Δ0 ura3Δ0 lys2Δ0 utp7Δ::Kan^r*
CCY1398-11B-23	**a** *his3Δ1::utp7-34::HIS3 leu2Δ0 ura3Δ0 lys2Δ0 utp7Δ::Kan^r*
CCY1488-5A-1	**α** *his3Δ1::UTP7::HIS3 leu2 ura3 lys2 utp7Δ::Kan^r::UTP7::LEU2*
CCY1398-12B-5-1	**α** *his3Δ1::utp7-14::HIS3 leu2Δ0 ura3Δ0 lys2Δ0 utp7Δ::Kan^r::utp7-14::LEU2*
CCY1398-12B-8-1	**α** *his3Δ1::utp7-17::HIS3 leu2Δ0 ura3Δ0 lys2Δ0 utp7Δ::Kan^r::utp7-17::LEU2*
CCY1398-12B-17-1	**α** *his3Δ1 leu2Δ0 ura3Δ0 lys2Δ0 utp7Δ::Kan^r*::2X *utp7-26::HIS3::LEU2*
CCY1687-8B-1	**α** *his3Δ1::utp7-29::HIS3 leu2 ura3 lys2 utp7Δ::Kan^r::utp7-29::LEU2*
CCY1681-4A-1	**α** *his3Δ1::utp7-30::HIS3 leu2 ura3 lys2 utp7Δ::Kan^r::utp7-30::LEU2*
CCY1689-3A-1	**α** *his3Δ1::utp7-32::HIS3 leu2 ura3 lys2 utp7Δ::Kan^r::utp7-32::LEU2*
CCY1690-8D-1	**α** *his3Δ1::utp7-34::HIS3 leu2 ura3 lys2 utp7Δ::Kan^r::utp7-34::LEU2*

All of the strains were constructed specifically for this study.

transformed into appropriate yeast strains and transformants that resulted from integration of PCR fragment into the genomic locus by homologous recombination were selected as described in section 2.1. The integration was validated by band shift in Western blot and/or genomic DNA PCR.

2.3. Construction of the temperature-sensitive *utp7-26* mutant allele

Mutagenesis of *UTP7* was carried out by *in vitro* PCR and *in vivo* gapped-repair as described (Muhlrad, 1992). In brief, T3 and T7 primers (Promega) were used in a standard 30-cycle PCR reaction with *Taq* DNA polymerase (Promega) to amplify the *UTP7* gene present on the *LEU2*-CEN-plasmid pCC863. Approximately 0.5 µg of the ~3.6-kb PCR product and ~0.1 µg of the ~7.5-kb *Bgl*II-*Xba*I fragment of unmutagenized pCC863 were used to transform the yeast strain CCY1398-11B, which contained *UTP7* on a *URA3*-CEN-plasmid (pCC1000) as the only source of *UTP7*. Leu^+ Ura^+ transformants were selected at 26°C on supplemented SD medium. Transformants were tested for their ability to grow at 26 and 37°C on supplemented SD medium lacking leucine but containing uracil and 5-FOA (1 g/L for 26°C and 0.5 g/L for 37°C). Transformant colonies that could grow on 5-FOA plates at 26 but not 37°C were chosen. After colony purification by streaking, such Leu^+ Ura^+ transformants were retested for their differential sensitivity to 5-FOA at 37 but not 26°C. The *LEU2*-plasmids were recovered from 5-FOA-sensitive transformants into *E. coli*. The ability of each plasmid to support growth of CCY1398-12B (which contained *UTP7* on a *URA3*-CEN-plasmid (pCC1000) as the only source of *UTP7*) on 5-FOA plates at 26 and 37°C was retested. Cells from 26°C FOA plate were then tested for temperature-sensitivity at 37C on YEPD. From ~60,000 Leu^+ Ura^+ transformants screened, 25 plasmids (Table 1.3) containing temperature-sensitive *utp7* alleles (*utp7-10* to *utp7-34*) were isolated.

Preliminary cytological studies of these *utp7* mutants that had plasmid-borne *utp7* allele indicated two major phenotypes after 3 h at 37°C: enrichment of unbudded cells or large-budded cells with a short mitotic spindle that was suggestive of mitotic spindle

Table 2.3. Plasmids used in this study.

Name	Features
pRS303	*A*mp^R *HIS3*
pRS305	*A*mp^R *LEU2*
pCC476	*Amp*^{R} 2m *ADE3 URA3 IPL1*
pCC863	*Amp*^{R} *LEU2* CEN6 ARSH4 *UTP7*
pCC1000	*Amp*^{R} *URA3* CEN ARS *UTP7*
pCC1751	*A*mp^R *LEU2* CEN6 ARSH4 f1 ori *utp7-10*
pCC1752	*A*mp^R *LEU2* CEN6 ARSH4 f1 ori *utp7-11*
pCC1753	*A*mp^R *LEU2* CEN6 ARSH4 f1 ori *utp7-12*
pCC1754	*A*mp^R *LEU2* CEN6 ARSH4 f1 ori *utp7-13*
pCC1755	*A*mp^R *LEU2* CEN6 ARSH4 f1 ori *utp7-14*
pCC1756	*A*mp^R *LEU2* CEN6 ARSH4 f1 ori *utp7-15*
pCC1757	*A*mp^R *LEU2* CEN6 ARSH4 f1 ori *utp7-16*
pCC1758	*A*mp^R *LEU2* CEN6 ARSH4 f1 ori *utp7-17*
pCC1759	*A*mp^R *LEU2* CEN6 ARSH4 f1 ori *utp7-18*
pCC1760	*A*mp^R *LEU2* CEN6 ARSH4 f1 ori *utp7-19*
pCC1761	*A*mp^R *LEU2* CEN6 ARSH4 f1 ori *utp7-20*
pCC1762	*A*mp^R *LEU2* CEN6 ARSH4 f1 ori *utp7-21*
pCC1763	*A*mp^R *LEU2* CEN6 ARSH4 f1 ori *utp7-22*
pCC1764	*A*mp^R *LEU2* CEN6 ARSH4 f1 ori *utp7-23*
pCC1765	*A*mp^R *LEU2* CEN6 ARSH4 f1 ori *utp7-24*
pCC1766	*A*mp^R *LEU2* CEN6 ARSH4 f1 ori *utp7-25*
pCC1767	*A*mp^R *LEU2* CEN6 ARSH4 f1 ori *utp7-26*

pCC1768	*A*mp^R *LEU2* CEN6 ARSH4 f1 ori *utp7-27*
pCC1769	*A*mp^R*LEU2* CEN6 ARSH4 f1 ori *utp7-28*
pCC1770	*A*mp^R *LEU2* CEN6 ARSH4 f1 ori *utp7-29*
pCC1771	*A*mp^R *LEU2* CEN6 ARSH4 f1 ori *utp7-30*
pCC1772	*A*mp^R *LEU2* CEN6 ARSH4 f1 ori *utp7-31*
pCC1773	*A*mp^R *LEU2* CEN6 ARSH4 f1 ori *utp7-32*
pCC1774	*A*mp^R *LEU2* CEN6 ARSH4 f1 ori *utp7-33*
pCC1775	*A*mp^R *LEU2* CEN6 ARSH4 f1 ori *utp7-34*
pCC1776	*A*mp^R *LEU2* f1 ori *utp7-10*
pCC1777	*A*mp^R *LEU2* f1 ori *utp7-11*
pCC1778	*A*mp^R *LEU2* f1 ori *utp7-12*
pCC1779	*A*mp^R *LEU2* f1 ori *utp7-13*
pCC1780	*A*mp^R *LEU2* f1 ori *utp7-14*
pCC1781	*A*mp^R *LEU2* f1 ori *utp7-15*
pCC1782	*A*amp^R *LEU2* f1 ori *utp7-16*
pCC1783	*A*mP^R *LEU2* f1 ori *utp7-17*
pCC1784	*A*mp^R *LEU2* f1 ori *utp7-18*
pCC1785	*A*mp^R *LEU2* f1 ori *utp7-19*
pCC1786	*A*mp^R *LEU2* f1 ori *utp7-20*
pCC1787	*A*mp^R *LEU2* f1 ori *utp7-21*
pCC1788	*A*mp^R *LEU2* f1 ori *utp7-22*
pCC1789	*A*mp^R *LEU2* f1 ori *utp7-23*
pCC1790	*A*mp^R *LEU2* f1 ori *utp7-24*
pCC1791	*A*mp^R *LEU2* f1 ori *utp7-25*

pCC1792	*A*mp^R *LEU2* f1 ori *utp7-26*
pCC1793	*A*mp^R *LEU2* f1 ori *utp7-27*
pCC1794	*A*mp^R *LEU2* f1 ori *utp7-28*
pCC1795	*A*mp^R *LEU2* f1 ori *utp7-29*
pCC1796	*A*mp^R *LEU2* f1 ori *utp7-30*
pCC1797	*A*mp^R *LEU2* f1 ori *utp7-31*
pCC1798	*A*mp^R *LEU2* f1 ori *utp7-32*
pCC1799	*A*mp^R *LEU2* f1 ori *utp7-33*
pCC1800	*A*mp^R *LEU2* f1 ori *utp7-34*
pCC1781	*A*mp^R *LEU2* f1 ori *UTP7*
pCC1782	*A*mp^R *LEU2* f1 ori *UTP7*
pCC1840	*A*mp^R *HIS3* f1 ori *UTP7*
pCC1841	*A*mp^R *HIS3* f1 ori *utp7-10*
pCC1842	*A*mp^R *HIS3* f1 ori *utp7-11*
pCC1843	*A*mp^R *HIS3* f1 ori *utp7-13*
pCC1844	*A*mp^R *HIS3* f1 ori *utp7-14*
pCC1845	*A*mp^R *HIS3* f1 ori *utp7-15*
pCC1846	*A*mp^R *HIS3* f1 ori *utp7-16*
pCC1847	*A*mp^R *HIS3* f1 ori *utp7-17*
pCC1848	*A*mp^R *HIS3* f1 ori *utp7-18*
pCC1849	*A*mp^R *HIS3* f1 ori *utp7-20*
pCC1850	*A*mp^R *HIS3* f1 ori *utp7-21*
pCC1851	*A*mp^R *HIS3* f1 ori *utp7-22*
pCC1852	*A*mp^R *HIS3* f1 ori *utp7-23*
pCC1853	*A*mp^R *HIS3* f1 ori *utp7-24*

pCC1854	*A*mp^R *HIS3* f1 ori *utp7-25*
pCC1855	*A*mp^R *HIS3* f1 ori *utp7-26*
pCC1856	*A*mp^R *HIS3* f1 ori *utp7-27*
pCC1857	*A*mp^R *HIS3* f1 ori *utp7-29*
pCC1858	*A*mp^R *HIS3* f1 ori *utp7-30*
pCC1859	*A*mp^R *HIS3* f1 ori *utp7-31*
pCC1860	*A*mp^R *HIS3* f1 ori *utp7-32*
pCC1861	*A*mp^R *HIS3* f1 ori *utp7-33*
pCC1862	*A*mp^R *HIS3* f1 ori *utp7-34*

Most of the plasmids were constructed specifically for this study with the following exceptions: Plasmids pRS303, pRS305, pCC476, pCC863 and pCC1000 are from C. Chan's laboratory collection.

assembly checkpoint activation, with different mutants exhibiting one or both of these phenotypes. To integrate each *utp7* mutant allele into the chromosome, I cloned the ~3.5-kb *Sac*I/*Bam*HI fragment that contains each mutant allele into the *Sac*I/*Bam*HI sites of the integrating *LEU2*-plasmid pRS305. The resulting plasmid was linearized at the unique *Sph*I site and used to transform CCY1398-12B, resulting in the integration of the *utp7* mutant allele downstream of the *utp7-Δ* locus on the chromosome. To my surprise, mutants containing a single copy of chromosomally integrated *utp7* as the only source of *UTP7* either had no observable cytological phenotype or were arrested mostly as unbudded cells after 3 h at 37°C. I reasoned that the difference in phenotype between cells with CEN-plasmid-borne and chromosomally integrated *utp7* mutant alleles might have to do with differences in the copy number of the *utp7* mutant allele. The copy number of CEN-plasmids in yeast can be over 5 (Futcher, 1986). Thus, I cloned a subset (*utp7-14, -17, -20, -26, -29, -30, -32, and -34*) of the *utp7* alleles into the *Xba*I/*Bam*HI sites of the *HIS3* integrating plasmid pRS303. The resulting plasmid was linearized by *Bss*HII and used to integrate a second copy of *utp7* onto the chromosome. One such doubly integrated mutant (*utp7-26*) exhibited a strong chromosome missegregation phenotype and is the subject of this study.

2.4. Recovery of plasmids from yeast

Yeast cells were collected from 0.5 ml overnight liquid culture or from half a frog spot on agar plate. 200 μl of STES (1% SDS, 0.2μ Tris-HCl [pH7.5], 10 mM EDTA, 0.5 M NaCl) were added to the cell pellets and acid-washed glass beads (425-600 microns; Sigma) were added to right below liquid surface. Cells were lysed using a multi-tube vortexer for 2 min with the maximum speed set at 10. Cell extract was extracted with same volume of phenol:chloroform and then chloroform:isoamyl alcohol. In each step, reagents were mixed well by 1-min-vortexing that was followed by centrifugation at 14,000 rpm for 10 min. Supernatant was recovered and EtOH-precipitated. Resulting nucleic acid pellet was dissolved in 20 μl of 10mM Tris-HCl [pH7.5] and 5 μl of nucleic acid solution was immediately transformed into *E.coli* DH5α.

2.5. High efficiency *E. coli* transformation

Here I describe a procedure to prepare *E.coli* competent cells that gives very high efficiency of plasmid transformation. This protocol is from Inoue et al (1990). I usually achieve ~ 5 x 10^8 cfu/μg plasmid DNA when DH5α cells are prepared by this method. This protocol might be considered when very rare DNA needs to be dealt with: when DNA libraries need to be constructed or amplified, or when one encounters problem in *E.coli* transformation due to very low amount of transforming plasmids. The major characteristic of this method is to grow *E.coli* at lower temperature, 18°C, to prepare competent cells.

Growth media such as LB (Luria broth) liquid medium and LB agar with or without ampicillin (50 μg/ml for liquid medium or at 100 μg/ml for agar) can be prepared as described in general lab protocols. TB is composed of 10 mM Pipes, 55 mM $MnCl_2$, 15 mM $CaCl_2$, 250 mM KCl. To make TB, all the reagents except $MnCl_2$ are mixed in ddH_2O and the pH is adjusted to 6.7 with KOH. Then, $MnCl_2$ is added otherwise it will not go into solution. The resulting TB solution is sterilized by filtration through a 0.45 μm filter unit and stored at 4°C as aliquots.

DH5α from frozen stock is streaked on LB agar and incubated for about 1 day at 37°C. One large colony is inoculated into 5 ml LB medium and incubated at 18°C for 1 day. The whole 5 ml culture is added to 45 ml LB medium and further incubated at 18°C until cell density reaches 0.3~0.4 at A_{600}. It may take 2 days to reach a proper cell density from the initial inoculation: If start culture was incubated at 37°C and then diluted and incubated 18°C, it might lower transformation efficiency by about 10 fold. The cell culture is removed from 18°C and placed on ice for 10 min. The culture is transferred to pre-chilled centrifugation tube and spun down by centrifugation at 4,000 rpm for 10 min at 4°C. The cell pellet is gently resuspended in 16 ml of ice-cold TB, incubated on ice for 10 min, and spun down as above. The cell pellet is gently resuspended in 3.72 ml of ice-cold TB. 0.28 ml of DMSO (i.e., to the final concentration of 7 %) is then added with gentle swirling of cell suspension. The cells are further incubated on ice for 10 min and

200 µl-aliquots are transferred into pre-chilled 1.5 ml Eppendorf tubes. The competent cells can be immediately used for plasmid transformation or they can be chilled by liquid N_2 and kept frozen at -80°C. 50 ml of cell culture will give rise to 20 transformations and the volume of cell culture and reagents can be proportionally adjusted when necessary.

For transformation, 200 µl of competent cells is thawed on ice, and plasmid solution (usually not exceeding 10 % of the volume of competent cells) is added. The cells are incubated on ice for 30 min followed by heat shock at 42°C for 1.5 min. The tube is transferred to ice and 0.3 ml of LB medium is added. The cells are incubated at 37°C for 45 min, plated on LB agar with 100 µg/ml ampicillin, and incubated overnight at 37°C.

2.6. Cell synchrony

Cell synchrony experiments were performed as essentially described by Burk et al (2000).

2.6.1. α-factor

MATa cells are arrested at START of G1 in the cell cycle by using α-factor. All the strains that I used for α-factor arrest experiments contained wild type *BAR1* gene, which encodes a protease that is secreted out of cells and destroys α-factor. This activity could be somewhat avoided if cell number in culture is low, which might be only useful for experiments that need a small number of cells. Since I needed large number of pre-synchronized cells that would be subsequently released and allowed to enter cell cycle, this approach seemed not useful. Since the protease activity of Bar1 could be partially suppressed at acidic pH, I grew cells in acidic YEPD (pH 3.5; adjusted with HCl). Using this method I usually achieved around 98% arrest. α-factor (custom made) stock was made at 10 mg/ml in 100% ethanol and kept at -20°C. Overnight culture of yeast cells in regular (i.e., not acidic) YEPD was washed once with sterile ddH_2O, once with acidic YEPD, diluted in acidic YEPD to $O.D._{600}$ of ~ 0.1, and then allowed to grow for about 4 h. When $O.D._{600}$ has reached 0.2–0.3, α-factor was added to the final concentration of 10

μg/ml and incubation was continued for 1.5-2 h. When necessary, α-factor was added to the additional final concentration of 5 μg/ml 1 h after the first addition, and incubation was continued for one more hour. To release cells from the arrest, cells were washed once with sterile ddH_2O, once with regular YEPD, and then cells were resuspended and theincubated in regular YEPD.

2.6.2. Hydroxyurea

Hydroxyurea is a drug that inhibits the enzymatic activity of ribonucleotide synthetase. Upon treatment, cells suffer from diminished pool of dNTPs and cannot finish DNA replication, leading to cell cycle arrest in S phase. Overnight culture of yeast cells was diluted in fresh medium and incubated for at least two generation. Powder of Hydroxyurea (Sigma) was added directly into actively growing cell culture to give the final concentration of 0.2μ. When temperature shift was required, culture was split after 1-h incubation at 26°C in the presence of hydroxyurea, Half of it was shifted to 37°C for 2 h while the other half stayed at 26°C as a control. I usually achieved 80–90 % arrest as judged by counting large-budded cells. Indirect tubulin immunofluorescence staining revealed that most of these cells contained undivided DAPI and short spindle.

2.6.3. Nocodazole

Nocodazole is a microtubule-destabilizing drug. Cells in the presence of nocodazole cannot complete mitosis and arrest cell cycle at pre-anaphase. The nocodazole (Sigma) stock was made at 1.5 mg/ml in DMSO and stored at -20°C. Overnight culture of yeast cells was diluted to fresh medium and incubated for at 2-3 generations. Nocodazole stock was diluted 100-fold into the cell culture to give final contration of 15 μg/ml. When needed, cell culture was immediately shifted to 37°C for 2-3 h. Typically, ~ 85 % of cells become arrested as large-budded cells. Treated cells showed no microtubule staining and if any, contained dot(s) at the periphery of DAPI-stained area, most likely microtubule patches that might be less accessible by nocodazole due to their close proximity to spindle pole bodies.

2.7. Cytological Techniques

All the images were collected through a Zeiss Axioscope (Carl Zeiss) with a MicroMax CCD camera (Princeton Instruments) using IPLab spectrum 3.1.1 software (Scanalytics Inc.).

2.7.1. Imaging GFP and RFP fusion proteins

To stain DNA in live cells, DAPI (4', 6'-diamidino-2-phenylindole; Accurate Chemical Co.) was directly added to cell culture to give final conentration of 1-5 μg/ml 15-20 min prior to microscopy. Stained cells were collected by brief centrifugation and resuspended in PBS (40 mM K_2HPO4, 10 mM KH_2PO4, 0.15 M NaCl) to remove excessive DAPI from media and to minimize background. For colocalization of Utp7-GFP and Nop1-RFP, actively growing cells ($O.D._{600}$ E 0.5) were fixed with ice-cold 100% ethanol for several seconds, washed twice with PBS and then subjected to DAPI staining at the final concentration of 1 μg/ml for 5-10 min. For orientation of old and new spindle pole body in wild type and *utp7-26* cells expressing Spc110-RFP (N1T1), cells were arrested at G1 by α-factor treatment, released in fresh medium and concomitantly shifted to 37°C. 80 min after release and temperature shift, cells were collected, fixed with 5% formaldehyde for 10 min at room temperature, washed once with PBS and stained with DAPI at 1 μg/ml for 5 min.

To test if kinetochores are bioriented and under tension in wild type and various mutant cells expressing Spc110-RFP as a spindle pole marker and TetR-GFP that binds to tandem array of TetO sites located 1.4-kb away from CEN5, cells in early log phase were shifted to 37°C for 3 h, fixed with 5% formaldehyde at room temperature for 10 min, washed once with PBS and stained with DAPI at 1 μg/ml for 5 min.

To study sister chromatid separation, wild-type and various mutant cells were genetically manipulated in such a way that they expressed TetR-GFP that binds to tandem arrays of TetO sites located 35-kb away from CEN5. Cells in early log phase

were shifted to 37°C for 3 h, fixed with 5% formaldehyde at room temperature for 10 min, washed once with PBS and stained with DAPI at 1 μg/ml for 5 min.

2.7.2. Indirect Immunofluorescence staining

Indirect immunostaining was performed as described by Pringle et al (1989). For indirect tubulin immunofluorescence staining, Rat YOL1/34 (Serotec) that recognizes yeast α-tubulin was used at 1:250 dilution. Goat FITC-conjugated anti-rat sIgG (Cappel) was used at 1:200 dilution to recognize YOL1/34 antibodies. Antibodies used in co-staining are listed in Table 2.4.

Table 2.4. Antibodies used in indirect immunofluorescence co-staining and chromatin spread.

Co-stain	Primary antibodies		Secondary antibodies	
	Description	Dilution	Description	Dilution
Sli15-Myc or Ipl1-Myc	c-myc 9E10 (mouse, ascites fluid)	1:500	FITC-conjugated anti-mouse IgG (goat, affinity purified)	1:200
Tubulin	YOL1/34 (rat, affinity purified)	1:250	rhodamin-conjugated anti-rat IgG (goat, affinity purified)	1:200
Cdc14-Myc or Net1-Myc	c-myc 9E10 (mouse, ascites fluid)	1:500	FITC-conjugated anti-mouse IgG (goat, affinity purified)	1:200
Nop1-HA	HA 3F10 (rat, monoclonal)	1:200	rhodamin-conjugated anti-rat IgG (goat, affinity purified)	1:200
Chromosome spread	Primary antibodies	Dilution	Secondary antibodies	Dilution
Scc1-HA	α-HA (mouse, ascites fluid)	1:500	FITC-conjugated anti-mouse IgG (goat, affinity purified)	1:200

Sources of antibodies:
c-myc 9E10 and α-HA antibodies were purchased from Covance; FITC-conjugated anti-mouse IgG and rhodamin-conjugated anti-rat IgG from Cappel; HA 3F10 from Boehringer Mannheim.

2.7.3. Chromatin spreads

10ml of yeast cells that have grown in appropriate condition to the cell density of ~ 0.5 (i.e. equivalent to 5 $O.D._{600}$) were harvested by centrifugation at 4,000 rpm for 3 min, washed once with 5 ml of spheroplasting solution (1.2 M sorbitol, 0.1 M KPO_4 [pH 7.0]), and resuspended in 0.5 ml of spheroplasting solution in a 1.5 ml Eppendorf tube: One may keep these cells on ice if more samples are to be collected as in a time course experiment. The next spheroplasting step is critical to success of the experiment. Poor spheroplasting would likely cause failure in attachment of cells onto glass slide as well as lysis of cell membrane, resulting in false negative results. This step should be done rapidly- possibly within 10 min- as cells are not fixed. If cells were grown at low temperature and therefore they must be spheroplasted at the same temperature, one may not get good spheroplasting efficiency within given 10 min since low temperature slows down spheroplasting. One may overcome this by using more zymolase and achieve similar efficiency. Below, I provide a guide for the amounts of zymolase to be used for achieving rapid and efficient spheroplasting at 26 and 37°C.

Zymolase 100T (US Biological) was prepared in 1 M sorbitol as a 1 mg/ml stock and stored at -20°C. This is the same reagent that is routinely used in indirect immunofluorescence staining in the Chan laboratory. For incubation at 37°C, 3.5 µl of β-mercaptoethanol and 40 µl of 1 mg/ml zymolase were added to 200 µl of cell suspension in speroplasting solution. For incubation at 26°C, 40 µl of 3X concentrated zymolase (3 mg/ml) was used. Resulting cell suspension was incubated for 10 min in a water bath that was set at the appropriate temperature. After 7-min incubation, 5 µl of cells were mixed with the same volume of 2% SDS and cell lysis was monitored under the light microscope. If ~ 80% of the cells are lysed by the contact with SDS by 7 min, one would likely achieve over 90% efficiency by 10 min. Once 80-90% of the cells were lysed, spheroplasting was stopped by transferring whole spheroplast suspension into an ice-cold small glass tube containing 5 ml of ice-cold stop solution (0.1 M MES [pH6.4], 1 mM EDTA, 0.5 mM $MgCl_2$, 1 M sorbitol). Spheroplasts were harvested by centrifugation at 2,000 rpm for 5 min and immediately resuspended in 200 µl ice-cold stop solution by

gentle swirling.

Before proceeding to spread, one should make sure that glass slides and reagents are ready. To clean glass slides, submerge regular microscopic glass slides for 20 min in a container that is filled with 100% ethanol, rub clean with Kimwipes, wash several times with ddH_2O, and wipe dry. One slide should contain only one strain or condition. Once cleaned, label the slides at their side using a marker pen that writes thick. Otherwise the writing would be washed off upon subsequent contact with washing solution. The fixative is paraformaldehyde solution that is composed of 4% paraformaldehyde and 3.4% sucrose. One can easily make it by mixing 1/5 volume of 20% paraformaldehyde stock solution and 4/5 volume of 4.25% sucrose stock solution. To make 50 ml of 20% paraformaldehyde stock solution, add 10 g of paraformaldehyde to 40 ml of ddH_2O in 50 ml cornical tube, add ~ 0.5 ml of 1 N NaOH and place the tube in 65°C water bath. When completely dissolved, bring the volume to 50 ml with ddH_2O and filter-sterilize it. This solution can be stored at room temperature and is good for 1 year. 1% Lipsol (LIP LTD) and 0.4% photoflow-200 (Kodak) should be made fresh by diluting in ddH_2O.

To make chromatin spread, the following solutions were pipeted onto the same spot of a slide, and mixed gently after each addition by tilting the slide back and forth several times: 20 μl of spheroplast suspension, 40 μl of paraformaldehyde solution, 80 μl of 1% Lipsol, and 40 μl of paraformaldehyde solution again. Once all the solution had been added, I used the side (and not the tip) of a blue pipet tip to spread the contents very gently and slowly back and forth over most of the length (and width) of the slide (that would be covered subsequently by a coverslip). I made sure that the blue pipet tip went over each area of the slide surface several times. Process slides one by one from beginning to end, but be sure not to take too long for each slide as cells are not fixed yet. The slides were dried overnight at room temperature.

To perform immunofluorescence staining, the slides were washed with Pasteur pipet-full (~ 3 ml) of 0.4% photoflow-200 by gently applying it onto the tilted slide and letting it flow down over chrmatin. Slides were submerged for 10 min in a glass jar that contained 1X PBS. In this step, make sure the level of PBS is below the label on the slide

to avoid being washed off. For this reason, I prefer tall jars to wide ones. Excess liquid was shaken off, and 200 µl of blocking solution (20% fetal calf serum in 1x PBS with 0.02% NaN_3) was added immediately. After incubation in blocking solution for 10 min in a humid chamber, excess solution was shaken off. 100 µl of blocking solution that contained diluted primary antibodies was added to the spread and a coverslip was carefully placed from its side to avoid trapping air bubbles, which could be pushed out by gently shaking the slide. After 1-h incubation in a humid chamber, Pasteur pipet-full 1x PBS was applied onto the tilted slide to remove the cover slip and to rinse off the antibodies. To further wash off antibodies, the slide was placed in a jar containing 1x PBS for 5 min. Incubation with diluted secondary antibodies was done similarly as with primary antibodies, but in the dark. After the coverslip was removed, the slide was washed twice by submerging it for 5 min each in two different jars containing 1x PBS. 300 µl of DAPI (1µg/ml in PBS) was pipeted onto the spread and the slide was incubated for 5 min in the dark. Excess DAPI was rinsed off with Pasteur pipet-full 1x PBS. The slide was let dry in the dark, mounted with ~50 µl of mounting solution (100 mg p-phenylenediamine, 1 ml of 10x PBS, 9 ml of 100% glycerol; pH 9.0) and sealed with coverslip.

2.8. Proteins and immunological techniques

Protease inhibitor cocktail I and II can be made as follows and stored at -20°C. Cocktail I contains 0.5 mM each of antipain, leupeptin, pepstatin A, chymostatin, and aprotinin in ddH_2O. Cocktail II contains 1 mg/ml phenanthroline, 1.6 mg/ml benzamidine-HCl and 1 mM PMSF that are all dissolved in isopropanol. All protease inhibitors were purchased from Sigma. Unless stated, the cocktail I and II were used at 1:500 and 1:100 dilution, respectively. Acid-washed glass beads (425-600 microns; Sigma) were autoclaved, dried well, and stored at room temperature until use.

2.8.1. Western blot analysis

3 $O.D._{600}$ units of exponentially growing yeast cells were transferred to small glass tube, collected by centrifugation at 4,000 rpm for 3 min, and washed once with 2 ml of 25 mM Tris-HCl (pH 7.5) that contains 10 mM NaN_3. Residual liquid was completely sucked out using vacuum. Cell pellet was boiled for 3 min using a heat block that was set at 100°C, transferred to ice, added with 20 μl of ESB (2% SDS, 10% glycerol, 80 mM Tris-HCl [pH 6.8], 0.3% bromophenol blue, 100 mM DTT). One scoop (~50 μl equivalent) of glass beads was added to the cell pellet in ESB. Cells were lysed using a multitube vortexer that was set at the maximum speed (10) for 4 min. Additional 80 μl of ESB was added to the cell lysate and mixed well by brief vortexing. The crude lysate was transferred to a 1.5 ml Eppendorf tube and cleared by centrifugation at 14,000 rpm for 1 min. Supernatant was collected to another 1.5 ml Eppendorf tube and stored at -80°C until use. I do not use the cell lysates that have been repeatedly frozen and thawed for analysis, as I have found that the total amounts of some proteins (e.g., Ipl1 and Dam1) are greatly reduced in cell lysates once they have been thawed twice. I have also noticed that in some cases, phosphorylated Sl15 seems more affected than unphosphorylated Sli15. Therefore, when multiple analyses are expected, I make several aliquots of cell lysate and use one aliquot at a time. Usually, cell lysates were prepared immediately after harvesting of cells. However, for time course experiments in which I needed to collect cells at multiple time points that are not spaced far apart, I stopped right after the boiling step and kept boiled cell pellets in the small glass tube at -80°C. Once all cell pellets were collected at the end of the time course, I took frozen cell pellets out of the -80°C freezer and proceeded with the rest of the steps.

Proteins in cell lysates were electrophoretically separated under Laemmli or Anderson SDS-PAGE condition. The latter was optimizes the resolution of phosphoproteins. Laemmli gels were made as described in the Chan laboratory protocol using 40% acrylamide/bis solution (37.5:1, 2.6% C; Biorad). Gels usually were made 0.75 mm thick, and electrophresed at 20 mA for ~ 4 h. Some proteins (e.g., Scc1) can be better separated on Laemmli gel if the gel is made thicker (1.5 mm). For the resolution of some phosphoproteins that are hardly separated into multiple migrating bands under

Laemmeli condition, I have modified the concentration of bisacrylamide in Anderson gels that were initially described in Anderson et al. (1973). Gels were made 1.5 mm thick. Stacking gel was made up of 5% acrylamide and 0.13% bisacrylamide. Unlike Laemmli gel, the bisacrylamide concentration in separating Anderson gel is not fixed but varies with acrylamide concentration, which is determined by molecular weight of protein of interest: 7.5 % acrylamide and 0.12 % bis; 10 % acrylamide and 0.107 % bis; 12.5 % acrylamide and 0.1 % bis. Anderson gels were run at 15 mA for ~ 9 h.

Once separated on gel, proteins were transferred in the cold room onto nitrocellulose membrane (0.45 μm; Intermountain Scientific Corp.) with the exception of gels for Myc-Kip1 blot that were transferred onto PVDF membrane. The nitrocellulose membrane with proteins was briefly stained with Ponceau S solution (Sigma) to monitor protein transfer and then destained with ddH_2O. The membrane was incubated for 30 min in blocking solution of 5% nonfat milk (store bought) in Western washing buffer (10 mM Tris-HCl [pH7.5], 150 mM NaCl, 0.05% Tween 20 [v/v]). To detect specific protein, the membrane was incubated in blocking solution for 1 h each with primary and then secondary antibodies. Antibody dilutions are listed in Table 2.5. Incubation with antibodies was followed by 3 times of 10-min washing with western washing buffer. When crude serum was used, the membrane was washed 6 times for 5 min each with stringent washing buffer that contained increased concentration of Tween 20 (0.15% instead of 0.05%).

Antibody-bound proteins were visualized by using a chemiluminescence system of luminol and peroxide (the SuperSignal West Pico; Pierce. The membrane was incubated for 5 min with a 1:1 mixture of the peroxide and luminol/enhancer solution. The chemiluminescent signals were exposed and detected onto Hyperfilm ECL (Amersham Biosciences).

2.8.2. Co-immunoprecipitation

30~40 $O.D._{600}$ units of actively growing yeast cells were harvested by centrifugation at 4,000 rpm for 3 min and washed once with 10 ml of ice-cold IP washing

buffer (20 mM HEPES-KOH [pH7.4], 50 mM KCl). Cell pellet was transferred to a 1.5 ml Eppendorf tube and centrifuged at 14,000 rpm for 1 min to remove residual liquid, and then stored at -80°C until use. Lysis buffer was made fresh from stock solutions: 50 mM HEPES-KOH [pH7.4], 200 mM KCl, 10% glycerol [v/v], 1% NP-40 [v/v], 1 mM EDTA, 1 mM DTT, 50 mM NaF, 0.1 mM Na_3VO_4, 5 mM β-glycerophosphate. Protease inhibitor cocktail I and II were usually diluted 500- and 100-fold, respectively, for cell lysis, and bothe were diluted 1,000 fold for washing. I have found that some proteins (e.g., Sl15 and Net1) appear to be more sensitive to proteolysis once cells are lysed. In such cases, adding more protease inhibitor cocktails during lysis and washing greatly diminished the proteolysis problems. I used 1:100 dilution of both cocktails for Co-IP assays that involved Net1, and 1:50 dilution of both cocktails for Co-IP assays with Sli15.

Frozen cell pellets were resuspended in 300 μl of lysis buffer, repelleted by centrifugation at 14,000 rpm for 1 min, resuspended in 200 μl of lysis buffer, transferred to a small glass tube, and kept on ice. Acid-washed glass beads (0.45-0.55 mm; Sigma) were added to the cell suspension to right below liquid surface. Using a multitube vortexer with the highest setting at 10, cells were vortexed 5 times for 2 min each with 2-min incubation on ice. To increase efficiency of recovery of extract, 200 μl of lysis buffer was added to the cell lysate and mixed well by brief vortexing. Cell lysates were transferred to a 1.5 ml Eppendorf tube and cleared by centrifugation at 14,000 rpm for 5 min at 4°C. Some supernatnant (typically 20 μl) was set aside as an input control, mixed with the same volume of 2x SDS sample buffer (100 mM Tris-HCl [pH6.8], 200 mM DTT, 4% SDS, 20% glycerol [v/v], 0.2% bromophenol blue), heated at 100°C for 5 min, and kept at -80°C until SDS-PAGE. The rest supernatant was trasferred to a 1.5 ml Eppendorf tube, incubated with 40 μl of 50 % slurry of protein A-sepharose CL-4B beads (Pharmacia) in equlibrium buffer (20 mM HEPES-KOH [pH7.4], 50 mM KCl, 0.02% NaN_3) for 30 min in the cold room to remove the proteins that nonspecifically interact with the beads. After supernatant was recovered to a 1.5 ml Eppendorf tube by centrifugation at 2,000 rpm for 1 min, appropriate primary antibodies were added, and incubated for 1 h with constant but slow rocking in the cold room. 50 μl of 50% slurry of

protein A CL-4B beads (Pharmacia) was added to lysates and incubated one more hour as in the previous step. Beads-bound proteins were pulled down by centrifugation at 2,000 rpm for 1 min, washed twice or three times with 1.5 ml of lysis buffer with protease inhibitor cocktails for 5 min each time. I usually wash twice since I have empirically learned that this is sufficient to remove most nonspecific interactions. Proteins were eluted from the beads in 60 μl of 1x SDS sample buffer (50 mM Tris-HCl [pH6.8], 100 mM DTT, 2% SDS, 10% glycerol [v/v], 0.1% bromophenol blue) by heating at 100°C for 5 min. Input samples that have been kept at -80°C were taken out and reheated at 100°C for 5 min. All the samples were centrifuged at 14,000 rpm for 1 min before loading onto a Laemmeli SDS polyacrylamide gel.

5-10 μl of input and 10-15 μl of immunoprecipitated proteins were immediately analysed and the remained was stored frozen at -80°C.

2.8.3. GST pull-down assay

A *GAL*$^+$ yeast strain, TD4 was transformed with two kinds of plasmids, one encoding either GST alone or GST-Utp7, of which expression is driven under *GAL1/10* promoter, and the other encodes either Sli15-Myc or HA-Ipl1 under control of its native promoter. Resulting transformants were grown at 26°C in 50ml of supplemented SD medium that contained 2% glucose as a carbon source. When saturated, cells were diluted 50-fold in similar medium that contained 2% raffinose instead of glucose, and incubated for 6 h at 30°C. To induce expression of Gal-driven GST fusion proteins, galactose was added to the culture at the final concentration of 4%, and cells were further incubated for 4 h at 30°C. Yeast extracts were prepared as described in section 2.8.2. Cell lysate was incubated with 50 μl of 50% slurry of glutathione-agarose beads (Sigma) in equlibrium buffer (20 mM HEPES-KOH [pH7.4], 50 mM KCl, 0.02% NaN_3) with constant agitation for 2 h in the cold room. The rest of the procedure (washing, elution, and SDS-PAGE) was done similarly as described in section 2.8.2.

2.8.4. Chromatin immunoprecipitation (ChIP)

5 ml of saturated yeast cell culture that has been incubated at 26°C was diluted into 50 ml of the same medium. Diluted cells were grown to log phase (0.5-0.8 at A_{600}) at 26°C or shifted to 37°C for 3 h. Cells were crosslinked with 1% formaldehyde for 15 min at room temperature. Cross-linking was then stopped by 5-min incubation with 125 mM glycine. Fixed cells were collected by centrifugation at 4,000 rpm for 3 min, washed twice with 50 ml of ice-cold TBS (20 mM Tris-HCl [pH7.6], 200 mM NaCl) and resuspended in 400 μl of ice-cold FA-lysis buffer (50 mM HEPES-KOH [pH7.5], 140 mM NaCl, 1 mM EDTA, 1% Triton X-100 [v/v], 0.1% SDS) containing protease inhibitor cocktails I and II that were diluted 500- and 100-fold, respectively. Cell suspension was stored in a 1.5 ml Eppendorf tube at 4°C until use. Cells can be stored for a few days at 4°C. To lyse cells and to fragment genomic DNA into average size of less than 0.5-kb, cell suspension was sonicated for 14 times of 10 sec each with incubation on ice between rounds of sonication. I used an Ultrasonic Inc. sonicator with a microtip that was set at 5 and 60% duty cycle. Resulting cell lysate was cleared by two-step centrifugation at 14,000rpm for 5 min and then 15 min at 4°C. Supernatant was transferred to new 1.5 ml Eppendorf tube and volumed up to 850 μl with FA-lysis buffer with protease inhibitor cocktails as above. 50 μl of the lysate was set aside as an input control (IN) and stored at 4°C while one of 400 μl lysate was incubated with specific antibodies (+Ab) and remaining 400 μl was mock-treated (-Ab) for 4 h with constant agitation in the cold room. Antibodies and their working dilutions used in ChIP assays are listed in Table 2.5. After incubation with antibodies, 50 μl of 50 % slurry protein A-sepharose CL-4B beads in equlibrium buffer (20 mM HEPEs-KOH [pH7.4], 50 mM KCl, 0.02% NaN_3) was added to both 400-μl lysates followed by further 1-h incubation. Chromatin-bound beads were precipitated by centrifugation at 2,000 rpm for 1 min at 4°C, washed 3 times without incubation with 1.5 ml of FA-lysis buffer containing 1:1,000 diluted protease inhibitor cocktails I and II. To reverse crosslink and to remove proteins that were precipitated with chromatin, washed beads were resuspended in 200 μl of TE (10 mM Tris-HCl [pH8.0], 1 mM EDTA) that was adjusted with 0.25% SDS and

250 μg/ml proteinase K (10 mg/ml stock; Promega). 0.625 μl of 20% SDS and 1.25 μl of 10 mg/ml proteinase K were added to 50-μl input control sample that has been kept at 4°C (see above). All the samples were incubated overnight at 37°C and then incubated at 65°C for at least 6 h. After crosslink was reversed, the volume of the input sample was increased to 200 μl with 10 mM Tris-HCl [pH7.5]. All the samples were phenol:chloroform extracted and the organic phase was back-extracted with one volume of 10 mM Tris-HCl [pH8.0]. In each step, the aqueous phase was separated by centrifugation at 14,000 rpm for 10 min. The combined aqueous fractions were extracted once with one volume of chloroform:isoamyl alcohol and centrifugated at 14,000 rpm for 5 min. 0.3 M Na_2CO_3 and 2 volumes of ice-cold 100% ethanl were added to the recovered aqueous fraction. The resulting solution was incubated overnight at -80°C and then the nucleic acid was precipitated by centrifugation at 14,000 rpm for 20 min at 4°C. The nucleic acid pellet was washed with 300 μl of 70% ethanol, re-pelleted by centrifugation at 14,000 rpm for 10 min at 4°C and resuspended in 20 μl of ddH_2O. 2 μl of the solution was analysed by a standard 30-cycle PCR reaction using *Taq* DNA polymerase (NEB). Primers that are specific to CEN3 and CEN16 are described in Meluh and Koshland (1997). A part of the *CIT3* sequence that is located ~ 1-kb from CEN16 was amplified with CEN16 proximal primers (5'-ACACCATGGTAGCGGTTCTA-3' and 5'-GGTAGAAGCCTTTGTACCAT-3').

2.8.5. Purification of proteins from *E.coli*

To express proteins in *E.coli*, plasmids that allow expression of proteins under control of IPTG (isopropyl-D-thiogalactopyranoside; Sigma)-inducible *tac* promoter were transformed into *E.coli* strain BL21 (DE3) pLysS (*E.coli B F⁻ ompT hsdS(r_B^- m_B^-) dcm^+ Tet^r gal λ(DE3) endA Hte [pLysS Cam^r]*; Stratagene) or BL21 Codon Plus (DE3) – RIPL (*E.coli B F⁻ ompT hsdS(r_B^- m_B^-) dcm^+ Tet^r gal λ(DE3) endA Hte* [*argU proL Cam^r*][*argU ileY leuW Strep/$Spec^r$*]; Stratagene). Transformants were incubated overnight at 37°C in LB (Luria broth) liquid media containing 50 μg/ml ampicillin and diluted then 100-fold in 30 or 50 ml of the same media, and incubated at 37°C for 3 h until cell

density has reached ~ 0.3 at A_{600}. To induce expression of proteins, IPTG was added to the final concentration of 1 mM, and cultures were further incubated at 37°C for 3 h or at 26°C for 4 h. In general, smaller proteins such as GST or MaBP (maltose-binding protein) that are fused to truncations of yeast proteins seem to express relatively well at 37°C, whereas full-length fusions seem poorly expressed at this temperature. Often expression of such larger proteins was improved when cells were incubated at 26°C. After induction, cells were harvested by centrifugation at 6,000 rpm for 10 min at 4°C, washed once with 5 ml of ice-cold washing solution (50 mM HEPES-KOH [pH 7.5], 200 mM KCl) and kept frozen at -80°C until use.

To lyse the cells, frozen cell pellet was resuspended in 1.5 or 2 ml of ice-cold lysis buffer (50 mM HEPES-KOH [pH 7.5], 200 mM KCl, 1% NP-40 [v/v], 1 mM EDTA [pH 8.0], 2 mM DTT) that contained protease inhibitor cocktail I and II at dilution of 1:500 and 1:100, respectively. Cells were lysed using a French press at 16,000 psi, and cell lysates were cleared by centrifugation at 14,000 rpm for 10 min at 4°C. 60 μl of either 50% slurry of glutathione-agarose beads or 50% slurry of maltose-agarose beads (NEB) in equilibrium buffer (20 mM HEPES-KOH [pH 7.5], 50 mM KCl, 0.02% NaN_3) was added to the recovered supernatant. After 2-h incubation with constant agitation in the cold room, protein-bound beads were collected by centrifugation at 2,000 rpm for 1 min at 4°C, washed twice for 5 min each with 1.5 ml of lysis buffer containing protease inhibitor cocktails at 1:1,000 dilution. GST- or MaBP-fusion proteins were eluted from beads by incubating with 100 μl of elution buffer (20 mM reduced glutathione, 50 mM Tris-HCl [pH 8.0], 50 mM KCl; 20 mM maltose, 50 mM HEPES-KOH [pH 7.4], 50 mM KCl) for 10 min with constant agitation in the cold room. Supernatant that contained eluted proteins were recovered by centrifugation at 2,000 rpm for 1 min at 4°C and stored in aliquots at -80°C until use.

2.8.6. Purification of proteins from yeast

The purification of GST-fusion proteins from the *GAL*$^+$ strain TD4 was performed as described in section 2.8.3 with the following modification. To elute GST-fusion

proteins from glutathione-agarose beads, protein-bound beads were washed three times for 5 min each at 4°C with 1 ml of lysis buffer (50 mM HEPES-KOH [pH7.4], 200 mM KCl, 10% glycerol [v/v], 1% NP-40 [v/v], 1 mM EDTA, 1 mM DTT, 50 mM NaF, 0.1 mM Na_3VO_4, 5 mM β-glycerophosphate) that contained protease inhibitor cocktail I and II at 1:1,000 dilution. The beads were washed once for 5 min at 4°C with 1ml of washing buffer (20 mM HEPES-KOH [pH7.4], 50 mM KCl) containing protease inhibitor cocktails as described above. Finally, the beads were incubated with 60 μl of elution buffer (20 mM reduced glutathione, 50 mM Tris-HCl [pH8.0], 50 mM KCl) for 10 min at 4°C in the cold room. These eluted proteins were kept at -80°C until used in *in vitro* kinase assays.

2.8.7. Direct binding assay

To test if Utp7 binds directly to Sli15 and if so, which domain of Utp7 is responsible for the binding, expression of MaBP (maltose-binding protein)- and GST-fusion proteins were induced by IPTG in BL21 Codon Plus (DE3)–RIPL cells as described in section 2.8.5. The proteins used were MaBP, MaBP-Utp7, MaBP-Utp7-N, MaBP-Utp7-M, MaBP-Utp7-C, GST and GST-Sli15. Efficiency of protein expression was checked by Coommassie staining of SDS polyacrylamide gel of cell lysate that was prepared from small fraction of induced cells while the rest of cell pellet was kept frozen at -80°C. Based on the intensity of staining, lysate volume was determined to give rise to similar molar amount of MaBP fusions or GST fusion proteins.

Once cell lysates were made, the same volume of lysates was put aside as input control, mixed with one volume of 2x SDS sample buffer (100 mM Tris-HCl [pH6.8], 200 mM DTT, 4% SDS, 20% glycerol [v/v], 0.2% bromophenol blue), heated at 100°C for 5 min, and kept at -80°C until SDS-PAGE. From the rest of the cell lysates, MaBP fusion proteins were precipitated with maltose-agarose beads as previously described in section 2.8.5. After 1.5-h incubation in the cold room, protein-bound beads were spun down by centrifugation at 2,000 rpm for 1 min and combined with cell lysate that contained similar amount of either GST or GST-Sli15. After 1.5-h incubation, protein-

bound beads were centrifugated, washed three times with lysis buffer as described in section 2.8.5, and proteins were eluted into 60 μl of 1x SDS sample buffer (50 mM Tris-HCl [pH6.8], 100 mM DTT, 2% SDS, 10% glycerol [v/v], 0.1% bromophenol blue) by heating at 100°C for 5 min.

Proteins that have been precipitated with glutathione-agarose beads were separated on Laemmeli SDS-polyacrylamide gel, and analysed by Western blotting using α-GST or α-MaBP antibodies as shown in Table 2.5.

2.8.8. Competitive binding assay

To test if Ipl1 and Utp7 compete to bind to Sli15, *in vitro* competitive binding assays were performed with increased amounts of MaBP-Utp7 but with constant amounts of His_6-Ipl1 and GST-Sli15. All proteins were purified from *E.coli*. BL21 Codon Plus (DE3)-RIPL cells. Protein expression was induced by IPTG, and cell lysates were prepared as described in section 2.8.5. While GST or GST-Sli15 were precipitated with glutathione-agarose beads, cell lysate containing His_6-Ipl1was split into multiple portions of equal volumes. Combinations of lysates of MaBP or MaBP-Utp7 were prepared in such a way that concentration of MaBP-Utp7 increased by the factor of 2– i.e. 0, 1x, 2x, 4x, and 8x (i.e., equivalent to 1 μg) and the difference in the amount of MaBP-Utp7 between samples was filled by MaBP. As described in section 2.8.7, GST or GST-Sli15-bound glutathione beads were precipitated, and lysate of His_6-Ipl1 and lysate mixture of MaBP and MaBP-Utp7 were added to the glutathione beads. After 2-h incubation in the cold room, the beads were centrifugated and washed three times with lysis buffer containing 1,000-fold diluted protease inhibitor cocktails I and II. Duplicate of Laemmeli 10% SDS-polyacrylamide gels were prepared to separate proteins from input and precipitated samples; One was stained with Coomassiee blue for the purpose of quantitation of proteins used and the other was subjected to Western blotting using guinea pig α-Ipl1 or α-MaBP antibodies to analyze MaBP-Utp7 and His_6-Ipl1 that were co-precipitated with GST-Sli15 or GST.

2.8.9. In vitro kinase assay

Kinase reaction was carried out in 30 µl of mixture that contained 5 µl of 6X kinase buffer (60 mM $MgCl_2$, 60 mM $MnCl_2$, 6 mM DTT, 0.6 mM Na_3VO_4, 30 mM ß-glycerophosphate), 1 µl of 5 mCi/ml [γ-^{32}P] ATP and 8 µl of 200 µM ATP. The rest of the reaction volume was taken up by a kinase, substrates, and elution buffer as used to elute proteins (see section 2.8.5). GST-Ipl1 was routinely used kinase at 200-300 ng with or without its stimulator, either GST-Sli15 or GST-Sli15-C at 100 ng or 1 µg, respectively. Bovine myelin basic protein (MyBP; Sigma) was used as an *in vitro* substrate at ~ 5 µg. Potential substrates of GST-Ipl1 kinase that were purified from *E.coli* as a fusion to GST or MaBP (see section 2.8.5) were used at various amounts mainly depending on how much of intact proteins were purified. GST or MaBP was used as a negative control at ~ 1 µg. After 15-min incubation at 30°C, reactions were stopped by adding 10 µl of 4x SDS sample buffer (200 mM Tris-HCl [pH6.8], 400 mM DTT, 8% SDS, 40% glycerol [v/v], 0.4% bromophenol blue) and heated at 100°C for 5 min. Proteins in reactions were electrophoretically separated on 12.5% Laemmeli SDS-polyacrylamide gel. After electrophoresis, gels were strained with Coommassie blue for 10 min, destained in destaining buffer (15% methanol, 7% acetic acid), dried on Whatman paper, exposed to phosphoimager screen overnight at room temperature. Phosporylation was analysed using a phosphoimager.

2.8.10. Immunocomplex kinase assay

To test if the *scd5-PP1Δ2* mutation affects *in vivo* kinase activity of Ipl1, Ipl1 immunocomplex was purified from wild-type and *scd5-PP1Δ2* cells that expressed Ipl1-13x Myc. In detail, cells growing exponentially in YEPD were shifted to 37°C for 3 h. As described in section 2.8.2, cell lysates were made and Ipl1-Myc was immunoprecipitated using mouse α-Myc at 1:100 dilution and 50 µl of 50% slurry of protein A−sepharose CN-4B beads. Ipl1 immunocomplex-bound beads were washed twice for 5 min each at 4°C with 1 ml of lysis buffer that contained protease inhibitor cocktail I and II at 1:1,000 dilution (see section 2.8.2) and washed twice more for 5 min each with 1ml of 1x kinase

buffer (10 mM $MgCl_2$, 10 mM $MnCl_2$, 1 mM DTT, 0.1 mM Na_3VO_4, 5 mM β-glycerophosphate) containing protease inhibitor cocktails as above. The washed beads were used in 30-µl kinase reaction which also included 6-fold diluted 6x kinase buffer, 1 µl of 5 mCi/ml [γ-^{32}P] ATP, 8 µl of 200 µM ATP and substrate. Substrate used was either MyBP or GST-Dam1-C that were purified from *E.coli*. GST purified from *E.coli* was used as a negative control. The total volume of substrates used was kept constant by adding elution buffer (20 mM reduced glutathione, 50 mM Tris-HCl [pH 8.0], 50 mM KCl). The rest of the kinase assay was carried out as described in section 2.8.9. Total lysates and kinase reaction samples were subject to Western blot to validate that similar amount of Ipl1-Myc was precipitated and used in kinase reactions.

2.9. Analysis of ribosome profile

Overnight culture of yeast cells in YEPD was diluted into 150 ml of liquid YEPD. Diluted cells were incubated at 26°C to early log phase ($O.D._{600}$ E ~ 0.3) or shifted to 37°C for 3 h. In experiments using cells expressing GST-fused Utp7 full length or its truncations under the control of *GAL1-10* promoter, cells were incubated in inducing media at 30°C for 4 h as described in section 2.8.3. Cycloheximide (10 mg/ml stock in ddH_2O) was added at the end of incubation to the final concentration of 200 µg/ml and mixed well by swirling culture flasks for 1 min at room temperature. Cells were transferred into pre-chilled centrifugation tubes and spun down using a refrigerated (4°C) centrifuge at 6,000 rpm for 10 min. Cell pellets were transferred to 1.5 ml Eppendorf tubes and kept frozen at -80°C until use.

Described below is how one tube of 7-47 % sucrose gradient was made. Volume of reagents can be multiplied by the number of samples that are to be analyzed. Each 5 ml of 7, 27.5 and 47% sucrose solutions was freshly supplemented with β-mercaptoethanol to the final concentration of 12 mM and with cycloheximide to the final concentration of 200 µg/ml. Using a 5 ml glass pipet, 4.2 ml of 47% sucrose solution was introduced slowly into a tilted tube, making sure that the flow of liquid was constant. This was

followed by 4.2 ml of 27.5% and 7% sucrose solution. Tubes were tightly sealed using parafilm and placed gently on their side in a refrigerator for 2 h to get continuous 7-47%

Table 2.5. Antibodies used in Immunoblotting (IB) and chromatin immunoprecipitation (ChIP) analysis.

Primary antibodies	Host/Form	Source/Batch	Dilution	
			IB	ChIP
α-Myc	mouse; Ascites fluid	Covance	1:1,000	1:100
α-HA	mouse; Ascites fluid	Covance	1:1,000	1:100
α-Ipl1	guinea pig; crude serum	Chan lab; CP2-18	1:2,000	1:100
	rabbit; crude serum	Chan lab; CC1-40, CC2-1	1:5,000	N/A
α-Scd5	rabbit; crude serum	Chan lab; 1652-7	1:5,000	1:200
α-Glc7	rabbit; crude serum	Chan lab;1649-7, 1650-7	1:2,000	1:100
α-Glc8	rabbit; crude serum	Chan lab;1653-5	1: 5,000	1:200
α-Pwp1*	rabbit; crude serum	Chan lab;7-71-1	N/A	1:200
α-Yor342c*	rabbit; crude serum	Chan lab;1655-6	N/A	1:100
α-Dam1	rabbit; affinity purified	D. Drubin lab; 2674	1:1,000	1:100
	guinea pig; affinity purified	D. Drubin lab; Myria (GP3)	1:1,000	N/A
α-Duo1	rabbit; affinity purified	D. Drubin lab	1:2,000	1:100
α-Tub4	rabbit; affinity purified	L. Marschall	1:5,000	1:100
α-G6PDH	rabbit; affinity purified	Sigma	1:250,000	N/A
α-GFP	goat; affinity purified	Rockland	1:5,000	N/A
α-GST	rabbit; affinity purified	Molecular Probes	1:5,000	N/A
α-MaBP	rabbit; affinity purified	New England BioLabs	1:5,000	N/A
Secondary antibodies†	Host/Form	Source	Dilution used in IB	
α-mouse IgG	sheep; affinity purified	Amersham Biosciences	1:5,000	
α-rabbit IgG	donkey; affinity purified	Amersham Biosciences	1:5,000	
α-guinea pig IgG	goat; affinity purified	Cappel	1:5,000	
α-goat IgG	donkey; affinity purified	Jackson ImmunoResearch Laboratories, Inc.	1:5,000	

NA: Not applicable
*Pwp1 and Yor342c are also known as Bro1 and Mip14 respectively in Chan laboratory.
†All secondary antibodies are HRP (horseradish peroxidase)-conjugated.

sucrose gradient.

While incubating gradient tubes, yeast cell lysates were prepared. Cell pellets were thawed on ice, resuspended in 200 μl of polysome buffer (10 mM Tris-HCl [pH7.4], 0.2 mM EDTA, 16 mM $MgCl_2$, 12 mM β-mercaptoethanol, 200 μg/ml cycloheximide), and transferred to small glass tubes. Pre-chilled acid-washed glass beads (425-600 μm; Sigma) were added to slightly below the surface of cell suspension. Cells were lysed by vortexing 4 times for 30 sec each at magnitude of 5 with chilling on ice between rounds of vortexing. Phase-dark cells that are indicative of cell lysis were checked using a light microscope. Once over 30-40% of cells were lysed, 100 μl of polysome buffer was added to cell lystate. Cell lysate was transferred to a 1.5 ml Eppendorf tube and cleared by centrifugation at 14,000 rpm at 4°C for 10 min. The amount of total RNA was measured by absorbance at 260 nm, and a total of 9 A_{260} units was layed onto the continuous sucrose gradient tube that has been kept in the refrigerator and subjected to ultracentrifugation at 40,000 rpm at 4°C for 2.5 h.

After ultracentrifugation, absorbance at 260 nm was measured using a density gradient monitor and plotted by an absorbance monitor.

2.10. Flow cytometry

1 ml of yeast cells that has grown to a cell density of 0.5 at A_{600} was harvested by centrifugation at 4,000 rpm for 3 min, washed once with 1 ml of PBS (40 mM K_2HPO4, 10 mM KH_2PO4, 0.15 M NaCl) and resuspended in 0.5 ml of PBS. To fix and permeabilize cells, 1 ml of 100% ethanol was added to 0.5 ml of cell suspension to reach the final ethanol concentration of ~ 70%. The mixture was allowed sit for 1 h at room temperature and then stored at 4°C overnight. Fixed cells were washed with 1 ml of 10 mM Tris-HCl [pH7.5] and reususpended in 100 μl PBS. To remove RNA, whole cell suspension was adjusted with pancreatic DNase-free RNase to the final concentration of 1 mg/ml and then incubated at 37°C for 2 h. Complete RNase digestion is critical. This

can be checked by examining propidium iodide-stained cells under a fluorescence microscope with a rhodamine filter. Nucleus should be brightly stained and cytoplasm should be lack of stain except for mitochondrial DNA. If necessary, one can prolong this incubation step. Once yeast RNA was completely digested, the whole cell suspension was adjusted with proteinase K (Sigma) to the final concentration of 10 μg/ml and further incubated at 65°C for 1 h. The cells were harvested as before and washed once with 1 ml of PBS and resuspended in 1 ml of PBS. To disperse cell aggregation, the cell suspension was sonicated for several seconds using an Ultrasonic sonicator with a microtip that was set at 1 with 50% duty cycle. The cells were collected by centrifugation as above, resuspended in 200 μl of 100 μg/ml propidium iodide (Roche), and incubated overnight at room temperature in the dark.

Propidium iodide-stained cells were analyzed by flow cytometry. The DNA content of ~20,000 cells per sample was determined using a FACS Calibur Systems (BD Bioscience) and the Cellquest software.

CHAPTER THREE

Regulation of Sli15/INCENP complex, kinetochore and Cdc14 protein phosphatase functions by the ribosome biogenesis protein Utp7

3.1. Introduction

Ipl1 of the budding yeast *Saccharomyces cerevisiae* is the first reported member of the conserved Aurora family of protein kinases and it is essential for proper chromosome segregation during mitosis and meiosis (Chan and Botstein, 1993; Francisco et al., 1994; Monje-Casas et al., 2007). It functions in a complex with Sli15 and Bir1 (Cheeseman et al., 2002; Kim et al., 1999), with Sli15 serving as a stimulator and targeting partner of Ipl1 (Kang et al., 2001). One of the mammalian homologs of Ipl1 (Aurora-B) also exists in a similar complex (termed the chromosomal passenger complex) that contains homologs of Sli15 (INCENP) and Bir1 (Survivin) as well as the protein Borealin (Vader et al., 2006; Vagnarelli and Earnshaw, 2004). The Sli15-Ipl1-Bir1 complex regulates diverse cellular processes during mitotic M phase, including histone H3 phosphorylation (Hsu et al., 2000), kinetochore microtubule-attachment and bi-orientation (Biggins et al., 1999; Dewar et al., 2004; He et al., 2001; Sandall et al., 2006; Tanaka et al., 2002); spindle assembly checkpoint activation in response to lack of kinetochore tension (Biggins and Murray, 2001; King et al., 2007; Pinsky et al., 2006); spindle stability and elongation during anaphase (Bouck and Bloom, 2005; Buvelot et al., 2003; Higuchi and Uhlmann, 2005; Pereira and Schiebel, 2003; Widlund et al., 2006); condensation and complete segregation of the ribosomal DNA locus in late anaphase (Lavoie et al., 2004; Sullivan et al., 2004); and coordination of cytokinesis to the clearance of chromosomes from the spindle midzone (Norden et al., 2006).

The Sli15-Ipl1-Bir1 complex, like the mammalian chromosomal passenger complex, undergoes changes in its subcellular localization to accomplish its many functions through M phase (Buvelot et al., 2003; He et al., 2001; Tanaka et al., 2002).

Before anaphase onset, a low level of the Sli15 complex is present throughout the interior of the nucleus, with this level being higher during earlier parts of the cell cycle. In addition, the Sli15 complex is concentrated at kinetochores and the spindle, with the concentration being much higher at kinetochores. Upon anaphase onset, the level of the Sli15 complex that is present throughout the nucleus becomes greatly diminished. Furthermore, this complex also redistributes from kinetochores to the elongating anaphase spindle. The redistribution of the Sli15 complex from kinetochores to the anaphase spindle requires dephosphorylation of Sli15 by the Cdc14 protein phosphatase, and activation of Cdc14 is necessary and sufficient for the redistribution of the Sli15 complex (Pereira and Schiebel, 2003).

The nucleolus is the site of ribosomal RNA (rRNA) transcription and processing. The small subunit (SSU) processome (or 90S pre-ribosome), consisting of ≥40 U3 snoRNA-associated proteins, is required for the processing of the 35S pre-rRNA to generate the mature 18S rRNA that is needed for the biogenesis of the 40S small ribosomal subunit (Bernstein et al., 2004; Dragon et al., 2002; Grandi et al., 2002; Schäfer et al., 2003). In addition to proteins that are involved in ribosome biogenesis (e.g., the SSU processome), the nucleolus also contains many proteins with no known functions in this process (reviewed in (Shaw and Doonan, 2005)). The RENT complex – consisting of the Cdc14 protein phosphatase, its inhibitor Net1/Cfi1, and the transcriptional silencer Sir2 – represses ectopic gene transcription within the rDNA locus and also promotes cell cycle progression (Shou et al., 1999; Straight et al., 1999; Visintin et al., 1999). Before anaphase onset, Cdc14 is sequestered and kept inactive in the nucleolus through its binding to Net1. Two signaling networks regulate activation of Cdc14. During early anaphase, activation of the FEAR network leads to the release of a fraction of the total pool of Cdc14 into the nucleoplasm (reviewed in (D'Amours and Amon, 2004)), where it can dephosphorylate cyclin-dependent kinase (CDK) substrate proteins such as Sli15. Nuclear Cdc14 also promotes condensin enrichment at the rDNA locus and efficient segregation of rDNA and telomeres (D'Amours et al., 2004; Machín et al., 2005; Sullivan et al., 2004). At the end of M phase, activation of the mitotic exit

network (MEN) leads to further release of Cdc14 from the nucleolus into the nucleoplasm and cytoplasm, and Cdc14 dephosphorylates a key set of CDK substrates to promote mitotic exit (reviewed in (Simanis, 2003; Stegmeier and Amon, 2004)). Interestingly, the Cdc15 kinase and the Mob1-Dbf2 kinase complex of the MEN are also required for the concentration of the Sli15 complex on the anaphase spindle, with Cdc15 being required for the early anaphase redistribution of the Sli15 complex from kinetochores and the Mob1-Dbf2 complex being required for the maintenance of the Sli15 complex on the late anaphase spindle (Stoepel et al., 2005).

Here I show that Utp7, a subunit of the SSU processome, functions not only in the nucleolus but also at kinetochores. Utp7 is required for proper chromosome segregation in addition to ribosome biogenesis. It associates with and regulates the localization of Sli15, Cdc14 and Net1. The regulation of Sli15 localization by Utp7 does not depend entirely on Cdc14 function. Furthermore, the mitotic exit defect caused by Cdc14 inactivation is partially relieved by the simultaneous inactivation of Utp7.

3.2. The *utp7-1* mutation is synthetic lethal with *ipl1-2*

To identify proteins that interact functionally with the Ipl1 protein kinase complex, we have carried out a synthetic lethal genetic screen for *sli* mutations that cause *sli ipl1-2* double mutants to grow very slowly or become inviable at 26°C, the permissive growth temperature for *sli* and *ipl1-2* single mutants (Kim et al., 1999). One such *sli* mutation (*utp7-1*) resides within the essential *UTP7* gene, which encodes a WD40-repeat-containing component of the small subunit (SSU) processome (or ~90S pre-ribosome) that is essential for 35S pre-rRNA processing and 40S ribosomal subunit biogenesis (Bernstein et al., 2004; Dragon et al., 2002; Grandi et al., 2002; Schäfer et al., 2003). Utp7 is conserved from yeast to humans, with the human homolog (BING4) being present in the nucleolus (Andersen et al., 2002). As might be expected, the *utp7-1* mutant is partially defective in 40S ribosomal subunit biogenesis. In contrast, *ipl1-2*^{ts} and *sli15-3*^{ts} cells are not defective in this process even after a 3-h incubation at the restrictive growth temperature of 37°C (data not shown). Furthermore, *ipl1-2* does not interact genetically with other mutations that compromise 40S (*rps27A*) or 60S (*rai1* or *spb2*)

ribosomal subunit biogenesis. Thus, the synthetic lethal relationship between *utp7-1* and *ipl1-2* is unlikely to be caused by a total failure in ribosome biogenesis in *utp7-1 ipl1-2* double mutant cells.

3.3. Utp7 associates with Sli15 and is present at kinetochores

Utp7 is present throughout the interior of the nucleus, but with especially high concentration in the nucleolus as would be expected for a ribosome biogenesis protein ((Dragon et al., 2002; Grandi et al., 2002); data not shown). In contrast, Ipl1 and Sli15 are not detectable in the nucleolus. To find out why a mutation affecting a protein that is concentrated predominantly in the nucleolus would interact genetically with *ipl1-2*, I explored the possibility that Utp7 might also function at kinetochores. Thus, I carried out chromatin immunoprecipitation (ChIP) assays with cells that had Utp7 or one of four other SSU processome subunits (Nan1, Nop1, Rrp5 and Utp10) tagged by the HA-epitope. Our results showed that immunoprecipitation of Utp7-HA but not the other SSU processome subunits tested led to the co-precipitation of centromere (CEN) 3 and 16 sequences (Fig. 3.1A; data not shown). The association between Utp7-HA and centromeres is specific since immunoprecipitation of Utp7-HA did not result in the co-precipitation of a *CIT3* gene sequence that is located ~1-kb from CEN16 (Fig. 3.1A) or sequences from the more centromere-distal *IPL1* and *SLI15* loci (data not shown). Furthermore, Utp7 is known to not associate detectably with the 5'ETS/TIR region of the rDNA repeats (Gallagher et al., 2004). As for most other kinetochore proteins, the association of Utp7-HA with centromeres is abolished in *ndc10-1*^{ts} mutant cells that have a defective inner kinetochore (Fig. 3.1A). Since I have not been able to detect cytologically the presence of Utp7 at kinetochores, our positive ChIP results suggested that Utp7 may associate transiently with kinetochores or that a very small amount of Utp7 may be present at kinetochores**.**

The finding that Utp7 is present at kinetochores prompted us to check by immunoprecipitation assays whether Utp7 might associate with Sli15 and Ipl1. Our results showed that Utp7-HA could be co-precipitated with Sli15-Myc but not with Ipl1-

Myc (Fig. 3.1B). Furthermore, purification of GST-Utp7 led to the co-purification of Sli15-Myc and to a much lesser degree Ipl1-HA (data not shown). Since Sli15 exists in at least two complexes in yeast, one containing Bir1 and the other containing Bir1 and Ipl1 (Sandall et al., 2006; Widlund et al., 2006), our results suggested that Utp7 may associate preferentially with the Sli15 complex that does not contain Ipl1. The fraction of Utp7-HA that was co-precipitated with Sli15-Myc was very small, possibly because the cellular abundance of Sli15 is ~20-fold lower than that of Utp7 (Ghaemmaghami et al., 2003). I have also carried out binding experiments with fusion proteins expressed in *E. coli* and showed that GST-Sli15 could pull down MaBP-Utp7 (data not shown). Thus, Sli15 likely binds directly to Utp7. In spite of the association of Utp7 with Sli15, the association of Utp7-HA with centromeres is not affected in *sli15-3* or *ipl1-2* mutant cells (Fig. 3.1A). Since the association of Sli15 and Ipl1 with centromeres is abolished in *sli15-3* cells (see Fig. 3.3A and 3.3B), the kinetochore localization of Utp7 does not depend on the kinetochore localization of Sli15 or Ipl1.

3.4. *utp7-26* mutant cells missegregate chromosomes

The *utp7-1* mutant that I identified initially in the synthetic lethal screen is partially Cs^- for growth at 13°C. Although this mutant exhibits an ~6-fold increase in the frequency of chromosome gain in a genetic assay (Chan and Botstein, 1993), it does not exhibit any drastic cytological phenotypes (data not shown). Thus, we carried out *in vitro* mutagenesis of the *UTP7* gene and screened for *utp7* mutant alleles that confer a Ts^- growth phenotype at 37°C. I have focused on the analysis of one such allele, *utp7-26*. At 26°C, *utp7-26* cells have a reduced growth rate (see Fig. 3.6B) and are partially defective in 40S ribosomal subunit biogenesis (data not shown). At 26°C or after 3 h at 37°C, the total cellular abundance of mutant Utp7-HA in *utp7-26-HA* cells was greatly reduced (Fig. 3.1C) and the association between mutant Utp7-HA and Sli15-Myc could no longer be detected by co-immunoprecipitation (data not shown). However, I do not know whether this negative result reflects the inability of mutant Utp7-HA to associate with

Sli5-Myc or simply a problem with detection due to the greatly reduced abundance of mutant Utp7-HA.

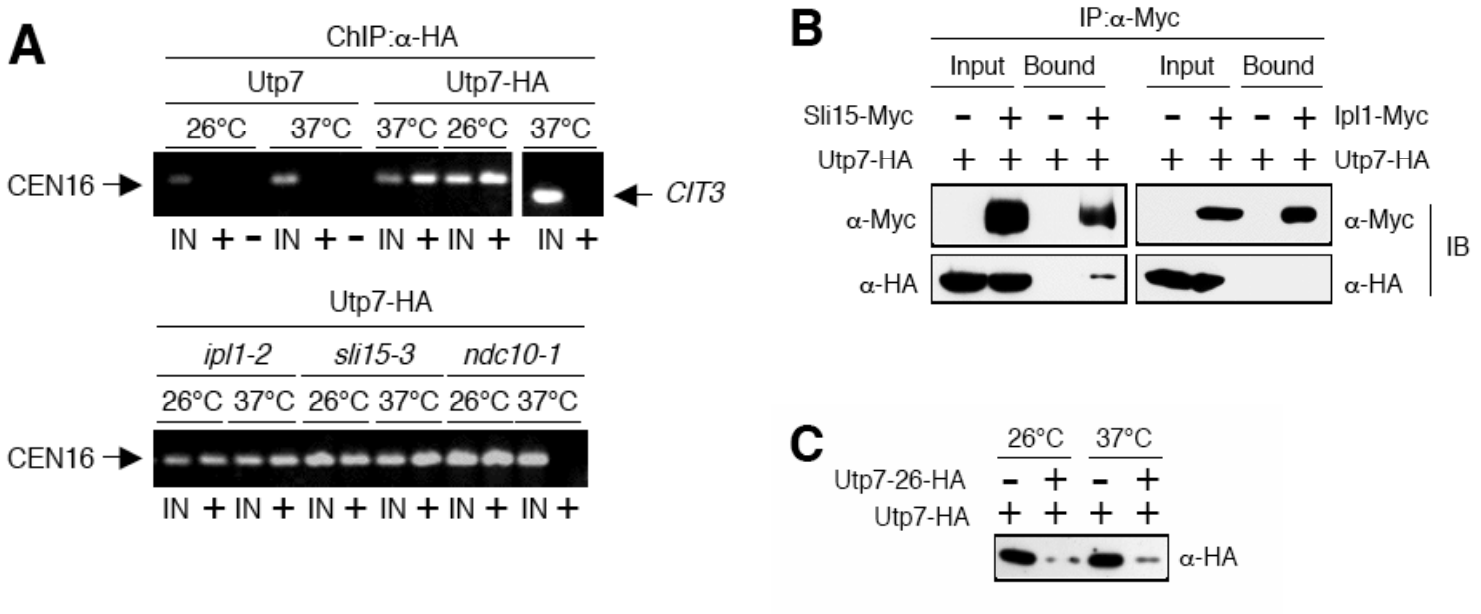

Figure 3.1. Utp7 associates with Sli15 and centromere DNA.

(A) Chromatin immunoprecipitation (ChIP) was carried out with anti-HA antibodies, using extracts from cells that were incubated at 26°C or shifted to 37°C for 3 h. Wild-type cells expressing untagged Utp7 or Utp7-HA, and mutant (*ipl1-2*, *sli15-3* or *ndc10-1*) cells expressing Utp7-HA were used. CEN16 and *CIT3* sequences were amplified by PCR from the total input chromatin (IN), antibody-immunoprecipitated samples (+), or mock treated no-antibody controls (–). (B) Sli15-Myc or Ipl1-Myc was immunoprecipitated (IP) from extracts of wild-type cells growing at 26°C that expressed (+) Utp7-HA in combination with Sli15-Myc or Ipl1-Myc. Immunoprecipitated proteins were analyzed by immunoblotting (IB) with anti-Myc- or anti-HA antibodies. (C) Cells expressing Utp7-HA or mutant Utp7-26-HA were incubated at 26°C or shifted to 37°C for 3 h. Extracts from these cells were immunoblotted with anti-HA antibodies.

To study chromosome segregation, I shifted asynchronous cultures of wild-type and *utp7-26* cells from 26 to 37°C. 3 h after shift, ~45% of *utp7-26* cells became unbudded, with the remainder becoming mostly large-budded (Fig. 3.2A). Since unbudded cells are known to accumulate upon depletion of Utp7 and other SSU components (Bernstein and Baserga, 2004; Bernstein et al., 2007), the slight enrichment in unbudded *utp7-26* cells might have resulted from the ribosome biogenesis defect of such cells. Staining of microtubules and DNA revealed significant chromosome missegregation in *utp7-26* cells. After 3 h at 37°C, ~80% of the large-budded *utp7-26* cells were in anaphase and they showed heterogeneous cytological phenotypes, the most common and striking of which is uneven chromosome segregation (Fig. 3.2B; panels c, d and f). ~68% of cells with separated chromosome masses had this phenotype. Chromosome missegregation was nonrandom, with the mother half of the cell receiving more chromosomal DNA in ~80% of the time when uneven chromosome segregation occurred. This bias is opposite to that reported for *ipl1-2* and *sli15-3* cells (Tanaka et al., 2002) and is similar but not identical to that observed in cells that simultaneously have the kinetochore protein Cse4 depleted and the mitotic spindle assembly checkpoint inactivated by the *mad2* mutation (Collins et al., 2005). By observing the segregation of spindle pole bodies marked by Spc42-RFP (Pereira et al., 2001), I have also shown that this unusual bias is not caused by abnormal segregation of the old and new spindle pole bodies (data not shown).

In addition to uneven chromosome segregation, some chromosomal DNA was often found spanning the bulk of the separated chromosomes, especially in cells with spindles that were not fully elongated (panels d, e and g). This result suggested that some chromosomes might have lagged behind the separating spindle poles, or that the separation of some sister chromatid arms might have been delayed. This lagging or bridging chromosome phenotype is similar to but more severe than that observed in *cdc14* mutants (D'Amours et al., 2004; Machín et al., 2005; Sullivan et al., 2004)). Similar chromosome segregation defects were observed when *utp7-26* cells pre-synchronized in G1 by a-factor treatment at 26°C were allowed to enter the cell cycle at 37°C (data not shown). Under such conditions, all *utp7-26* cells budded and progressed

through the first cell cycle (see Fig. 3.6D). Furthermore, when these G1-arrested cells were allowed to enter the cell cycle at 37°C in the presence of the microtubule-depolymerizing drug nocodazole, *utp7-26* cells, unlike wild-type cells, did not arrest as large-budded cells with unseparated chromosome mass (data not shown), thus indicating that these cells are defective in mitotic spindle assembly checkpoint control. This defect likely explained why *utp7-26* cells could enter and progress through anaphase while missegregating chromosomes.

Since the *utp7-26* mutant is defective in both 40S ribosomal subunit biogenesis and chromosome segregation, it is possible that the chromosome missegregation phenotype observed in *utp7-26* cells might occur as a consequence of the failure to synthesize certain proteins that are required for kinetochore or microtubule functions. However, I consider this possibility unlikely since over-expression of GST-NLS-Utp7-C (containing the C-terminal 149 residues of Utp7) from the galactose-inducible *GAL1-10* promoter causes chromosome missegregation without affecting ribosome biogenesis (data not shown).

3.5. Abnormal kinetochore behavior in *utp7-26* cells

To better understand the nature of chromosome missegregation in *utp7-26* cells, I examined chromosome segregation in wild-type and *utp7-26* cells that had the spindle pole body marked by Spc110-RFP (Yoder et al., 2003) and CEN5 marked by the binding of TetR-GFP to tandem TetO sites located ~1.4-kb from CEN5 (Tanaka et al., 2000). After 3 h at 37°C, most pre-anaphase/metaphase wild-type cells with well-separated spindle pole bodies had two TetR-GFP dots that were almost always located close to the spindle axis defined by the separated spindle pole bodies (Fig. 3.2C). This expected result reflected the normal, precocious separation (and occasional re-association) of sister kinetochores that were bi-oriented and under tension (Goshima and Yanagida, 2000; Goshima and Yanagida, 2001; He et al., 2000; Pearson et al., 2001; Tanaka et al., 2000). The majority of pre-anaphase/metaphase *utp7-26* cells with well-separated spindle pole bodies also had two TetR-GFP dots (Fig. 3.2C). Thus, sister kinetochores in these cells

were bi-oriented and under at least some tension. However, one or both of these TetR-GFP dots was often located way off the spindle axis.

After 3 h at 37°C, all early-anaphase wild-type cells had two TetR-GFP dots, with each locating very close to a different spindle pole body (Fig. 3.2D). This expected result reflected the rapid movement of separated sister kinetochores to opposite spindle poles during anaphase A (Pearson et al., 2001; Straight et al., 1997). Early-anaphase *utp7-26* cells also had two TetR-GFP dots (Fig. 3.2D). However, one or both of these TetR-GFP dots often was not located close to the spindle pole bodies, and such TetR-GFP dots were often located way off the spindle axis. One possible interpretation for the abnormal behavior of sister kinetochores in *utp7-26* cells is that kinetochore-microtubule attachment for the bi-oriented sister chromatids may be unstable. Upon kinetochore-microtubule detachment, previously bi-oriented and thus aligned sister kinetochores may diffuse through the nucleoplasm. If the separated sister kinetochores do not snap back together instantaneously (e.g., as in *slk19Δ* mutants (Zhang et al., 2006)), sister kinetochores would appear separated and off the spindle axis. Since *utp7-26* cells are defective in mitotic spindle assembly checkpoint control, these unattached kinetochores would not prevent entry into anaphase. Thus, detached kinetochores would fail to migrate towards the spindle pole during anaphase A. This kinetochore-microtubule detachment would also explain the lagging or bridging chromosomes seen in many late-anaphase *utp7* cells. Future studies with live cell imaging would help us determine whether this interpretation is correct.

3.6. Mislocalization of multiple kinetochore proteins in *utp7-26* cells

Since Utp7 associates with Sli15 and *utp7-26* cells missegregate chromosomes, I wondered if the kinetochore localization of Sli15, Ipl1 and Bir1 might be compromised in *utp7-26* cells. Thus, I carried out ChIP assays with wild-type and *utp7-26* cells that expressed Sli15-Myc or HA-Bir1 to monitor the associations of these proteins with centromeres. In these ChIP assays, I interpreted a loss of CEN DNA PCR signal as a loss of centromere-association for a specific immunoprecipitated protein, although other

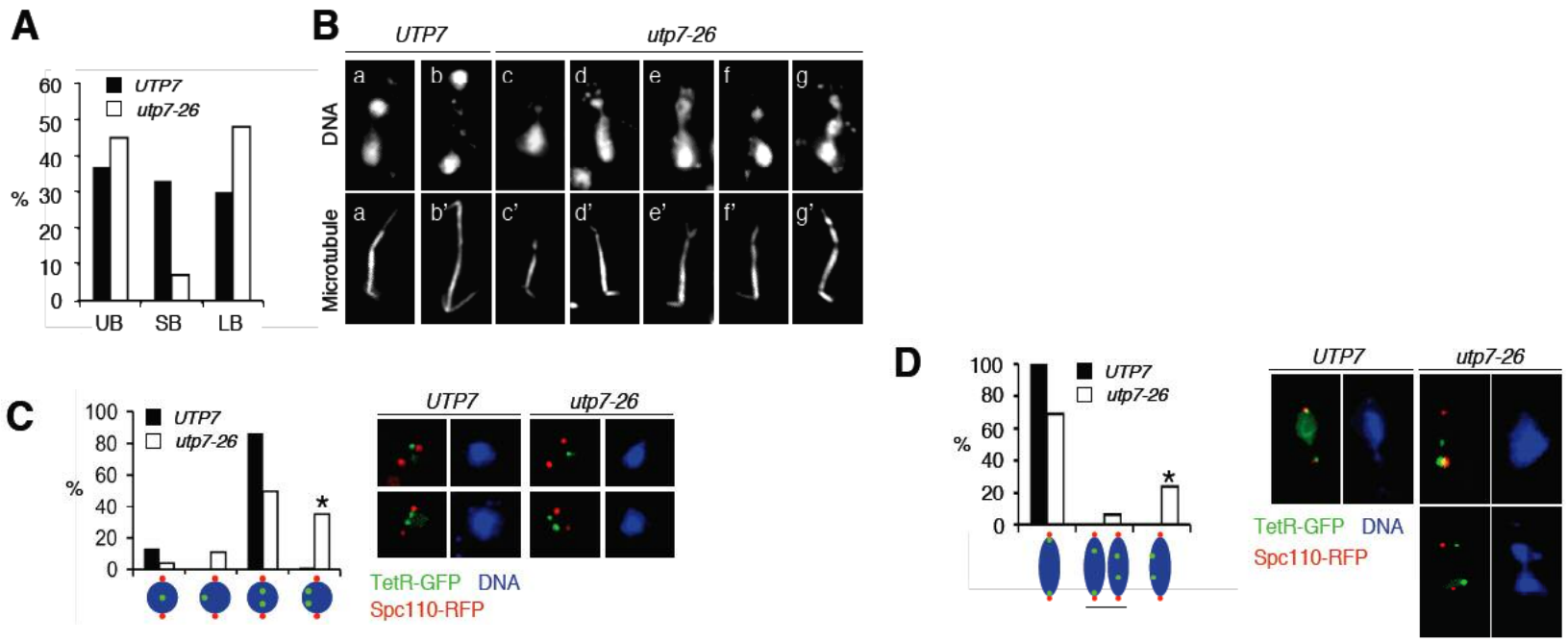

Figure 3.2. *utp7-26* mutant cells missegregate chromosomes.
(A) Wild-type and *utp7-26* cells growing exponentially at 26°C were shifted to 37°C for 3 h. Budding index (UB, unbudded; SB, small-budded; LB, large-budded) of 100 cells each was scored. (B) The microtubule and DNA (DAPI) in these cells were stained and images of stained large-budded cells are shown. Most of the small dots in the DAPI-stained images came from mitochondrial DNA. (C) Wild-type and *utp7-26* cells expressing Spc110-RFP and TetR-GFP that binds to tandem TetO sites located ~1.4 kb from CEN5 were grown to log phase at 26°C and then shifted to 37°C for 3 h. DNA was stained with DAPI and cells with well-separated spindle poles that were in pre-anaphase, or (D) early anaphase were imaged. 100 cells at each stage were scored. Some cells with 2 TetR-GFP dots may have one or both dots off the spindle axis (*).

changes (e.g., masking of epitopes caused by rearrangement in the organization of kinetochore proteins) might also cause a loss of PCR signal. Our results showed that the association of Sli15-Myc with centromeres was greatly reduced in *utp7-26* cells after a 3-h incubation at 37°C (Fig. 3.3A), although the association of mutant Utp7 with centromeres was unaffected in these cells (Fig. 3.3B). Since the centromere-association of both Ipl1 and mutant Sli15 was abolished in *sli15-3* cells (Fig. 3.3A and 3.3B) although the abundance of mutant Sli15 was unaffected in such cells (Fig. 3.3D), I expected the centromere-association of Ipl1 (and HA-Bir1) to also be reduced or abolished in *utp7-26* cells. Surprisingly, the centromere-association of Ipl1 and HA-Bir1 was unaffected in these cells (Fig. 3.3A).

I carried out additional ChIP assays to check whether the apparent Sli15-independent centromere-association of Ipl1 in *utp7-26* cells might be caused by a more broadly perturbed organization of kinetochore proteins in these cells. For this purpose, I monitored proteins that belong to the outer (Bik1, Bim1, Dam1, Kip1, Slk19, Stu2), central (Ctf19, Mtw1, Ndc80), or inner (Cse4, Ndc10) kinetochore (McAinsh et al., 2003). Our results showed that centromere-association was abolished or greatly reduced for Ctf19-HA, Dam1 and Myc-Kip1 (Fig. 3.3A), and was significantly reduced for Bim1-Myc and Ndc80-Myc in *utp7-26* cells (data not shown). Thus, the organization of the outer and central kinetochore is greatly perturbed in *utp7-26* cells and this perturbation likely contributes to the missegregation of chromosomes in these cells. The greatly reduced centromere-association of Sli15-Myc, Ctf19-HA, Dam1 and Myc-Kip1 in *utp7-26* cells was not caused by a significant reduction in the total cellular abundance of these proteins (and the abundance of HA-Bir1 was reduced without affecting its centromere-association) (Fig. 3.3C). Interestingly, the centromere-association of Ipl1 and Ctf19-HA is affected differentially in *utp7-26* and *sli15-3* cells, thus suggesting that the perturbed organization of kinetochore proteins in *utp7-26* cells is not caused entirely by the reduced centromere-association of Sli15 in these cells. This differential effect is also consistent with the distinct chromosome missegregation phenotypes observed in *sli15-3* and *utp7-26* mutants.

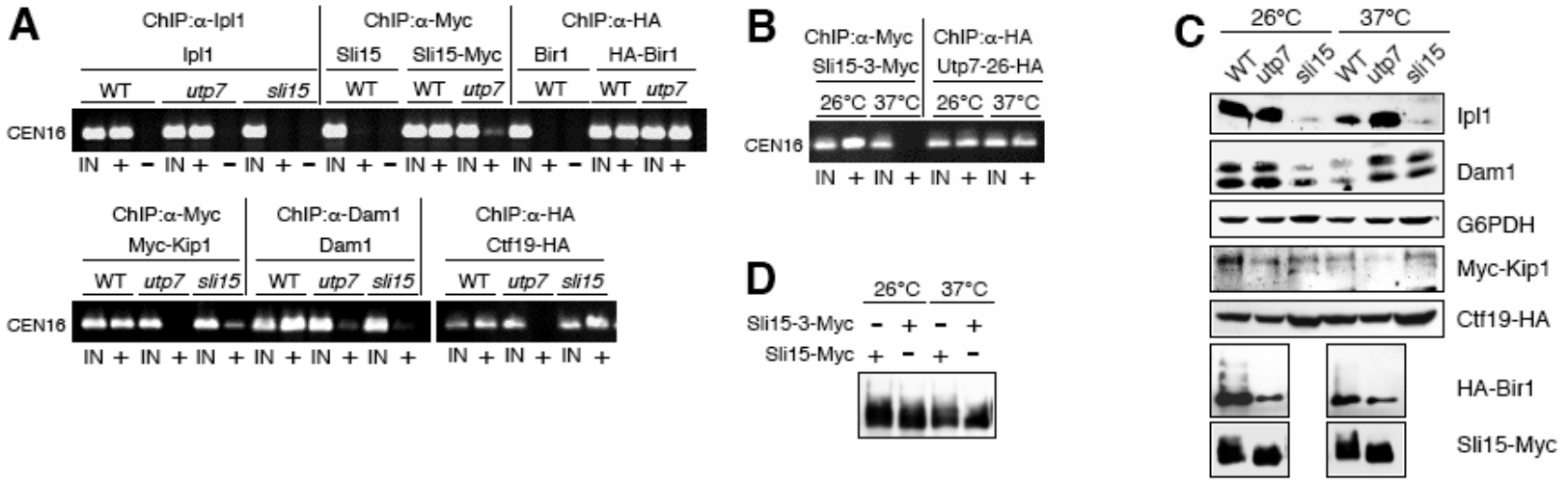

Figure 3.3. Sli15 and other kinetochore proteins mislocalize in *utp7-26* cells.
(A) Chromatin immunoprecipitation (ChIP) was carried out with anti-Ipl1, anti-Dam1, anti-Myc- or anti-HA antibodies, using extracts from cells that were incubated at 26°C and then shifted to 37°C for 3 h. The yeast cells used were: untagged wild-type, *utp7-26* and *sli15-3* cells; wild-type and *utp7-26* cells expressing Sli15-Myc; wild-type and *utp7-26* cells expressing HA-Bir1; wild-type, *utp7-26* and *sli15-3* cells expressing Myc-Kip1; wild-type, *utp7-26* and *sli15-3* cells expressing Ctf19-HA. CEN16 was amplified by PCR from the total input chromatin (IN), antibody-immunoprecipitated samples (+), or mock treated no-antibody controls (–). (B) ChIP was carried out as in (A), but with cells that were incubated at 26°C or shifted to 37°C for 3 h. These cells expressed mutant Sli15-3-Myc or mutant Utp7-26-HA. (C) Immunoblotting of extracts from some of the cells listed in (A). (D) Immunoblotting of extracts from cells that were incubated at 26°C or shifted to 37°C for 3 h. These cells expressed Sli15-Myc or mutant Sli15-3-Myc.

3.7. Altered microtubule localization of Sli15 in *utp7-26* cells

In pre-anaphase wild-type cells, Sli15 is concentrated at kinetochores, which tend to be located near the spindle poles. The abundance of Sli15 near the middle of the spindle is relatively low (Buvelot et al., 2003; Pereira and Schiebel, 2003; Tanaka et al., 2002). Upon anaphase onset, much of Sli15 redistributes to the length of the elongating anaphase spindle. During no part of the cell cycle is Sli15 detected on cytoplasmic microtubules. Our immuno-staining of Sli15-Myc in wild-type cells showed that the localization pattern of Sli15-Myc was not affected by a 3-h incubation at 37°C (Fig. 3.4A). In contrast, after a 3-h incubation at 37°C, Sli15-Myc was present on the cytoplasmic microtubules of *utp7-26* cells that were in all cell cycle stages. Furthermore, *utp7-26* cells that had a short spindle and were thus presumably in pre-anaphase (metaphase) had abnormally high levels of Sli15-Myc along the length of the spindle (Fig. 3.4B).

To confirm that Sli15-Myc was concentrated abnormally on the spindle of pre-anaphase *utp7-26* cells, I treated yeast cells at 26°C with hydroxyurea for 1 h to arrest cell cycle in S phase. These cells were then shifted to 37°C for 2 h in the presence of hydroxyurea. Under such conditions, wild-type and *utp7-26* cells arrested as large-budded cells with a short spindle. Sli15-Myc remained concentrated at kinetochores (near the spindle poles) and was not uniformly localized on the spindle in wild-type cells (Fig. 3.4C). In contrast, Sli15-Myc was concentrated abnormally on the spindle and cytoplasmic microtubules of *utp7-26* cells. Consistent with the idea that Sli15-Myc redistributed abnormally from the kinetochores of pre-anaphase *utp7-26* cells, our ChIP assays also showed that the amount of Sli15-Myc that was associated with centromeres was reduced in *utp7-26* cells that were arrested by hydroxyurea-treatment (Fig. 3.4D). Thus, Sli15-Myc is present abnormally on cytoplasmic microtubules during all cell cycle stages and is redistributed prematurely from kinetochores to the spindle in pre-anaphase *utp7-26* cells. Mutant Sli15 that associates prematurely with the spindle also targets Ipl1 to the spindle (Pereira and Schiebel, 2003). Thus, I also examined the localization of Ipl1-Myc in *utp7-26* cells. Unfortunately, the staining intensity for Ipl1-Myc was much

weaker than that for Sli15-Myc even in wild-type cells. Nevertheless, it was clear that Ipl1-Myc, like Sli15-Myc, was present on cytoplasmic microtubules of *utp7-26* but not wild-type cells in all cell cycle stages. I was unable to determine definitively whether Ipl1-Myc was also concentrated prematurely on pre-anaphase spindles of *utp7-26* cells.

3.8. Mislocalization of Cdc14 and Net1 in *utp7-26* cells

The Cdc14 protein phosphatase is sequestered in the nucleolus for much of the cell cycle through its binding to the inhibitor protein Net1. At the onset of anaphase, activation of the FEAR network leads to the partial release of Cdc14 but not Net1 from the nucleolus (D'Amours and Amon, 2004). Cdc14 dephosphorylates Sli15, and this dephosphorylation is necessary and sufficient for redistribution of the Sli15 complex from kinetochores to the spindle (Pereira and Schiebel, 2003). Since Sli15 is concentrated prematurely on the spindle of pre-anaphase *utp7-26* cells, I examined whether Cdc14 is abnormally present throughout the nucleoplasm of such cells. For this purpose, I carried out the hydroxyurea-treatment and temperature-shift experiment described above with yeast cells that expressed the nucleolar protein Nop1-HA in combination with Cdc14-Myc or Net1-Myc. As expected, Cdc14-Myc and Net1-Myc were localized exclusively to the nucleolus, mostly in a relatively condensed structure, in hydroxyurea-arrested, pre-anaphase wild-type cells (Fig. 3.5A; panels a' and d'). In contrast, Cdc14-Myc in pre-anaphase *utp7-26* cells was found throughout the entire nucleoplasm (~25%; panels c and c') or in a substantial part of the nucleoplasm that contained much chromosomal DNA but no Nop1-HA (~75%; panels b and b'). Thus, Cdc14-Myc is no longer localized exclusively in the nucleolus when Utp7 is inactivated at 37°C in pre-anaphase *utp7-26* cells. Furthermore, I have carried out ChIP assays and showed that Cdc14-Myc that was present in the nucleoplasm in pre-anaphase *utp7-26* cells associated with centromeres (Fig. 3.5B).

Interestingly, the subcellular localization of Net1-Myc was also altered in most (~89%) hydroxyurea-arrested pre-anaphase *utp7-26* cells. The delocalization of Net1-Myc differed from that of Cdc14-Myc. Although Net1-Myc appeared to remain in the

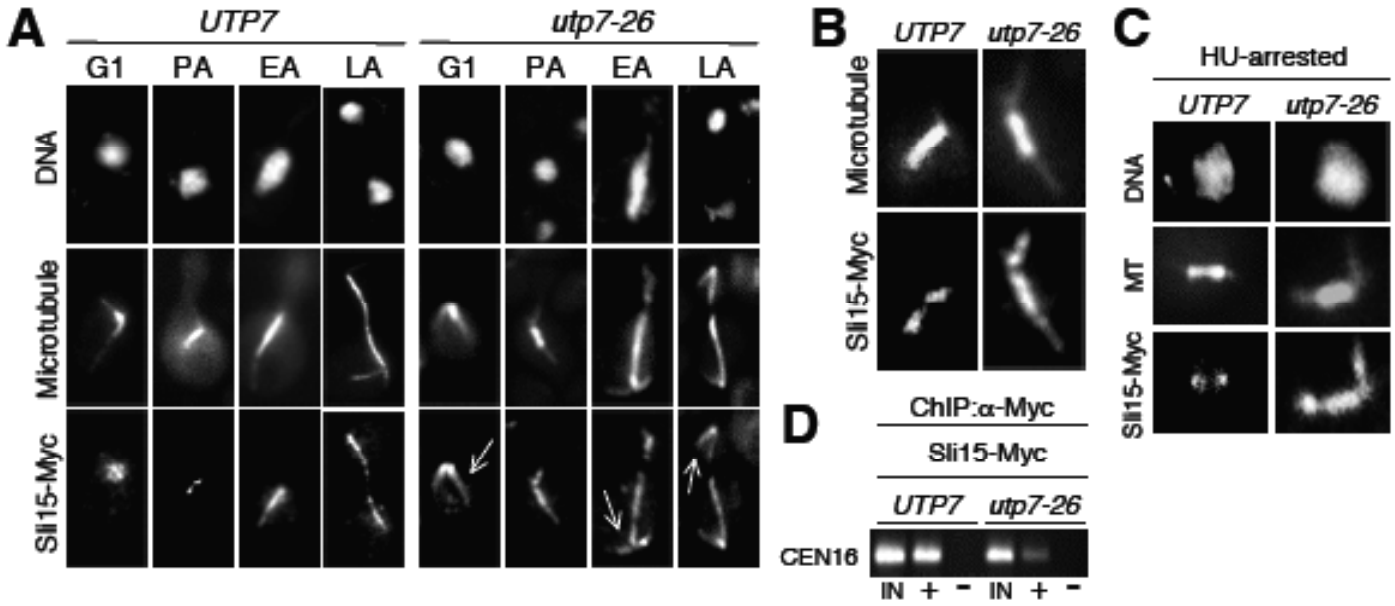

Figure 3.4. Sli15-Myc mislocalizes on microtubules in *utp7-26* cells.
(A) Wild-type and *utp7-26* cells expressing Sli15-Myc were incubated at 26°C and then shifted to 37°C for 3 h. DNA was stained with DAPI, microtubules with anti-tubulin antibodies and Sli15-Myc with anti-Myc antibodies. Representative images from unbudded (UB), pre-anaphase (PA), early-anaphase (EA) and late-anaphase (LA) cells are shown. Sli15-Myc on cytoplasmic microtubules is marked by arrows in some images. (B) Images of pre-anaphase cells from (A) are shown at 3X magnification and with slight changes in contrast. (C) Similar to (A), except cells were first incubated at 26°C for 1 h in the presence of hydroxyurea (HU) and then shifted to 37°C for 2 h. MT = microtubule. (D) Chromatin immunoprecipitation was carried out with anti-Myc antibodies, using extracts from cells shown in (C). CEN16 was amplified by PCR from the total input chromatin (IN), antibody-immunoprecipitated samples(+), or mock treated no-antibody controls.

nucleolus in most (~91%) *utp7-26* cells, it was very often (~80%; panels e and e') not restricted to the rod-like structure seen in wild-type cells. In a small fraction (~9%) of *utp7-26* cells, a low level of Net1-Myc was also found throughout the nucleoplasm (data not shown). However, Net1-Myc (unlike Cdc14-Myc) could not be detected at kinetochores of pre-anaphase *utp7-26* cells by our ChIP assay (Fig. 3.5B). The altered localization of Cdc14-Myc and Net1-Myc in *utp7-26* cells was not caused by a general disruption of nucleolar structure since the localization of the nucleolar protein Nop1-HA was mostly unaffected in these cells (Fig. 3.5A).

I have also repeated these temperature-shift experiments with asynchronously growing cultures of wild-type and *utp7-26* cells. Our results showed that Cdc14-Myc was similarly delocalized in unbudded and small-budded *utp7-26* cells and Net1-Myc was similarly delocalized through the entire cell cycle (data not shown). Thus, Utp7 is required for the proper organization of Net1 and the nucleolar sequestration of Cdc14 from G1 to early anaphase. Since the abundance of Cdc14-Myc and Net1-Myc was not affected in *utp7-26* cells (data not shown), the untimely nucleolar release of Cdc14 in these cells was not caused by a great excess of Cdc14 over its sequestering partner Net1.

3.9. Physical interactions between Utp7, Cdc14 and Net1

Since Utp7, Cdc14 and Net1 are all concentrated in the nucleolus and both Cdc14 and Net1 are delocalized in *utp7-26* cells, I wondered whether Utp7 might regulate the localization of Cdc14 and Net1 through an association with these proteins. Thus, I carried out immunoprecipitation experiments with wild-type cells that expressed Utp7-HA in combination with Cdc14-Myc or Net1-Myc. Our results showed that precipitation of either Cdc14-Myc or Net1-Myc led to the co-precipitation of Utp7-HA (Fig. 3.5C and 3.5D). In reciprocal experiments, immunoprecipitation of Utp7-HA also led to the co-precipitation of Cdc14-Myc and Net1-Myc (data not shown). Thus, Utp7 associates with Cdc14 and Net1 in wild-type cells. In parallel co-immunoprecipitation experiments with *utp7-26* cells, I was unable to detect association between Cdc14-Myc and mutant Utp7-HA. However, I do not know whether this negative result reflects the inability of mutant

Utp7-HA to associate with Cdc14-Myc or simply a problem with detection due to the greatly reduced abundance of mutant Utp7-HA.

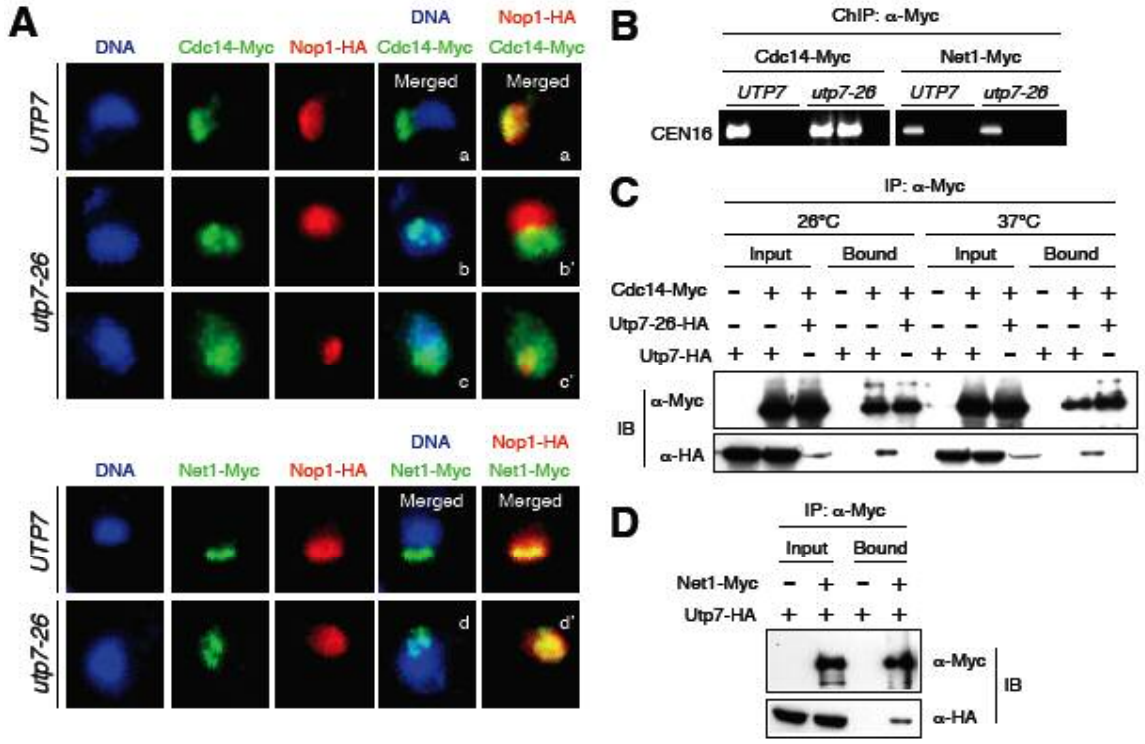

Figure 3.5. Utp7 associates with and regulates the localization of Cdc14 and Net1.
(A) Wild-type and *utp7-26* cells expressing Nop1-HA and Cdc14-Myc expressing Nop1-HA and Net1-Myc were first incubated at 26°C for 1 h in the presence of hydroxyurea and then shifted to 37°C for 2 h. DNA was stained with DAPI; Nop1-HA with anti-HA antibodies; Cdc14-Myc and Net1-Myc with anti-Myc antibodies. (B) Chromatin immunoprecipitation was carried out with anti-Myc antibodies, using extracts from cells shown in (A). CEN16 was amplified by PCR from the total input chromatin (IN), antibody-immunoprecipitated samples (+), or mock treated no-antibody controls (–). (C) Cells that expressed (+) Cdc14-Myc in combination with Utp7-HA or mutant Utp7-26-HA were incubated at 26°C or shifted to 37°C for 3 h. Cdc14-Myc was immunoprecipitated (IP) from cell extracts with anti-Myc antibodies. Immunoprecipitated proteins were analyzed by immunoblotting (IB) with anti-Myc- or anti-HA antibodies. (D) Similar to (C), except that extracts from wild-type cells that expressed (+) Utp7-HA in combination with Net1-Myc (or untagged Net1) were used and cells were incubated at 26°C.

3.10. Genetic interactions between Utp7, Cdc14 and Net1

In addition to physical interactions, I also observed interesting genetic interactions between the genes encoding Utp7, Cdc14 and Net1. First, *NET1-Myc* exacerbated the Ts^- phenotype of *utp7-26* cells, lowering the restrictive growth temperature of such cells from 37 to 30°C (Fig. 3.6A). One possible interpretation of this result is that Net1 function might be compromised by the *NET1-Myc* mutation, resulting in partial premature release of Cdc14 that is tolerated by otherwise wild-type cells. Similarly, the *utp7-26* mutation might also cause partial premature release of Cdc14 at 30°C, which may be tolerated by an otherwise wild-type cell. However, additive premature release mediated by the *NET1-Myc* and *utp7-26* mutations might not be tolerated at 30°C.

Second, the *utp7-26* and *cdc14-3* mutations exhibited reciprocal suppression, with the *cdc14-3* mutation (Sharon and Simchen, 1990) suppressing the slow-growth phenotype of *utp7-26* cells at 26°C (Fig. 3.6B) and the *utp7-26* mutation partially suppressing the Ts^- growth phenotype of *cdc14-3* cells (Fig. 3.6C). Since *utp7-26* cells are defective in 40S ribosomal subunit biogenesis at 26°C, I assumed that the slow-growth phenotype of *utp7-26* cells at this temperature was caused by the ribosome biogenesis defect. Thus, I was surprised to learn that *utp7-26 cdc14-3* cells were similarly defective in 40S ribosomal subunit biogenesis (data not shown). Thus, the slow-growth phenotype of *utp7-26* cells at 26°C might not be caused by the ribosomal biogenesis defect and *cdc14-3* suppresses this unknown defect of *utp7-26* cells.

Since Cdc14 is essential for mitotic exit, I also examined the ability of the *utp7-26* mutation to affect the mitotic exit defect of *cdc14-3* cells. For this purpose, I pre-synchronized yeast cells in G1 with a-factor treatment and then monitored budding as these cells progressed through the cell cycle at 37°C, a temperature restrictive for all mutant cells. As expected, *cdc14-3* cells budded with wild-type kinetics but then arrested in telophase as large-budded cells (Fig. 3.6D). In contrast, budding of *utp7-26* cells was delayed by ~30-45 minutes and these cells were able to exit mitosis and undergo cell division. Interestingly, budding occurred at close to wild-type kinetics in *utp7-26 cdc14-3* cells. These cells reached the large-budded stage with kinetics intermediate between

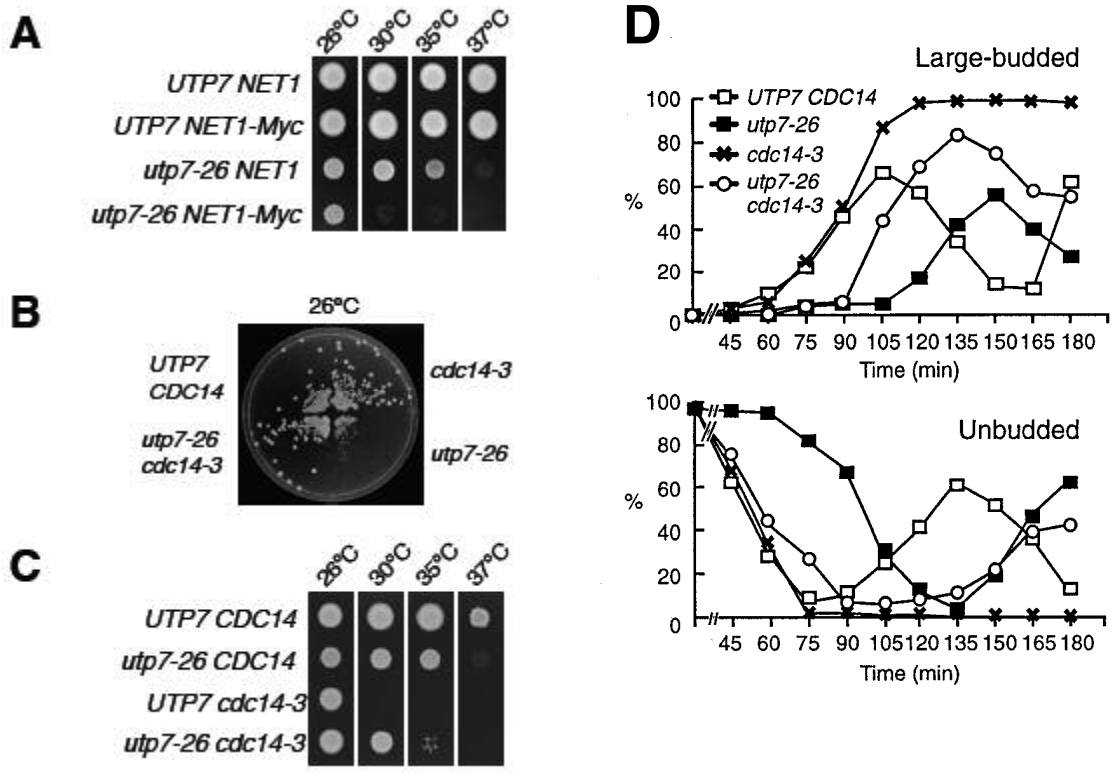

Figure 3.6. *UTP7* interacts genetically with *CDC14* and *NET1*.
(A) Suspensions of yeast cells with the indicated genotypes were spotted on YEPD agar and allowed to grow for 2 days at the indicated temperatures. (B) Yeast cells with the indicated genotypes were streaked on YEPD agar and allowed to grow at 26°C for 3 days. (C) Similar to (A), but with cells from (B). (D) Yeast cells from (B) were first incubated at 26°C for 1.5 h in the presence of α-factor and then shifted to 37°C in the absence of α-factor. The budding index of 100 cells was scored at each time point.

those of *utp7-26* and *cdc14-3* cells. Thus, *cdc14-3* suppresses the slow "growth" phenotype of *utp7-26* cells at 37 as well as 26°C. Furthermore, a substantial fraction of *utp7-26 cdc14-3* cells exited mitosis and divided to yield unbudded cells. Thus, the mitotic exit defect of *cdc14-3* cells is partially suppressed by the *utp7-26* mutation. These genetic results together indicate that the functions of Utp7, Cdc14 and Net1 are intimately related.

3.11. Functional relationship between Utp7 and Cdc14

If the extra-nucleolar localization of Cdc14 in pre-anaphase *utp7-26* cells is entirely responsible for the abnormal concentration of Sli15 on the spindle in such cells, I might expect inactivation of Cdc14 to abolish the abnormal concentration of Sli15-Myc on the pre-anaphase spindle of *utp7-26* cells. Thus, I further examined Sli15-Myc localization in wild-type, *utp7-26*, *cdc14-3* and *utp7-26 cdc14-3* cells. In our initial experiment, I shifted asynchronous cell cultures from 26 to 37°C for 3 h and focused on cells that were in late anaphase, which represented the terminal arrest point for *cdc14-3* cells. As expected, Sli15-Myc was concentrated on the spindle of late-anaphase wild-type and *utp7-26*, but not *cdc14-3*, cells since Cdc14 is required for the concentration of Sli15 on the anaphase spindle (Fig. 3.7A; (Pereira and Schiebel, 2003)). Interestingly, the concentration of Sli15-Myc on the spindle was largely restored in *cdc14-3 utp7-26* cells, thus indicating that Cdc14 function is not absolutely required for the concentration of Sli15-Myc on the late-anaphase spindle when Utp7 function is also compromised. In contrast, the localization of Sli15-Myc on cytoplasmic microtubules in late-anaphase *utp7-26* cells is dependent on Cdc14 function since Sli15-Myc was absent on the cytoplasmic microtubules of *utp7-26 cdc14-3* cells.

Furthermore, while the spindles in *cdc14-3* cells appeared relatively short and broken since spindle-association of Sli15 is required for spindle stability during anaphase (Pereira and Schiebel, 2003), the spindles in *utp7-26 cdc14-3* cells appeared intact and more normal in length, perhaps because the spindle-association of Sli15-Myc was restored in these cells. In addition, the chromosome segregation defect (uneven chromosome segregation and lagging/bridging chromosomes) commonly seen in *utp7-26* cells was much less commonly seen or severe in *utp7-26 cdc14-3* cells (Fig. 3.2B and 3.7A). This observation suggested that the abnormal localization and functioning of Cdc14 in the nucleoplasm and at kinetochores of pre-anaphase *utp7-26* cells might contribute to chromosome missegregation in these cells. These phenotypes of *utp7-26 cdc14-3* cells are also consistent with the reciprocal genetic suppression observed between *utp7-26* and *cdc14-3* (Fig. 3.6B and 3.6C).

To address the issue of Sli15-Myc localization in pre-anaphase cells, I repeated the temperature-shift experiment with cells that were arrested in S phase by hydroxyurea-treatment. After 2 h at 37°C, Sli15-Myc remained concentrated at kinetochores in wild-type and *cdc14-3* cells, whereas Sli15-Myc became concentrated abnormally on the spindle and cytoplasmic microtubules of *utp7-26* and *utp7-26 cdc14-3* cells (Fig. 3.7B). Thus, the concentration of Sli15-Myc on the spindle of pre-anaphase as well as late-anaphase *utp7-26* cells does not absolutely require Cdc14 function. Furthermore, unlike the situation in late-anaphase cells, the abnormal location of Sli15-Myc on cytoplasmic microtubules in pre-anaphase *utp7-26* cells also does not absolutely require Cdc14 function.

I have also carried out ChIP assays to examine the association of Sli15-Myc with centromeres in these hydroxyurea-arrested pre-anaphase cells. As I have shown earlier (Fig. 3.4D), the amount of Sli15-Myc that was associated with centromeres was greatly reduced in *utp7-26* cells after 2 h at 37°C (Fig. 3.7C). Centromere-association of Sli15-Myc was increased, but perhaps not quite back to wild-type level, in *utp7-26 cdc14-3* cells. Thus, the loss of Sli15-Myc from the pre-anaphase kinetochores in *utp7-26* cells might be due at least partly to the premature presence and functioning of Cdc14 at the kinetochores of these cells (Fig. 3.5B).

In immunoblots of extracts prepared from asynchronous cell cultures, I noticed that the electrophoretic mobility of Sli15-Myc in SDS-PAGE was increased in *utp7-26* cells (Fig. 3.3C). Since reduced electrophoretic mobility of Sli15-Myc is caused by phosphorylation (Kang et al., 2001), this observation indicated that Sli15-Myc was under-phosphorylated in *utp7-26* cells. Similarly, Sli15-Myc was also under-phosphorylated in hydroxyurea-arrested pre-anaphase *utp7-26* cells (Fig. 3.7D). This was especially apparent in *utp7-26* cells that had not been shifted to 37°C (since Sli15-Myc in wild-type cells also became less phosphorylated at 37°C). In contrast, Sli15-Myc was hyper-phosphorylated in pre-anaphase *cdc14-3* cells, especially after 2 h at 37°C. This was a surprising finding since according to current models of Cdc14 regulation, the Cdc14 protein phosphatase is not thought to be present outside the nucleolus before anaphase

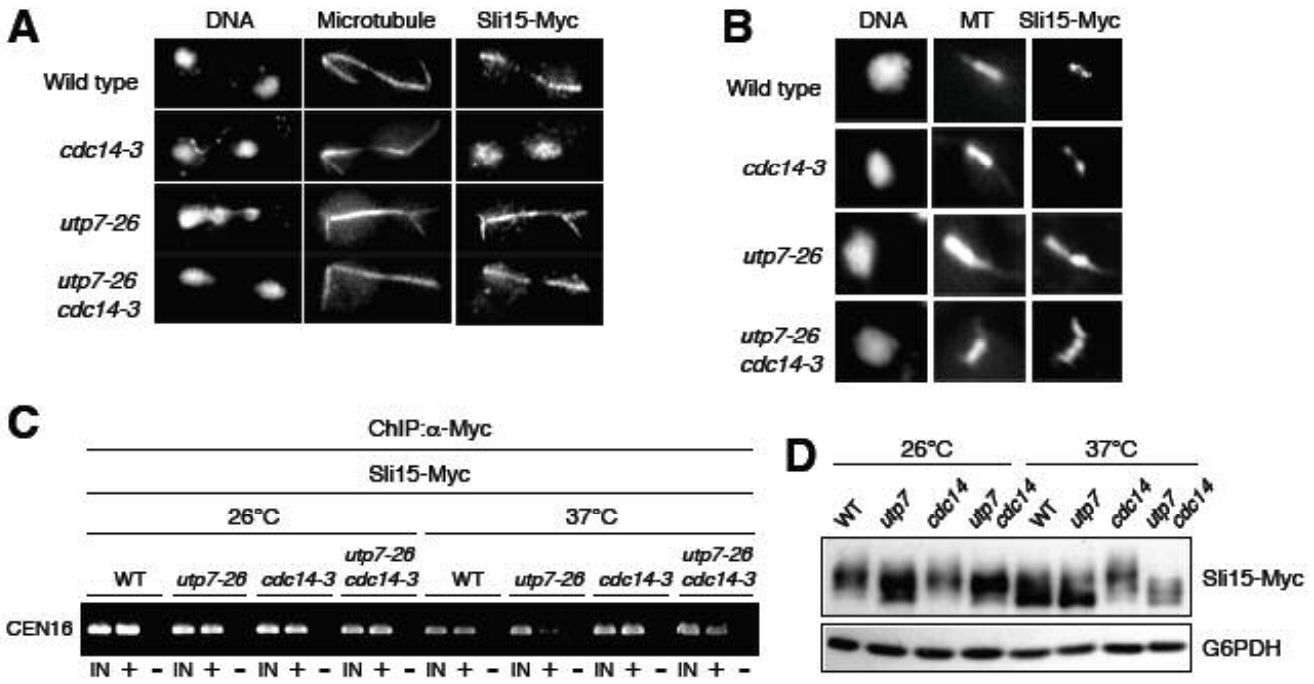

Figure 3.7. Utp7 regulates Sli15 localization and phosphorylation by Cdc14-dependent and Cdc14–independent mechanisms.
(A) Yeast cells with the indicated genotypes that expressed Sli15-Myc were incubated at 26°C and then shifted to 37°C for 3 h. DNA was stained with DAPI, microtubules with anti-tubulin antibodies and Sli15-Myc with anti-Myc antibodies. Representative images of cells in telophase are shown. (B) Similar to (A), except cells were first incubated at 26°C for 1 h in the presence of hydroxyurea and then shifted to 37°C for 2 h. MT = microtubule. Images are shown at 3X magnification relative to those shown in (A). (C) Chromatin immunoprecipitation was carried out with anti-Myc antibodies, using extracts from cells shown in (B) before and after the 2-h shift to 37°C. CEN16 was amplified by PCR from the total input chromatin (IN), antibody-immunoprecipitated samples (+), or mock treated no-antibody controls (–). (D) Immunoblotting of extracts from the cells shown in (C), using anti-Myc and anti-G6PDH antibodies.

onset (in wild-type and *cdc14-3* cells) and thus is not expected to dephosphorylate Sli15 at this stage of the cell cycle. Nevertheless, the phosphorylation state of Sli15-Myc in pre-anaphase *utp7-26 cdc14-3* cells was intermediate between that in wild-type and *cdc14-3* cells. Thus, Utp7 can regulate the phosphorylation state of Sli15 independent of Cdc14.

3.12. Discussion

I have shown here that the predominantly nucleolar ribosome biogenesis protein Utp7 associates with Sli15, Cdc14 and Net1. It is present at kinetochores and is required for normal organization of kinetochore proteins and proper chromosome segregation. When Utp7 is inactivated, Sli15 becomes concentrated on cytoplasmic microtubules and also prematurely on pre-anaphase spindles. Furthermore, Cdc14 is no longer sequestered in the nucleolus before anaphase onset. However, premature targeting of Sli15 to the pre-anaphase spindle of *utp7-26* cells is not caused entirely by the premature nucleolar release of Cdc14.

3.12.1. Utp7 and nucleolar sequestration of Cdc14

Cdc14 is sequestered and kept inactive from G1 to early anaphase in the nucleolus as part of the RENT complex, which also contains Net1 and Sir2 (Shou et al., 1999; Straight et al., 1999; Visintin et al., 1999). As part of the activation of the FEAR network upon anaphase onset (D'Amours and Amon, 2004), the sister chromatid-separating protease separase associates with and down-regulates the activity of the $PP2A^{Cdc55}$ protein phosphatase towards Net1 (Queralt et al., 2006), thus allowing phosphorylation of Net1 by mitotic CDK and partial release of Cdc14 from Net1-mediated nucleolar sequestration (Azzam et al., 2004). At the end of M phase, activation of the mitotic exit network (MEN) leads to further nucleolar release of Cdc14, probably involving phosphorylation of Cdc14 by protein kinases in this network (Stegmeier and Amon, 2004). I show here that inactivation of Utp7 in *utp7-26* cells leads to perturbation of the organization of Net1 mostly within the nucleolus and release of Cdc14 from the nucleolus through all cell cycle stages. Since Utp7 associates with Cdc14 and Net1, and

these proteins are present at roughly similar abundance (~5,800, 8,550 and 1,590 molecules/cell for Utp7, Cdc14 and Net1, respectively (Ghaemmaghami et al., 2003)), Utp7 potentially may function in a stable complex with Net1 to sequester Cdc14 in the nucleolus. I consider this unlikely since the abundance of mutant Utp7 protein in *utp7-26* cells is very greatly reduced even at the permissive growth temperature of 26°C. Yet dramatic untimely nucleolar release of Cdc14 occurs in *utp7-26* cells only at the restrictive growth temperature of 37°C. Thus, nucleolar sequestration of Cdc14 occurs even when the abundance of Utp7 is much lower than that of Cdc14. Furthermore, extensive mass spectrometric analysis of the purified RENT complex has not identified Utp7 as a stably bound component of this complex (Huang et al., 2006; Shou et al., 1999; Straight et al., 1999). Thus, I favor a model in which Utp7 associates loosely with the RENT complex to regulate its stability, possibly by causing conformation changes that favor Net1-Cdc14 association. In wild-type cells, the effect of Utp7 on the stability of the RENT complex is overridden by activation of the FEAR and mitotic exit networks. In addition, Utp7 potentially may inhibit untimely activation of the FEAR or mitotic exit network, possibly working with the known negative regulators Bub2, Bfa1, Fob1, Kin4 or $PP2A^{Cdc55}$ (D'Aquino et al., 2005; Queralt et al., 2006; Stegmeier and Amon, 2004). It remains to be determined whether untimely nucleolar release of Cdc14 in *utp7-26* cells requires functional components of the FEAR or mitotic exit network.

3.12.2. Utp7 and Sli15 localization

Inactivation of Utp7 in *utp7-26* cells affects the localization of Sli15 in two important ways. First, Sli15 becomes abnormally localized on cytoplasmic microtubules in all cell cycle stages. This abnormal localization potentially can be caused by a defect in the nuclear import or nuclear retention of a fraction of Sli15, which contains a putative nuclear localization signal (Kang et al., 2001), thus allowing it to associate with cytoplasmic microtubules. Interestingly, inactivation of Cdc14 (by the *cdc14-3* mutation) abolishes the abnormal localization of Sli15 on the cytoplasmic microtubules of late-anaphase but not pre-anaphase *utp7-26* cells. Genetic and biochemical studies have

previously linked components of the RENT complex with proteins that are involved in nuclear trafficking (Asakawa and Toh-e, 2002; Huang et al., 2006; Shou and Deshaies, 2002). If Cdc14 can regulate nuclear trafficking in late anaphase but not pre-anaphase, then inactivation of Cdc14 may affect the putative defect in Sli15 nuclear import or nuclear retention in late-anaphase but not pre-anaphase *utp7-26* cells.

Second, Sli15 becomes concentrated on the spindle prematurely in G1 to metaphase *utp7-26* cells. This is not a surprising result since Cdc14 is also released prematurely from the nucleolus of these *utp7-26* cells, and Cdc14 nucleolar release and dephosphorylation of Sli15 is known to be sufficient to redistribute Sli15 from kinetochores to the spindle (Pereira and Schiebel, 2003). However, Cdc14 function is not required for the concentration of Sli15 on the spindle of HU-arrested pre-anaphase or late-anaphase *utp7-26* cells. Thus, Utp7 regulates the spindle localization of Sli15 in at least two ways, one through its effect on the nucleolar sequestration of Cdc14 and another through a mechanism that is independent of Cdc14 function. I do not know yet how Utp7 performs its Cdc14-independent function. However, a clue comes from the analysis of the phosphorylation state of Sli15. I have shown that Sli15 is hyper-phosphorylated in HU-arrested pre-anaphase *cdc14-3* cells. This surprising result suggests that a small amount of active Cdc14 may actually be present outside the nucleolus before anaphase onset, or that Sli15 somehow has access to nucleolar Cdc14. Importantly, the phosphorylation state of Sli15 in HU-arrested pre-anaphase *utp7-26 cdc14-3* cells is intermediate between that of wild-type and *cdc14-3* cells. Thus, inactivation of Utp7 can lead to Sli15 dephosphorylation independent of Cdc14 function. Interestingly, Glc7, the catalytic subunit of protein phosphatase 1, and Cdc55, a regulatory subunit of protein phosphatase 2A, are both present in the nucleolus, where Utp7 is concentrated (Bloecher and Tatchell, 2000; Queralt et al., 2006). Utp7 may negatively regulate one of these protein phosphatases.

3.12.3. Utp7 and chromosome segregation

The centromere-association of at least 6 central or outer kinetochore proteins (Bim1, Ctf19, Dam1, Kip1, Ndc80 and Sli15) is greatly reduced or totally abolished in *utp7-26* cells. This severe perturbation of kinetochore structure almost certainly contributes to chromosome missegregation in *utp7-26* cells. The reduction but not loss of centromere-association for Sli15 in *utp7-26* cells can be explained by the premature nucleolar release of Cdc14, which is known to cause Sli15 to redistribute from kinetochores to the spindle (Pereira and Schiebel, 2003). Since the centromere-association of Bim1, Dam1, Kip1 and Sli15 is abolished or reduced in *sli15-3* cells, it is not surprising that the centromere-association of Bim1, Dam1 and Kip1 is also abolished or reduced in *utp7-26* cells. However, the centromere-association of Ctf19 is totally abolished in *utp7-26* but not *sli15-3* cells, and the centromere-association of Ipl1 is totally abolished in *sli15-3* but not *utp7-26* cells. Thus, the effect of the *utp7-26* mutation on kinetochore organization does not act entirely through Sli15. It is possible that the premature nucleolar release and centromere-association of Cdc14 in *utp7-26* cells contributes to the loss of centromere-association for Ctf19 (and possibly other kinetochore proteins). Premature nucleolar release of Cdc14 may also contribute to chromosome missegregation by affecting microtubule dynamics. Cdc14 dephosphorylates a number of spindle microtubule-stabilizing proteins, including Fin1. These dephosphorylated proteins associate with the anaphase spindle, where they cause a reduction in the dynamics of spindle microtubules, including kinetochore microtubules (Higuchi and Uhlmann, 2005; Woodbury and Morgan, 2007). Expression of a mutant Fin1 protein that mimics constitutive Cdc14 dephosphorylation leads to chromosome missegregation. However, since *cdc14-3* only partially suppresses the chromosome segregation defects of *utp7-26* cells, I do not believe that untimely activation of Cdc14 in *utp7-26* cells is responsible for all the chromosome segregation defects observed in *utp7-26* cells. Utp7 most likely also regulate chromosome segregation through a mechanism that is independent of Cdc14 activation.

3.12.4. Reciprocal suppression between *utp7-26* and *cdc14-3*

The *cdc14-3* mutation not only partially suppresses the chromosome segregation defects of *utp7-26* cells at 37°C, it also suppresses the growth of *utp7-26* cells in two other ways. First, it completely suppresses the slow-growth phenotype of *utp7-26* cells at 26°C without suppressing their 40S ribosomal subunit biogenesis defect. Second, it partially suppresses the delay in bud emergence and growth observed in *utp7-26* cells at 37°C. One possible explanation for these suppression results is that a very small amount of Cdc14 is released prematurely from the nucleolus in *utp7-26* cells even at 26°C (our unpublished results). The presence of Cdc14 outside the nucleolus before anaphase onset in *utp7-26* cells would lead to inappropriate dephosphorylation of CDK substrate proteins (including the CDK inhibitor Sic1 as well as transcription and DNA replication factors (Bloom and Cross, 2007; Geymonat et al., 2004; Visintin et al., 1998)), which might lead to slow growth at 26°C and delay in bud emergence and growth at 37°C. Reduction or abrogation of Cdc14 function by the *cdc14-3* mutation would thus alleviate these defects.

The *utp7-26* mutation also suppresses the Ts^- growth phenotype of *cdc14-3* cells at 30°C and the mitotic exit defect of these cells at 37°C. Since Sli15 is not required for mitotic exit and cell division, the ability of the *utp7-26* mutation to restore spindle-association of Sli15 in *cdc14-3* cells cannot explain the ability of *utp7-26 cdc14-3* cells to exit mitosis and divide at 37°C. Mitotic exit requires inactivation of mitotic CDK. Cdc14 triggers mitotic exit by dephosphorylating and positively regulating the CDK inhibitor Sic1, the Swi5 transcription factor for *SIC1*, and the Cdh1 subunit of anaphase-promoting complex that leads to the degradation of mitotic cyclin (Visintin et al., 1998). It remains to be determined whether the abundance and phosphorylation states of these three proteins are affected in *utp7-26* cells.

3.12.5. Ribosome biogenesis and other cellular processes

Ribosome biogenesis is an extremely energy-intensive process, consuming up to 80% of the energy of a rapidly growing eukaryotic cell. Consequently, ribosome biogenesis must be regulated according to all the other needs of a cell. In budding yeast, ribosome biogenesis is coordinated with other important cellular processes – e.g.,

secretion (Warner, 1999). The findings that some nucleolar ribosome biogenesis proteins associate and function with yeast DNA replication initiation proteins at replication origins (Du and Stillman, 2002; Zhang et al., 2002) or the mRNA splicing machinery (Combs et al., 2006) suggest coordination of these processes as well. Furthermore, the nucleolar proteins Csm1 and Lrs4 are recruited to the kinetochores of meiotic chromosomes, where they are required for homolog segregation during meiosis I (Rabitsch et al., 2003). In this context, the physical and functional interactions between Utp7 and the Sli15/INCENP as well as RENT complexes suggest a potential functional link of ribosome biogenesis to the processes of chromosome segregation and mitotic exit. Since Utp7, Sli15 and Cdc14 are conserved from yeast to humans, this potential functional link may extend to other organisms.

CHAPTER FOUR

Regulation of Ipl1-Sli15 kinase complex and Glc7/PP1c phosphatase functions by Glc7 regulatory subunit Scd5

4.1. Introduction

The Ipl1–Sli15–Bir1 Aurora kinase complex of the budding yeast *Saccharomyces cerevisiae* is essential for proper chromosome segregation during mitosis and meiosis (Chan and Botstein, 1993; Cheeseman et al., 2002; Francisco et al., 1994; Kim et al., 1999; Monje-Casas et al., 2007; Yoon and Carbon, 1999). Sli15 targets Ipl1 and Bir1 to kinetochores and the anaphase spindle (Kang et al., 2001). It also stimulates the kinase activity of Ipl1 and is in turn a physiological substrate of Ipl1 (Cheeseman et al., 2002; Kang et al., 2001). However, the effect of Sli15 phosphorylation by Ipl1 is unknown. A similar complex (termed the chromosomal passenger complex) that contains homologs of Ipl1 (Aurora-B), Sli15 (INCENP), Bir1 (Survivin) – and a fourth subunit in some organisms – is present in other eukaryotes, including humans (Vader et al., 2006). The Ipl1 complex regulates diverse cellular processes during mitotic M phase, including including histone H3 phosphorylation (Hsu, 2000), kinetochore microtubule-attachment and bi-orientation (Biggins et al., 1999; Dewar et al., 2004; He et al., 2001; Sandall et al., 2006; Tanaka et al., 2002); transient spindle assembly checkpoint activation in response to lack of kinetochore tension (Biggins and Murray, 2001; King et al., 2007; Pinsky et al., 2006b); anaphase spindle stabilization and elongation (Bouck and Bloom, 2005; Buvelot et al., 2003; Higuchi and Uhlmann, 2005; Pereira and Schiebel, 2003; Widlund et al., 2006); condensation and complete segregation of the ribosomal DNA locus in late anaphase (Lavoie et al., 2004; Sullivan et al., 2004); and coordination of cytokinesis to the clearance of chromosomes from the spindle midzone (Norden et al., 2006).

In many of the processes described above, the function of the Ipl1 complex must be attenuated or counteracted after the relevant process has been completed. For example, the Ipl1 complex phosphorylates kinetochore proteins to cause kinetochore-

microtubule detachment at kinetochores that are not under tension. After sister kinetochores have subsequently become bi-oriented, phosphorylated substrates must be dephosphorylated and Ipl1 kinase activity must be attenuated to avoid futile cycles of kinetochore-microtubule attachment and detachment. Protein phosphatase 1 (PP1 or Glc7) plays a key role in counteracting Ipl1 function. Partial loss of Ipl1 function can be compensated by perturbations that lead to reduced PP1 function, suggesting that PP1 dephosphorylates and attenuates the activity of the Ipl1 complex or dephosphorylates substrates of Ipl1 (Francisco et al., 1994; Hsu et al., 2000; Pinsky et al., 2006a; Tung et al., 1995). Studies with some *glc7* mutants also indicate that PP1 regulates aspects of kinetochore function (Andrews and Stark, 2000; Baker et al., 1997; Black et al., 1995; Bloecher and Tatchell, 1999; Hisamoto et al., 1994; Sassoon et al., 1999). The activity, localization and substrate specificity of PP1 are regulated by the binding of PP1 to one or more of a large number of regulatory subunits (Ceulemans and Bollen, 2004). The Ypi1 and Sds22 regulatory subunits together are at least partly responsible for targeting Glc7 into the yeast nucleus (Pedelini et al., 2007; Peggie et al., 2002). However, which regulatory subunit targets PP1 to the Ipl1 complex and Ipl1 substrates within the nucleus is not known.

Scd5 is a regulatory subunit of PP1 that plays a crucial role in endocytosis and cortical actin organization (Henry et al., 2002; Nelson et al., 1996; Tu and Carlson, 1994). Scd5 is present predominantly in the cytoplasm and, like many endocytic proteins, is especially concentrated at cortical patches, some of which contain actin filaments (Henry et al., 2002). In addition, it associates with the cortical patch endocytic proteins Sla2 and Rvs167. The ability of Scd5 to bind PP1 (Chang et al., 2002), but not its cortical localization (Chang et al., 2006), is essential for normal endocytosis and cortical actin organization. Since the *glc7-10* mutation also affects cortical actin organization (Andrews and Stark, 2000), Scd5 likely targets PP1 to its physiological substrates in the cytoplasm to regulate cortical actin organization and endocytosis. Although Scd5 is not detectable cytologically in the nucleus of wild-type cells, it accumulates in the nucleus of *crm1* mutant cells that are defective in protein nuclear

export, thus indicating that Scd5 undergoes constitutive nuclear-cytoplasmic shuttling, with the export process being very fast or efficient in wild-type cells (Chang et al., 2006). Since Scd5, but not endocytosis, is essential for cell viability at 26°C, Scd5 may perform a function in the nucleus that is essential for cell viability.

Here I show that Scd5 and PP1 are present at kinetochores. Scd5 targets PP1 to the Ipl1 complex. Surprisingly, genetic and biochemical results suggest that Scd5 plays a positive role not only in the functioning of PP1, but also that of the Ipl1 complex. It does so at least partly by stimulating the kinase activity of Ipl1 and regulating the abundance, phosphorylation state and localization of Sli15. Cytological studies of *scd5* mutant cells indicate that Scd5 is essential for kinetochore bi-orientation, sister chromatid separation and proper chromosome segregation.

4.2. Scd5 functions as a positive regulator of both PP1 and the Ipl1 complex

To identify gene products that function with the Ipl1 protein kinase complex to regulate chromosome segregation, the Chan lab has previously isolated genes that in high copy number (when present on a 2μ plasmid) can suppress the Ts^- growth defect of *ipl1-1* mutant cells. Characterization of two such genes – *GLC8* and a truncated, dominant negative version of *GLC7* – provided the first evidence that PP1 counteracts the function of Ipl1 *in vivo* (Francisco et al., 1994; Tung et al., 1995). Another such multicopy suppressor of *ipl1-1* is *SCD5* (Fig. 4.1A), which has been identified independently as a multicopy suppressor of *ipl1-321* (Pinsky et al., 2006a). As a multicopy suppressor of *ipl1* mutations, *SCD5* potentially might function as a positive regulator of Ipl1 or as a negative regulator of Glc7. The *scd5-PP1Δ2* mutation alters a PP1-binding motif present on Scd5 (Fig. 4.1B) and very greatly reduces the ability of mutant $Scd5^{PP1\Delta2}$ to associate with Glc7 in the two-hybrid assay (Chang et al., 2002). In immunoprecipitation assays, precipitation of HA-Glc7 led to the co-precipitation of wild-type Scd5 but not mutant $Scd5^{PP1\Delta2}$ (Fig. 4.2A, lanes 7 and 8). The Ts^- growth phenotype and cortical actin organization defects of *scd5-PP1Δ2* cells are suppressed by a 2μ plasmid containing *GLC7* (Fig. 4.1C; (Chang et al., 2002)). Furthermore, the *glc7-127* mutation, which can

suppress partially the *ipl1-2* mutation (Hsu et al., 2000), is synthetic-lethal with *scd5-PP1Δ2* at 26°C (data not shown). Thus, Scd5 is a positive regulator of PP1.

The unexpected finding that over-expression of Scd5 – a positive regulator of PP1 – suppresses *ipl1* mutations prompted me to check genetically whether Scd5 might also positively regulate the function of the Ipl1 complex. My results showed that a 2μ plasmid containing *IPL1*, *SLI15* or *BIR1* could suppress the Ts^- growth phenotype of *scd5-PP1Δ2* cells (Fig. 4.1C). Furthermore, the *scd5-PP1Δ2* mutation exacerbated the Ts^- growth defect of *ipl1-2* cells, with the *ipl1-2 scd5-PP1Δ2* double mutant growing extremely slowly at 26°C, the permissive growth temperature for the two single mutants (Fig. 4.1D). In addition, diploid cells heterozygous for both the *scd5-PP1Δ2* and *ipl1-2* mutations were inviable at ≥30°C, whereas diploid cells heterozygous for either mutation grew well up to 37°C (Fig. 4.1E). This uncommon genetic relationship of unlinked non-complementation is most often observed between mutations that affect two proteins whose shared functions require their close physical association (e.g., α- and β-tubulin (Stearns and Botstein, 1988); actin and fimbrin (Welch et al., 1993)). These genetic results together suggest that Scd5 positively regulates the Ipl1 complex and it might do so through an association with this complex.

To find out whether Scd5 and Glc7 associate with the Ipl1 complex, I carried out co-immunoprecipitation assays with wild-type and mutant cells that were incubated at 26°C or for 3 h at 37°C. Similar results were obtained with both incubation conditions.

4.3. Scd5 and Glc7 associate with the Ipl1 complex

My results showed that immunoprecipitation of Scd5 or HA-Glc7 from wild-type cells led to the co-precipitation of Ipl1-Myc (Fig. 4.2B, lane 4; Fig. 4.2C, lane 6) and Sli15-Myc (Fig. 4.2D, lane 4; Fig. 4.2E, lane 6). In contrast, immunoprecipitation of mutant $Scd5^{PP1\Delta2}$ or HA-Glc7 from *scd5-PP1Δ2* cells did not lead to the co-precipitation

My results showed that immunoprecipitation of Scd5 or HA-Glc7 from wild-type cells led to the co-precipitation of Ipl1-Myc (Fig. 4.2B, lane 4; Fig. 4.2C, lane 6) and Sli15-

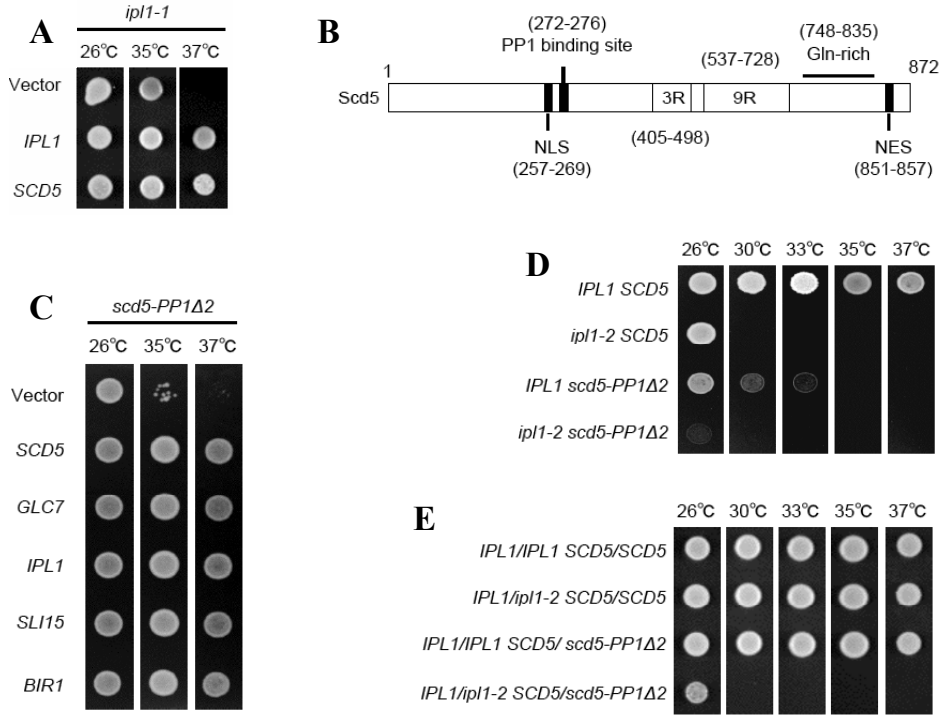

Figure 4.1. Scd5 functions as a positive regulator of both PP1 and the Ipl1 complex.
(A) Suspensions of *ipl1-1* cells carrying 2μ plasmid control, *IPL1*-containing CEN plasmid or *SCD5*-containing 2μ plasmid were spotted on YEPD agar and allowed to grow for 2 days at the indicated temperatures. (B) Features of Scd5 protein. NLS= nuclear localization signal; NES= nuclear export signal; PP1= Glc7 protein phosphatase 1; 3R= three repeats of 20 amino acids; 9R= nine repeats of 12 amino acids: GLN-rich= glutamine-rich. (C) Similar to (A) but with *scd5-PP1Δ2* cells carrying 2μ plasmid control, *SCD5*-containing CEN plasmid, or 2μ plasmid containing *GLC7, IPL1*, *SLI15*, or *BIR1*. (D) Similar to (A) but with haploid or (E) diploid yeast cells with the indicated genotype.

Myc (Fig. 4.2D, lane 4; Fig. 4.2E, lane 6). In contrast, immunoprecipitation of mutant Scd5$^{PP1\Delta2}$ or HA-Glc7 from *scd5-PP1Δ2* cells did not lead to the co-precipitation of Ipl1-Myc (Fig. 4.2B, lane 5; Fig. 4.2C, lane 7) or Sli15-Myc (Fig. 4.2D, lane 5; Fig. 4.2E, lane 7). Thus, the Scd5–Glc7 complex associates with the Ipl1 complex in wild-type cells and this association is abolished by the *scd5-PP1Δ2* mutation (which also abolishes the association between Scd5 and Glc7). This latter observation can be interpreted in two ways. First, Scd5 and Glc7 might need to be in a complex for them to associate with the

Ipl1 complex. Second, Scd5 might bridge the association between Glc7 and the Ipl1 complex, and the *scd5-PP1Δ2* mutation affects the structure of Scd5 in such a way that mutant Scd5$^{PP1\Delta2}$ can no longer bind Glc7 or the Ipl1 complex.

The association of Scd5–Glc7 with the Ipl1 complex prompted me to check whether the association between Scd5 and Glc7 requires a functional Ipl1 complex. My results showed that the association between HA-Glc7 and Scd5 could no longer be detected in *ipl1-2* cells (Fig. 4.2A, lane 10). Thus, a functional Ipl1 complex is required for the formation or stability of the Scd5–Glc7 complex (and Scd5 positively regulates the function of the Ipl1 complex). Since the ability of Scd5 to bind Glc7 is essential for normal endocytosis (Chang et al., 2002), I collaborated with the Sandy Lemmon lab to examine endocytosis in *ipl1-2* cells. Preliminary results from the Lemmon lab showed that *ipl1-2* cells are partially defective in endocytosis after a 15-min incubation at 37°C (data not shown).

4.4. Scd5 and Glc7 are present at kinetochores

The Ipl1 complex is present at kinetochores and the mitotic spindle. The Scd5–Glc7 complex potentially might associate with the Ipl1 complex at one or both of these sites. In wild-type cells, Scd5 cannot be detected cytologically in the nucleus (Henry et al., 2002). Thus, I used the more sensitive chromatin immunoprecipitation (ChIP) assay to check whether Scd5 and Glc7 are present at kinetochores, using wild-type and mutant cells that were incubated at 26°C or for 3 h at 37°C. Similar results were obtained with both incubation conditions, except when *ndc10-1* cells were used. My results showed that Scd5 and Glc7 could be crosslinked to centromeres (CEN) 3 and 16, but not to the *CIT3* locus located ~1 kb from CEN16 (Fig. 2F; data not shown). The centromere-association of Scd5 and Glc7 – like that of Ipl1-Myc, Sli15-Myc and most kinetochore proteins – was abolished by the *ndc10-1* mutation (at 37°C). Furthermore, the centromere-association of Scd5 and Glc7 was unaffected by the *scd5-PP1Δ2* or *ipl1-2* mutation. Thus, Scd5 and Glc7 can be recruited to kinetochores without associating with each other or with the Ipl1 complex.

4.5. Scd5 is an *in vitro* stimulator and substrate of the Ipl1 kinase

The genetic and co-immunoprecipitation results described above indicate that Scd5 associates with the Ipl1 complex and positively regulates its function. To find out whether Scd5 positively regulates Ipl1 by stimulating its kinase activity, I performed *in vitro* kinase assays with recombinant GST-Ipl1 and GST-Scd5 that were purified from *Escherichia coli*. As it has been shown previously (Kang et al., 2001), GST-Ipl1 efficiently phosphorylated GST-Dam1-C (containing the COOH-terminal 169 residues of Dam1). The ability of GST-Ipl1 to phosphorylate GST-Dam1-C was stimulated by the addition of GST-Scd5, and the extent of stimulation was dependent on the amount of GST-Scd5 used (data not shown). Thus, Scd5, like Sli15, is a stimulator of Ipl1. The ability of GST-Scd5 alone to stimulate the *in vitro* kinase activity of GST-Ipl1 also suggested that Scd5 that is not in a complex with Glc7 could bind directly (but not necessarily stably) to the Ipl1 complex.

In these *in vitro* kinase assays, GST-Scd5 but not GST was efficiently phosphorylated by GST-Ipl1. Thus, GST-Ipl1 phosphorylates Scd5 *in vitro*. In immunoblotting experiments with wild-type yeast extracts, multiple forms of Scd5 that differed in electrophoretic mobility could be detected (data not shown). The abundance of the slowest migrating (and presumably hyper-phosphorylated) form of Scd5 was greatly reduced in *ipl1-2* cells. Thus, Scd5 likely is a physiological substrate of Ipl1, and this phosphorylation might be important for the association of Scd5 with Glc7.

4.6. *scd5-PP1Δ2* cells missegregate chromosomes severely

Since the Ipl1 complex and PP1 are both required for proper chromosome segregation, I suspected that Scd5 is also required for this process. To study chromosome

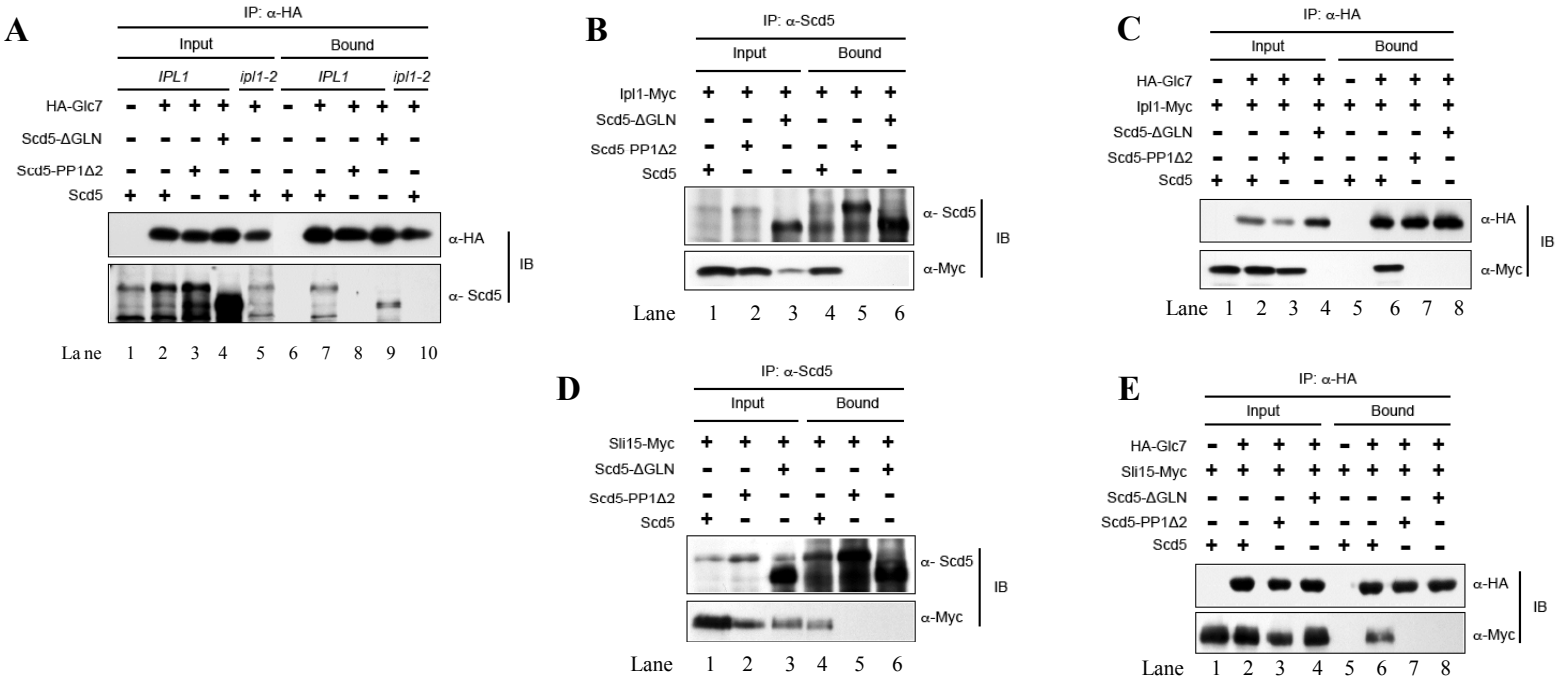

Figure 4.2. Scd5 and Glc7 associate with the Ipl1 complex.
(A) Wild-type, *scd5-PP1Δ2*, *scd5-ΔGLN* and *ipl1-2* cells that expressed (+) HA-Glc7 from CEN plasmid were shifted to 37°C for 3 h. HA-Glc7 was immunoprecipitated (IP) from cell extracts with anti-HA antibodies. Immunoprecipitated proteins were immunoblotted (IB) with anti-HA or anti-Scd5 antibodies. (B) Wild-type, *scd5-PP1Δ2* and *scd5-ΔGLN* cells that expressed (+) Ipl1-Myc alone or in combination with (C) HA-Glc7 from CEN plasmid were shifted to 37°C for 3 h. (B) Scd5 or (C) HA-Glc7 was immunoprecipitated (IP) from cell extracts with anti-Scd5 or anti-HA antibodies, respectively. Immunoprecipitated proteins were immunoblotted (IB) with anti-Myc, anti-HA or anti-Scd5 antibodies. (D) and (E) Similar to (B) and (C), respectively, but with the cells expressing Sli15-Myc instead of Ipl1-Myc.

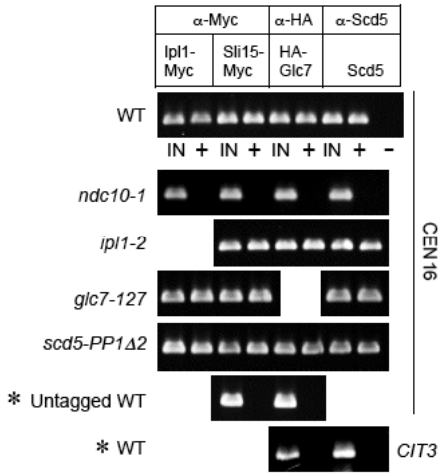

Figure 4.3. Scd5 is a kinetochore protein and does not affect the kinetochore association of Ipl1 kinase

Chromatin immunoprecipitation was carried out with anti-Myc, anti-HA or anti-Scd5 antibodies, using extracts from cells that were incubated at 26°C and then shifted to 37°C for 3 h. The yeast cells used were: wild-type, *ndc10-1*, *ipl1-2, gl7-127, scd5-PP1Δ2* cells; such cells expressing HA-Glc7 from CEN plasmid, Ipl1-Myc or Sli15-Myc. CEN16 and *CIT3* sequences were amplified by PCR from the total input chromatin (IN), antibody-immunoprecipitated samples (+),or mock treated no-antibody control (–).

segregation, I shifted asynchronous cultures of wild-type and *scd5-PP1Δ2* cells from 26 to 37°C. 3 h after shift, ~72% of *scd5-PP1Δ2* cells became large-budded (vs. ~35% for wild-type cells) (Fig. 4.4B). Staining of microtubules and DNA revealed that ~90% of these large-budded *scd5-PP1Δ2* cells had a short spindle (vs. ~20% for wild-type cells). In contrast, *scd5-PP1Δ2* cells that also contained the *mad2*Δ mutation did not accumulate as large-budded cells with a short spindle (data not shown). These results together indicated that the spindle assembly checkpoint was activated in many *scd5-PP1Δ2* cells, likely as a consequence of the presence of unattached kinetochores.

In support of this conclusion, the ~10% of large-budded *scd5-PP1Δ2* cells that entered anaphase missegregated chromosomes severely, with very uneven amounts of chromosomal DNA being distributed to the two poles of the elongated spindle (Fig. 4.4A). These phenotypes of *scd5-PP1Δ2* cells appear to be a combination of the phenotypes observed in *ipl1*/*sli15* and some *glc7* mutant cells. *glc7-129* mutant cells become arrested as large-budded cells with a short spindle due to spindle assembly checkpoint activation (Bloecher and Tatchell, 1999). In contrast, *ipl1* and *sli15* mutants readily enter anaphase and segregate chromosomes very unevenly (Biggins et al., 1999; Francisco et al., 1994; Kim et al., 1999).

The microtubules in *scd5-PP1Δ2* cells were also abnormal in a number of ways. First, the number of cytoplasmic microtubules was significantly increased in *scd5-PP1Δ2* cells (Fig. 4.4C). Second, cytoplasmic microtubules in *scd5-PP1Δ2* cells were often much longer than those in wild-type cells (Fig. 3A). Third, gaps in staining were often seen in the cytoplasmic and spindle microtubules of *scd5-PP1Δ2* cells (Fig. 4.4A; arrows). Thus, Scd5 plays a role in regulating microtubule structure and function in both the cytoplasm and the nucleus.

4.7. Unipolar kinetochore-microtubule attachment in *scd5-PP1Δ2* cells

To better understand the nature of chromosome missegregation in *scd5-PP1Δ2* cells, I examined chromosome segregation in wild-type and *scd5-PP1Δ2* cells that had the spindle pole body marked by Spc110-RFP (Yoder et al., 2003) and CEN5 marked by the binding of TetR-GFP to tandem TetO sites located ~1.4 kb from CEN5 (Tanaka et al., 2000). After 3 h at 37°C, all pre-anaphase/metaphase wild-type cells with well-separated spindle pole bodies had TetR-GFP dots that were always located close to the spindle axis defined by the separated spindle pole bodies because sister kinetochores were bi-oriented in these cells (Fig. 4.5A). Most (~84%) of such cells had two TetR-GFP dots due to the normal, precocious separation (and occasional re-association) of sister kinetochores that were bi-oriented and under tension (Goshima and Yanagida, 2000; He et al., 2000). In contrast, only ~12% of pre-anaphase/metaphase *scd5-PP1Δ2* cells had two TetR-GFP

dots that were located close to the spindle axis. The remainder had a single TetR-GFP dot, the majority (75/88) of which was located very close to the old spindle pole body that was destined for the bud. Since the spindle assembly checkpoint was activated in the majority of *scd5-PP1Δ2* cells, these results suggested that often only one of the two kinetochores in a sister pair was attached to a microtubule in these cells and this attachment was preferentially to a microtubule that emanated from the old spindle pole body. This bias in kinetochore-attachment to microtubules from the old spindle pole body is similar to that observed in *ipl11-2* and *sli15-3* cells (Tanaka et al., 2002). However, it should be noted that both sister kinetochores are thought to be attached to microtubules from the old spindle pole body in *ipl11-2* and *sli15-3* cells, whereas only one kinetochore of the sister pair is likely attached in *scd5-PP1Δ2* cells.

4.8. *scd5-PP1Δ2* cells are defective in sister chromatid separation

After 3 h at 37°C, all wild-type cells that were in late anaphase had 2 TetR-GFP dots, with each locating close to a different spindle pole body (Fig. 4.5B). In contrast, most (~84%) *scd5-PP1Δ2* cells that managed to reach late anaphase had a single TetR-GFP dot that was located very close to the spindle pole body in the bud. Thus, sister kinetochores of *scd5-PP1Δ2* cells failed to separate from each other during anaphase, indicating that *scd5-PP1Δ2* cells are defective in sister chromatid separation. To find out whether this sister chromatid separation defect affected only the kinetochore region, I examined the segregation pattern of TetR-GFP that binds to tandem TetO sites located 35 kb from CEN5. I shifted asynchronous cultures of wild-type, *mad2*Δ, *scd5-PP1Δ2* and *scd5-PP1Δ2 mad2*Δ cells from 26 to 37°C. The *mad2*Δ mutation allowed a greater fraction of *scd5-PP1Δ2* cells to enter anaphase and should alleviate potential problems caused by cell cycle arrest that resulted from spindle assembly checkpoint activation. After 3 h at 37°C, almost all wild-type (100%) and *mad2*Δ (98%) cells that were in late anaphase had two TetR-GFP dots, with each dot associating with each separated chromosomal DNA mass (Fig. 4.5C). In contrast, most *scd5-PP1Δ2* (79%) and *scd5-PP1Δ2 mad2*Δ (85%) cells that were in late anaphase had a single TetR-GFP dot. These

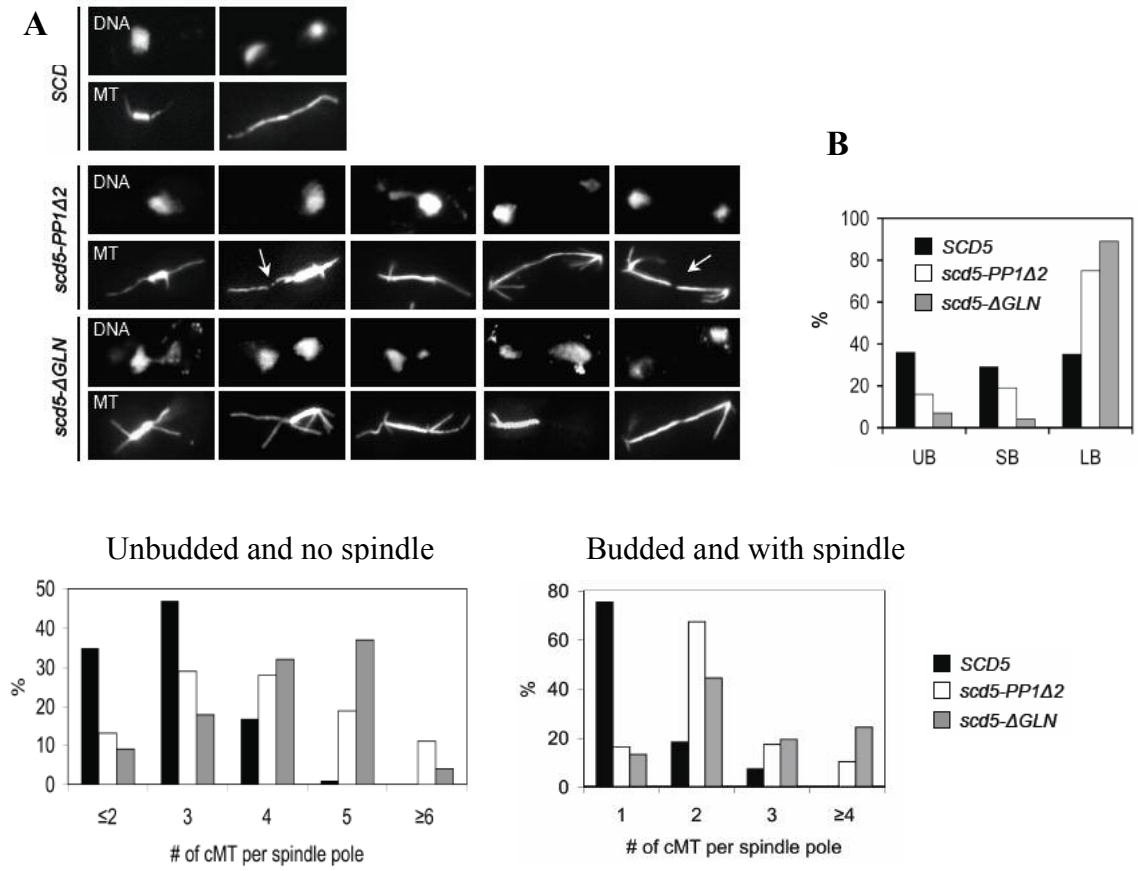

Figure 4.4. Mutations in *SCD5* cause chromosome missegregation and overproduction of cytoplasmic microtubule.
(A) Wild-type, *scd5-PP1Δ2* and *scd5-ΔGLN* cells growing exponentially at 26°C were shifted to 37°C for 3 h. Budding index (UB, unbudded; SB, small-budded; LB, large-budded) of 100 cells each was scored. (B) The microtubule (MT) and DNA in these cells were stained and images of large-budded cells are shown. Arrows point at broken microtubule. (C) The number of cytoplasmic microtubule (cMT) per spindle pole in these stained cells was counted. 100 cells that were unbudded or budded were scored.

results together indicate that *scd5-PP1Δ2* cells are defective in the separation of sister kinetochores and sister chromosome arms during anaphase.

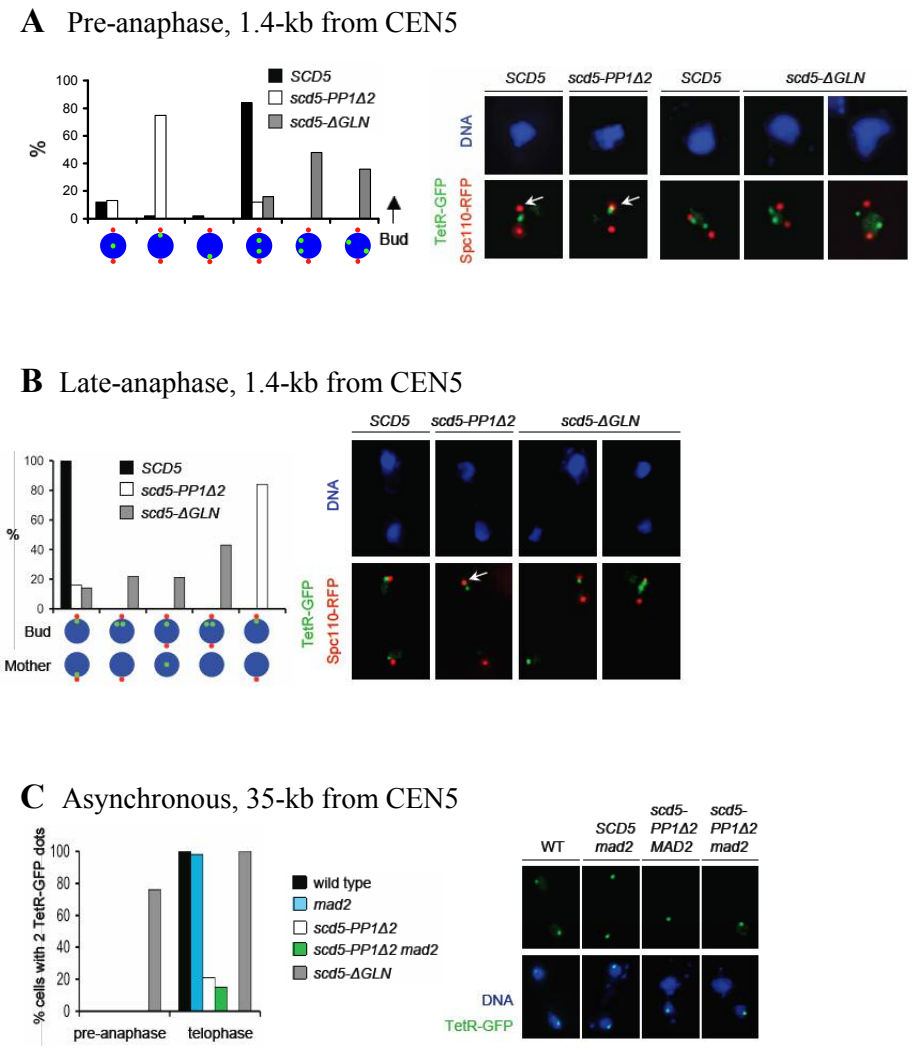

Figure 4.5. Scd5 regulates kinetochore bi-orientation and sister chromatid cohesion.
(A) Wild-type and *scd5-PP1Δ2* cells expressing Spc110-RFP and TetR-GFP that binds to tandem TetO repeats located 1.4-kb away from CEN5 were incubated at 26°C and then shifted to 37°C for 3 h. DNA was stained with DAPI and cells with well separated spindle poles that were in pre-anaphase, or (B) in late-anaphase were imaged. 100 cells at each stage were scored. (C) Yeast cells with the indicated genotype expressing TetR-GFP that binds to tandem TetO repeats located 35-kb away from CEN5 were incubated at 26°C and then shifted to 37°C for 3 h. DNA was stained with DAPI and 100 cells in pre-anaphase or telophase were scored. Images of representative cells in telophase are shown.

4.9. Discussion

I have shown here that the PP1-binding protein Scd5, which is present predominantly in the cytoplasm, is also present at kinetochores. Scd5 positively regulates PP1 function by targeting PP1/Glc7 to cortical actin patches and the Ipl1 complex at kinetochores. It is not known whether it also regulates the enzymatic activity of PP1. In addition, Scd5 also regulates positively the Ipl1 complex, at least partly by stimulating the kinase activity of Ipl1. Scd5 is required for proper kinetochore-MT attachment, sister chromatid separation and mitotic spindle stability.

4.9.1. Protein phosphatase 1 (PP1), Ipl1-Sli15 and chromosome segregation

Early work in the Chan lab with Glc7 and Glc8 led to the idea that PP1 counteracts the *in vivo* function of Ipl1 (Francisco et al., 1994; Tung et al., 1995), possibly by dephosphorylating and inactivating the Ipl1 complex or by dephosphorylating Ipl1 substrates. A similar functional relationship has since been established for the metazoan Aurora-B kinase complex and PP1 (Hsu et al., 2000; Murnion et al., 2001; Sugiyama et al., 2002). However, how PP1 is targeted to Ipl1/Aurora-B or its substrates is not known in yeast or any other organism. My work presented here shows for the very first time that the PP1-binding protein Scd5 targets PP1 to the Ipl1 complex at kinetochores. Surprisingly, Scd5 also positively regulates Ipl1 function, at least partly by stimulating the kinase activity of Ipl1. The observation that Scd5 associates with and positively regulates the functions of the Ipl1 complex and PP1 places Scd5 at the center of a regulatory circuit where Scd5 may control and coordinate the apparently opposing enzymatic activities of Ipl1 and Glc7. Obviously, how Scd5 carries out its function will be the focus of future work.

Before establishment of sister kinetochore bi-orientation, Ipl1 function is needed to correct inappropriate kinetochore-microtubule attachment. In this process, Ipl1 phosphorylates specific kinetochore proteins (e.g., Ndc80) to cause kinetochore-microtubule detachment. Once bi-orientation (or bipolar attachment) is established, Ipl1 function should be down-regulated to avoid futile cycles of microtubule attachment and

detachment. Proteins (e.g., Ndc80) previously phosphorylated by Ipl1 should also be dephosphorylated to prevent kinetochore-microtubule detachment. Down-regulation of Ipl1 could be achieved by increasing the abundance of the opposing PP1 at the site of Ipl1 function. In one model (Fig. 4.6A), Scd5 does not associate with PP1/Glc7 before sister kinetochore bi-orientation. Instead, it associates with the Ipl1 complex and stimulates Ipl1 kinase activity. After establishment of bi-orientation and tension between sister kinetochores, PP1/Glc7 is recruited to Scd5 and binding of PP1 to Scd5 inhibits the ability of Scd5 to stimulate the kinase activity of Ipl1 without affecting its ability to bind the Ipl1 complex. In this process, Glc7 is recruited to the Ipl1 complex, where it can dephosphorylate and inactivate the Ipl1 complex or Ipl1 substrates that are in the vicinity.

An alternative model predicts the presence of an unknown inhibitor of PP1/Glc7 at kinetochores (Fig. 4.6B). In this model, the Scd5-Glc7 complex associates with the Ipl1 complex at kinetochores that are not bi-oriented. Scd5 stimulates Ipl1 kinase activity and the inhibitor protein prevents PP1/Glc7 from dephosphorylating the Ipl1 complex or Ipl1 substrates. Once bi-orientation has occurred, the affinity of the inhibitor for PP1/Glc7 is reduced, possibly due to changes in the phosphorylation status of the inhibitor-Glc7 complex. Dissociation of the inhibitor from PP1/Glc7 allows PP1 to antagonize Ipl1 functions. One candidate for the hypothetic kinetochore inhibitor of Glc7 is Glc8, which is structurally and functionally related to mammalian inhibitor-2 (Tung et al., 1995). When present at physiological level, Glc8 functions as an activator for overall PP1 activity in a cell. However, when Glc8 is overproduced, it functions as a general inhibitor of PP1 activity. Furthermore, Glc8, like inhibitor-2, can inhibit the *in vitro* phosphatase activity of PP1. However, it is not known whether Glc8 functions as an *in vivo* inhibitor of PP1 at specific sites (e.g., kinetochores) within yeast. It is noteworthy that Glc8 is an *in vitro* substrate of Ipl1, and mutations in *GLC8* and *SCD5* exhibit unlinked noncomplementation genetic relationship (data not shown).

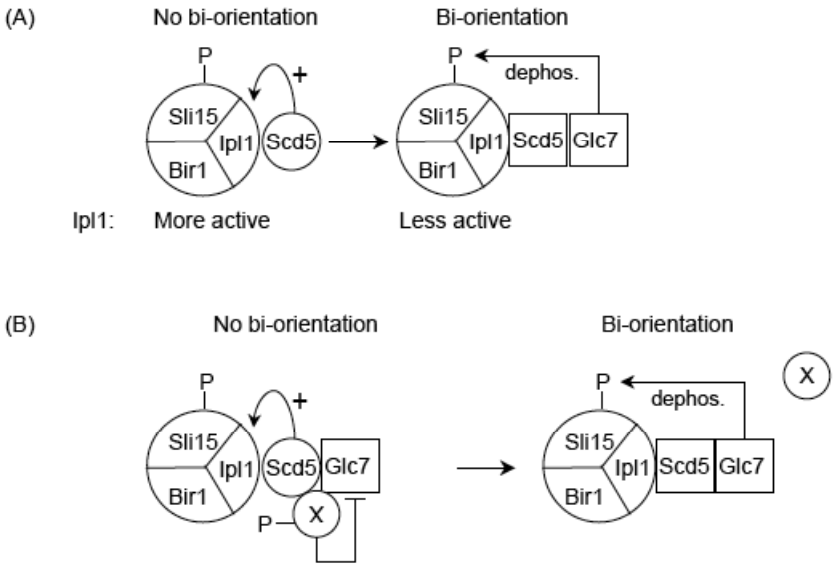

Figure 4.6. Models for Scd5 function.

X= a hypothetic inhibitor of PP1/Glc7; dephos. = dephosphorylation; (+) = stimulation of Ipl1 kinase activity; P = phosphate group. See text for detail.

4.9.2. Sister chromatid separation in *scd5-PP1Δ2* mutant cells

When the pre-anaphase block in *scd5-PP1Δ2* mutant cells is bypassed by simultaneous inactivation of Mad2, *scd5-PP1Δ2 mad2Δ* cells that are in anaphase fail to separate sister chromatids and the Scc1 cohesin subunit remains chromatin-bound (data not shown). In wild-type cells, activation of the anaphase-promoting complex (APC) leads to the multi-ubiquitination and degradation of securin (Pds1). This leads to activation of the securin-binding partner separase (Esp1), which cleaves the Scc1 subunit of the cohesin complex, resulting in the loss of Scc1 from chromatin and subsequent sister chromatid separation (Nasmyth, 2002). Persistent association of Scc1 on the chromatin of *scd5-PP1Δ2 mad2Δ* cells through anaphase suggests that these cells are defective in the degradation of securin, which can be monitored simply by immunoblotting. If securin is indeed not degraded, I doubt that defective APC is the cause of failure in securin degradation because *scd5-PP1Δ2 mad2Δ* cells progress

through anaphase and exit from mitosis, which require normal APC function to degrade a large number of proteins (e.g., mitotic cyclins such as Clb2; kinesin-like proteins such as Cin8 and Kip1; spindle midzone assembly proteins such as Ase1; DNA replication factor Dbf4; Swe1 inhibitor Hsl1). Instead, the phosphorylation and localization of securin may be abnormal in *scd5-PP1*Δ*2 mad2*Δ cells. In wild-type cells, securin and separase enter the nucleus in late G2 (Jensen et al., 2002), and nuclear entry requires phosphorylation of securin by CDK (Argawal and Cohen-Fix, 2002). In wild-type cells that have suffered DNA damage, activation of the Chk1 kinase leads to phosphorylation of securin by Chk1 and inhibition of securin degradation (Wang et al., 2001). The nuclear import and phosphorylation of Securin can be monitored by immunofluorescent microscopy and immunoblotting, respectively. These experiments should tell me which aspect of sister chromatid separation is defective in *scd5-PP1*Δ*2* cells. Results from these experiments might also reveal potential relationship of the *scd5-PP1*Δ*2* mutation with kinases (or phosphatases) other than Ipl1 (or PP1).

4.9.3. Separation of the multiple functions of Scd5

The cytological, molecular and genetic studies of *scd5-PP1Δ2* cells that I have shown here indicate that Scd5 performs multiple functions at least in part through its association with Ipl1 or PP1/Glc7. To understand the function of Scd5 in detail, it is important to know the biological consequence when only the interaction between Scd5 and the Ipl1 complex or only the interaction between Scd5 and PP1 is compromised. *scd5* mutations that affect the binding of Scd5 to only the Ipl1 complex or only PP1/Glc7 will enhance our understanding of the Ipl1- and PP1-specific functions of Scd5. In Fig. 4.6, I have proposed models for Scd5 functions at kinetochores. The models predict sequential activation of the Ipl1 complex and PP1/Glc7. These *scd5* mutations should block specific steps of this hypothetic sequential activation process and lead to specific phenotypic consequences.

Scd5 plays a role in sister chromatid separation. This function of Scd5 is likely independent of Ipl1 because *ipl1-321* mutant cells separate sister chromatids with wild-

type kinetics (Biggins et al., 1999). In addition, there has been no report so far that PP1 is involved in this process in yeast. Examination of sister chromatid separation in the many *glc7* mutants isolated by the Tatchell lab (Baker et al., 1997) may reveal that PP1 is required for this process. Furthermore, if the sister chromatid separation defect of *scd5-PP1Δ2* cells is caused by the failure of mutant Scd5 to associate with PP1, I would expect Scd5 mutants specifically defective in its association with PP1 (see last paragraph), but not mutants defective in its association with the Ipl1 complex, to fail in sister chromatid separation. Alternatively, Scd5 may regulate sister chromatid separation independent of its association with PP1 or the Ipl1 complex. A number of nuclear proteins that associate with Scd5 in two-hybrid assays have been identified (data not shown). One of these proteins may mediate the sister chromatid function of Scd5.

CHAPTER FIVE

Perspectives

The aim of this thesis was to understand how the Ipl1-Sli15-Bir1 kinase complex is regulated to maintain genomic stability in the budding yeast *Saccharomyces cerevisiae*. My work presented in Chapters 3 and 4 shows that the predominantly nucleolar protein Utp7 and the predominantly cytoplasmic protein Scd5 function at kinetochores to regulate the Ipl1-Sli15-Bir1 chromosomal passenger complex and chromosome segregation.

5.1. Ribosome biogenesis, other vital cellular processes and tumorigenesis

The nucleolus is a clearly differentiated nuclear sub-compartment. The most obvious function of the nucleolus is ribosome biogenesis and it has been a subject of research for decades. Emerging evidence points to additional unconventional roles for the nucleolus. Recent works in yeast have linked ribosome biogenesis to other cellular processes. Noc3, which is essential for pre-RNA processing and pre-ribosome maturation in the nucleolus, also associates with the origin recognition complex (ORC) and is required for the loading of specific DNA replication initiation proteins at chromosomal replication origins (Zhang et al., 2002). Yph1, which is required for the biosynthesis of the 60S large ribosomal subunit, also interacts with the ORC and controls initiation of chromosomal DNA replication (Du et al., 2002). In addition, Yph1 is required for entry into the cell cycle from G_0 (Du et al., 2002). This transition point is important for cell proliferation control since it dictates whether a cell would progress through the cell cycle or be quiescent. A key factor in this control for most cell types is the availability of energy source. Therefore, it would make sense to coordinate cellular processes that require high-energy input (e.g., ribosome biogenesis and chromosomal DNA replication) with cell cycle entry.

My work on Utp7 further links ribosome biogenesis to kinetochore function and mitotic exit. Interestingly, Rrb1, a Yph1-interacting protein, is implicated in the control

of kinetochore-microtubule attachment and chromosome segregation (Killian, et al., 2004). Inactivation of Rrb1 leads to spindle assembly checkpoint activation and chromosome instability (CIN), which is a hallmark of most human cancer cells (Lengauer et al., 1998). Ribosome biogenesis is the target of tumor suppresser genes (e.g., RB and TP53) and oncogenes (e.g., c-myc), and it is altered in cancer cells (reviewed in Ruggero and Pandolfi, 2003). Therefore, mutational alterations of proteins that link ribosome biogenesis and chromosome segregation (e.g., Utp7) may represent additional causes for CIN and may contribute to tumorigenesis. In this regard, alteration in ribosome biogenesis might also lead to de-regulation in DNA replication and cell proliferation, which would facilitate tumorigenesis and favor cancer cell proliferation.

Although it is possible that Utp7 is a multifunctional protein that independently controls or functions in ribosome biogenesis, chromosome segregation and mitotic exit, I favor the view that Utp7 coordinates ribosome biogenesis with chromosome segregation and mitotic exit control. It is currently not known whether there is crosstalk between these important cellular events. However, it is clear that other ribosome biogenesis proteins (e.g., possibly Rrb1) also function at kinetochores. The budding yeast protein Cbf5 was initially identified as a protein that binds centromere DNA with low affinity (Jiang et al., 1993). The presence of an extra copy or two of the essential *CBF5* gene partially suppresses the Ts^- phenotype caused by a mutation in the inner-kinetochore protein Ndc10 (Jiang et al., 1993). A recent large-scale mass spectrometric analysis of yeast protein complexes has also identified Cbf5 as one of 8 proteins that associate with Ipl1 (Krogan et al., 2006). Since Cbf5 is concentrated in the nucleolus where it associates with some subunits of the SSU processome (Grandi et al., 2002) and functions as a pseudouridine synthase to modify uracil residues present in rRNAs (Lafontaine et al., 1998), the potential function of Cbf5 in chromosome segregation has been largely ignored. However, a point mutation in *CBF5* that abolishes all measurable pseudouridylation of rRNA *in vivo* only compromises cell growth moderately (Zebarjadian et al., 1999), thus suggesting that rRNA pseudouridylation is not the essential function for Cbf5. Furthermore, the Ts^- *swoC1* mutation in the *Aspergillus*

nidulans homolog of Cbf5 compromises microtubule-dependent cellular processes without noticeably affecting rRNA pseudouridylation (Lin and Momany, 2003). Furthermore, germline mutation of the human Cbf5 homolog Dyskerin (or DKC1) causes X-linked dyskeratosis congenita, a genetic disease characterized by increased tumor susceptibility and is considered a CIN disorder (Heiss et al., 1998). Therefore, it is tempting to speculate that Cbf5 functions with Utp7 to link ribosome biogenesis with the Ipl1 complex, chromosome segregation and cell cycle regulation.

There are additional evidences that link kinetochores to the nucleolus, where ribosome biogenesis occurs. Human Aurora-B and INCENP (homologs of Ipl1 and Sli15, respectively) are present in highly purified preparations of nucleoli (Andersen et al., 2005), and human INCENP has been reported to be present in the nucleoli of interphase cells (Wong et al., 2007). Furthermore, Aurora-B phosphorylates the RNA methyltransferase NSUN2 to regulate the assembly of a nucleolar RNA-processing complex (Sakita-Suto et al., 2007). Budding yeast Ipl1 and Sli15 are not detectable cytologically in the nucleolus. However, it is not known whether these proteins may transit rapidly through the nucleolus. If they do, it is unlikely that they regulate ribosome biogenesis since the *ipl1-2* and *sli15-3* mutations do not affect ribosome biogenesis (data not shown). Instead, they may regulate the emerging number of non-ribosome biogenesis processes that occur within the nucleolus. These studies will take us one-step forward to understanding of how nuclear activities are coordinately integrated with the nucleolar activities.

5.2. Functional relationship between Ipl1, PP1 and Utp7 at kinetochores

As discussed in section 4.9.1, once tension and bi-orientation have occurred, Ipl1 function must be repressed or counteracted to prevent futile cycles of attachment and detachment. Ipl1 function at kinetochores may be repressed or counteracted in a number of ways, including: (a) removal of Ipl1 itself; (b) removal or inhibition of its stimulator Sli15 or Scd5, and (c) association of an unknown inhibitor or the counteracting PP1, which dephosphorylates at least some Ipl1 substrates and possibly down-regulates Ipl1

kinase activity. Utp7 also regulates Ipl1 complex function at kinetochores since the centromere-association of Sli15 but not Ipl1 is greatly reduced in *utp7-26* cells. What Utp7 does exactly at kinetochores is unknown, but it may regulate the association of Sli15 with Ipl1 until bi-orentation is established. To understand how Ipl1 function is regulated or counteracted during different stages of kinetochore-attachment, it would be interesting to analyze systematically: (a) which of the proteins mentioned above are present at kinetochores under different states of kinetochore-microtubule attachment; and (b) which protein associates with Ipl1 under each condition. This can be accomplished by using two sets of strains, each containing the *cdc26*Δ mutation that allows cell cycle synchronization in the pre-anaphase stage at 37ºC. One set of strains will also contain the *stu2-279* mutation, which abolishes sister kinetochore tension but not kinetochore-microtubule attachment (He et al., 2001; Severin et al., 2001; Gillett et al., 2004). This should create a situation analogous to monopolar attachment (i.e., both kinetochores attached to microtubules form the same pole and hence experience no tension). These strains will allow the examination of uniform populations of cells that have sister kinetochores that are attached and under tension (i.e., bi-oriented; condition (a) in Fig. 5.1) or sister kinetochores that are attached but not under tension (condition (b) in Fig. 5.1). In the presence of the microtubule-depolymerizing drug nocodazole, all kinetochores would be unattached (condition (c) in Fig. 5.1).

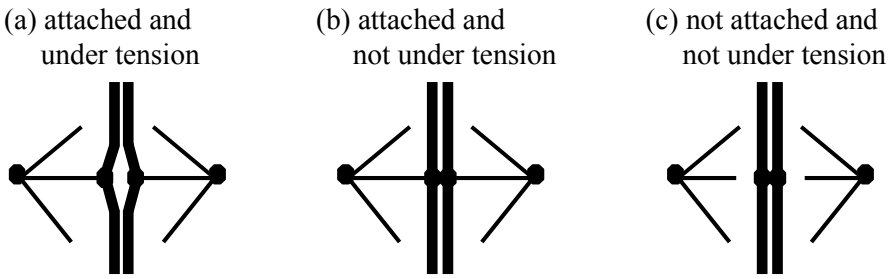

Figure 5.1. Possible kientochore status.

A combination of co-immunoprecipitation and chromatin immunoprecipitation should reveal which of these proteins is present at kinetochores and which associates with Ipl1 under the different states of kinetochore-microtubule attachment. The model described in Fig. 4.6A predicts that Scd5 should associate with Ipl1 and be present at kinetochores in both conditions (a) and (b), whereas PP1 should associate with Ipl1 (and be present at kinetochores) only in condition (a). In contrast, the model described in Fig. 4.6B predicts that PP1 would associate with Ipl1 and be present at kinetochores in both conditions (a) and (b), whereas the inhibitor of PP1 (X or possibly Glc8) should associate with Ipl1 (and be present at kinetochores) only in condition (b). Proteins that have different properties under conditions (c) vs. (a) and (b) are also interesting. For example, a protein involved in kinetochore-microtubule attachment checkpoint activation in response to unattached kinetochores (e.g., possibly Utp7) may be present at higher abundance at kinetochores that are not attached to microtubules (i.e., condition (c)). This systematic analysis will enhance our understanding of the molecular mechanism by which the Ipl1, Sli15, Bir1, PP1, Scd5 and Utp7 proteins regulate kinetochore-microtubule attachment. How the Ipl1 complex monitors tension at kinetochores and how it translates the tension into chemical signals to affect downstream events still remain to be determined.

REFERENCES

Adams, I. R. , and Kilmartin, J. V. (2000). Spindle pole body duplication, a model for centrosome duplication? Trends Cell Biol *10*, 329–335.

Agarwal, R., and Cohen-Fix, O. (2002). Phosphorylation of the mitotic regulator Pds1/securin by Cdc28 is required for efficient nuclear localization of Esp1/separase. Genes Dev *16*, 1371-1382.

Anderson, C. W., Baum, P. R., and Gesteland, R. F. (1973). Processing of adenovirus 2-induced proteins. J Virol *12*, 241-252.

Andersen, J. S., Lyon, C. E., Fox, A. H., Leung, A. K. L., Lam, Y. W., Steen, H., Mann, M., and Lamond, A. I. (2002). Directed proteomic analysis of the human nucleolus. Curr Biol *12*, 1-11.

Andersen, J. S., Lam, Y. W., Leung, A. K. L., Ong, S.-E., Lyon, C. E., Lamond, A. I., and Mann, M. (2005). Nucleolar proteome dynamics. Nature *433*, 77-83.

Andrews, P. D., and Stark, M. J. R. (2000). Type 1 protein phosphatase is required for maintenance of cell wall integrity, morphogenesis and cell cycle progression in *Saccharomyces cerevisiae*. J Cell Sci *113*, 507-520.

Arumugam, P., Gruger, S., Tanaka, K., Haering, C. H., Mechtler, K., and Nasmyth, K. (2003). ATP hydrolysis is required for cohesin's association with chromosomes. Curr Biol *13*, 1941–1953.

Asakawa, K., and Toh-e, A. (2002). A defect of Kap104 alleviates the requirement of mitotic exit network gene functions in *Saccharomyces cerevisiae*. Genetics *162*, 1545-1556.

Ault, J. G., and Rieder, C. L. (1992). Chromosome mal-orientation and reorientation during mitosis. Cell Motil Cytoskeleton *22*, 155–159.

Azzam, R., Chen, S. L., Shou, W., Mah, A. S., Alexandru, G., Nasmyth, K., Annan, R. S., Carr, S. A., and Deshaies, R. J. (2004). Phosphorylation by cyclin B-Cdk underlies release of mitotic exit activator Cdc14 from the nucleolus. Science *305*, 516-519.

Baker, S. H., Frederick, D. L., Bloecher, A., and Tatchell, K. (1997). Alanine-scanning mutagenesis of protein phosphatase type 1 in the yeast *Saccharomyces cerevisiae*. Genetics *145*, 615-626.

Bender, A., and Pringle, J. (1991). Use of a screen for synthetic lethal and multicopy suppressee mutants to identify two new genes involved in morphogenesis in *Saccharomyces cerevisiae*. Mol Cell Biol *11*, 1295-1305.

Bernstein, K. A., and Baserga, S. J. (2004). The small subunit processome is required for cell cycle progression in G1. Mol Biol Cell *15*, 5038-5046.

Bernstein, K. A., Bleichert, F., Bean, J. M., Cross, F. R., and Baserga, S. J. (2007). Ribosome biogenesis is sensed at the Start cell cycle checkpoint. Mol Biol Cell *18*, 953-964.

Bernstein, K. A., Gallagher, J. E. G., Mitchell, B. M., Granneman, S., and Baserga, S. J. (2004). The small-subunit processome is a ribosome assembly intermediate. Eukaryot Cell *3*, 1619-1626.

Biggins, S., Severin, F. F., Bhalla, N., Sassoon, I., Hyman, A. A., and Murray, A. W. (1999). The conserved protein kinase Ipl1 regulates microtubule binding to kinetochores in budding yeast. Genes Dev *13*, 532-544.

Biggins, S., and Murray, A. W. (2001). The budding yeast protein kinase Ipl1/Aurora allows the absence of tension to activate the spindle checkpoint. Genes Dev *15*, 3118-3129.

Black, S., Andrews, P. D., Sneddon, A. A., and Stark, M. J. R. (1995). A regulated *MET3-GLC7* gene fusion provides evidence of a mitotic role for *Saccharomyces cerevisiae* protein phosphatase 1. Yeast *11*, 747-759.

Bloecher, A., and Tatchell, K. (1999). Defects in *Saccharomyces cerevisiae* protein phosphatase type I activate the spindle/kinetochore checkpoint. Genes Dev *13*, 517–522.

Bloecher, A., and Tatchell, K. (2000). Dynamic localization of protein phosphatase type 1 in the mitotic cell cycle of *Saccharomyces cerevisiae*. J Cell Biol *149*, 125-140.

Bloom, J., and Cross, F. R. (2007). Novel role for Cdc14 sequestration, Cdc14 dephosphorylates factors that promote DNA replication. Mol Cell Biol *27*, 842-853.

Bouck, D. C., and Bloom, K. S. (2005). The kinetochore protein Ndc10p is required for spindle stability and cytokinesis in yeast. Proc Natl Acad Sci USA *102*, 5408-5413.

Burk, D., Dawson, D., and Sterns, T. (2000). Methods in Yeast Genetics (Cold Spring Harbor, NY, Cold Spring Harbor Laboratory Press).

Buvelot, S., Tatsutani, S. Y., Vermaak, D., and Biggins, S. (2003). The budding yeast Ipl1/Aurora kinase regulates mitotic spindle disassembly. J Cell Biol *160*, 329-339.

Cantor, S. B., Bell, D. W., Ganesan, S., Kass, E. M., Drapkin, R., Grossman, S., Wahrer, D. C., Sgroi, D. C., Lane, W. S., Haber, D. A., and Livingston, D. M. (2001). BACH1, a novel helicase-like protein, interacts directly with BRCA1 and contributes to its DNA repair function. Cell *105*,149–160.

Cantor, S., Drapkin, R., Zhang, F., Han, Y., Lin, J., Pamidi, S., and Livingston, D. M. (2004). The BRCA1-associated protein BACH1 is a DNA helicase targeted by clinically relevant inactivating mutations. Proc Natl Acad Sci USA *101*, 2357–2362.

Carazo-Salas, R. E., Gruss, O. J., Mattaj, I. W., and Karsenti, E. (2001). Ran-GTP coordinates regulation of microtubule nucleation and dynamics during mitotic-spindle assembly. Nature Cell Biol *3*, 228–234.

Carazo-Salas, R. E., and Karsenti, E. (2003). Long-range communication between chromatin and microtubules in *Xenopus* egg extracts. Curr Biol 13, 1728–1733.

Carvalho, P., Gupta, M. L. Jr., Hoyt, M. A., and Pellman, D. (2004). Cell cycle control of kinesin-mediated transport of Bik1 (CLIP-170) regulates microtubule stability and dynein activation. Dev Cell *6*, 815–829.

Caudron, M., Bunt, G., Bastiaens, P., and Karsenti, E. (2005). Spatial coordination of spindle assembly by chromosome-mediated signaling gradients. Science *309*, 1373–1376.

Ceulemans, H., and Bollen, M. (2004). Functional diversity of protein phosphatase-1, a cellular economizer and reset button. Physiol Rev *84*, 1-39.

Chan, C. S. M., and Botstein, D. (1993). Isolation and characterization of chromosome-gain and increase-in-ploidy mutants in yeast. Genetics *135*, 677-691.

Chang, J. S., Henry, K., Geli, M. I., and Lemmon, S. K. (2006). Cortical recruitment and nuclear-cytoplasmic shuttling of Scd5p, a protein phosphatase-1-targeting protein involved in actin organization and endocytosis. Mol Biol Cell *17*, 251-262.

Chang, J. S., Henry, K., Wolf, B. L., Geli, M. I., and Lemmon, S. K. (2002). Protein phosphatase-1 binding to Scd5p is important for regulation of actin organization and endocytosis in yeast. J Biol Chem *277*, 48002-48008.

Cheeseman, I. M., Enquist-Newman, M., Muller-Reichert, T., Drubin, D. G., and Barnes, G. (2001). Mitotic spindle integrity and kinetochore function linked by the Duo1p/Dam1p complex. J Cell Biol *152*, 197–212.

Cheeseman, I. M., Anderson, S., Jwa, M., Green, E., Kang, J.-s., Yates III, J. R., Chan, C.

S. M., Drubin, D. G., and Barnes, G. (2002). Phospho-regulation of kinetochore-microtubule attachments by the Aurora kinase Ipl1p. Cell *111*, 163-172.

Cimini, D., Moree, B., Canman, J. C., and Salmon, E. D. (2003). Merotelic kinetochore orientation occurs frequently during early mitosis in mammalian tissue cells and error correction is achieved by two different mechanisms. J. Cell Sci *116*, 4213–4225.

Ciosk, R., M. Shirayama, A. Shevchenko, T. Tanaka, A. Toth, A. Shevchenko, and K. Nasmth. (2000). Cohesin's binding to chromosomes depends on a separate complex consisting of Scc2 and Scc4. Mol Cell *5*, 243–254.

Collins, K. A., Castillo, A. R., Tatsutani, S. Y., and Biggins, S. (2005). *De novo* kinetochore assembly requires the centromeric histone H3 variant. Mol Biol Cell *16*, 5649-5660.

Combs, D. J., Nagel, R. J., Ares Jr., M., and Stevens, S. W. (2006). Prp43p is a DEAH-box spliceosome disassembly factor essential for ribosome biogenesis. Mol Cell Biol *26*, 523-534.

Crotti, L. B., and Basrai, M. A. (2004). Functional roles for evolutionarily conserved Spt4p at centromeres and heterochromatin in *Saccharomyces cerevisiae*. EMBO J *23*,1804–1814.

D'Amours, D., and Amon, A. (2004). At the interface between signaling and executing anaphase - Cdc14 and the FEAR network. Genes Dev *18*, 2581-2595.

D'Amours, D., Stegmeier, F., and Amon, A. (2004). Cdc14 and condensin control the dissolution of cohesin-independent chromosome linkages at repeated DNA. Cell *117*, 455-469.

D'Aquino, K. E., Monje-Casas, F., Paulson, J., Reiser, V., Charles, G. M., Lai, L., Shokat, K., and Amon, A. (2005). The protein kinase Kin4 inhibits exit from mitosis in response to spindle position defects. Mol Cell *19*, 223-234.

Dewar, H., Tanaka, K., Nasmyth, K., and Tanaka, T. U. (2004). Tension between two kinetochores suffices for their bi-orientation on the mitotic spindle. Nature *428*, 93-97.

De Wulf, P., McAinsh, A. D., and Sorger, P. K. (2003). Hierarchical assembly of the budding yeast kinetochore from multiple subcomplexes. Genes Dev *17*, 2902–2921.

Dragon, F., Gallagher, J. E. G., Compagnone-Post, P. A., Mitchell, B. M., Porwancher, K. A., Wehner, K. A., Wormsley, S., Settlage, R. E., Shabanowitz, J., Oshelm, Y.*, et al.* (2002). A large nucleolar U3 ribonucleoprotein required for 18S ribosomal RNA biogenesis. Nature *417*, 967-970.

Du, Y.-C. N., and Stillman, B. (2002). Yph1p, an ORC-interacting protein, potential links between cell proliferation control, DNA replication, and ribosome biogenesis. Cell *109*, 835-848.
Francisco, L., Wang, W., and Chan, C. S. M. (1994). Type-1 protein phosphatase acts in opposition to the Ipl1 protein kinase in regulating yeast chromosome segregation. Mol Cell Biol *14*, 4731-4740.

Futcher, B., and Carbon, J. (1986). Toxic effects of excess cloned centromeres. Mol Cell Biol *6*, 2213-2222.

Gallagher, J. E. G., Dunbar, D. A., Granneman, S., Mitchell, B. M., Osheim, Y., Beyer, A. L., and Baserga, S. J. (2004). RNA polymerase I transcription and pre-rRNA processing are linked by specific SSU processome components. Genes Dev *18*, 2506-2517.

Geymonat, M., Spanos, A., Wells, G. P., Smerdon, S. J., and Sedgwick, S. G. (2004). Clb6/Cdc28 and Cdc14 regulate phosphorylation status and cellular localization of Swi6. Mol Cell Biol *24*, 2277-2285.

Ghaemmaghami, S., Huh, W.-K., Bower, K., Howson, R. W., Belle, A., Dephoure, N., O'Shea, E. K., and Weissman, J. S. (2003). Global analysis of protein expression in yeast. Nature *425*, 737-741.

Gillespie, P. J., Hirano, T. (2004). Scc2 couples replication licensing to sister chromatid cohesion in *Xenopus* egg extracts. Curr Biol *14*, 1598–1603.

Gillett, E. S., Espelin, C. W., and Sorger, P. K. (2004). Spindle checkpoint proteins and chromosome-microtubule attachment in budding yeast. J Cell Biol *164*, 535-546.

Goh, P. Y., and Kilmartin, J. V. (1993). NDC10, a gene involved in chromosome segregation in *Saccharomyces cerevisiae*. J Cell Biol *121*, 503–512.

Gordon, D. M., and Roof, D. M. (1999). The kinesin-related protein Kip1p of *Saccharomyces cerevisiae* is bipolar. J Biol Chem *274*, 28779–28786.

Goshima, G., and Yanagida, M. (2000). Establishing biorientation occurs with precocious separation of the sister kinetochores, but not the arms, in the early spindle of budding yeast. Cell *100*, 619-633.

Goshima, G., and Yanagida, M. (2001). Time course analysis of precocious separation of sister centromeres in budding yeast, continuously separated or frequently reassociated? Genes Cells *6*, 765-773.

Grandi, P., Rybin, V., Baßler, J., Petfalski, E., Strauß, D., Marzioch, M., Schäfer, T., Kuster, B., Tschochner, H., and Tollervey, D*., et al.* (2002). 90S pre-ribosomes include the 35S pre-rRNA, the U3 snoRNP, and 40S subunit processing factors but predominantly lack 60S synthesis factors. Mol Cell *10*, 105-115.

Guacci, V., Hogan, E., and Koshland, D. (1994). Chromosome condensation and sister chromatid pairing in budding yeast. J. Cell Biol *125*, 517–530.

Haber, J. E. (1974). Bisexual mating behavior in a diploid of *Saccharomyces cerevisiae*, evidence for genetically controlled non-random chromosome loss during vegetative growth. Genetics *78*, 843–858.

Hanna, J. S., Kroll, E. S., Lundblad, V., and Spencer, F. A. (2001). *Saccharomyces cerevisiae* CTF18 and CTF4 are required for sister chromatid cohesion. Mol Cell Biol *21*, 3144–3158.

Haering, C. H., Schoffnegger, D., Nishino, T., Helmhart, W., Nasmyth, K., Lowe, J. (2004). Structure and stability of cohesin's Smc1–Kleisin interaction. Mol Cell *15*, 951–964.

Hauf, S., Cole, R. W., LaTerra, S., Zimmer, C., Schnapp, G., Walter, R., Heckel, A., van Meel, J., Rieder, C. L., and Peters, J.-M. (2003). The small molecule Hesperadin reveals a role for Aurora B in correcting kinetochore–microtubule attachment and in maintaining the spindle assembly checkpoint. J Cell Biol *161*, 281–294.

Hayden, J. H., Bowser, S. S., and Rieder, C. L. (1990). Kinetochores capture astral microtubules during chromosome attachment to the mitotic spindle, direct visualization in live newt lung cells. J. Cell Biol *111*, 1039–1045.

Hayashi, T., Fujita, Y., Iwasaki, O., Adachi, Y., Takahashi, K., and Yanagida, M. (2004). Mis16 and Mis18 are required for CENP-A loading and histone deacetylation at centromeres. Cell *118*, 715–729.

He, X., Asthana, S., and Sorger, P. K. (2000). Transient sister chromatid separation and elastic deformation of chromosomes during mitosis in budding yeast. Cell *101*, 763-775.

He, X., Rines, D. R., Espelin, C. W., and Sorger, P. K. (2001). Molecular analysis of kinetochore-microtubule attachment in budding yeast. Cell *106*, 195-206.

Hegemann, J. H., Shero, H., Cottarel, G., Philippsen, P., and Hieter, P. (1988). Mutational analysis of centromere DNA from chromosome VI of *Saccharomyces cerevisiae*. Mol Cell Biol *8*, 2523-2535.

Heiss, N. S., Knight, S. W., Vulliamy, T. J., Klauck, S. M., Wiemann, S., Mason, P. J.,

Poustka, A., and Dokal, I. (1998). X-linked dyskeratosis congenita is caused by mutations in a highly conserved gene with putative nucleolar functions. Nat. Genet *19*, 32-38.

Henry, K. R., D'Hondt, K., Chang, J., Newpher, T., Huang, K., Hudson, R. T., Riezman, H., and Lemmon, S. K. (2002). Scd5p and clathrin function are important for cortical actin organization, endocytosis, and localization of Sla2p in yeast. Mol Biol Cell *13*, 2607-2625.

Higuchi, T., and Uhlmann, F. (2005). Stabilization of microtubule dynamics at anaphase onset promotes chromosome segregation. Nature *433*, 171-176.

Hildebrandt, E. R., and Hoyt, M. A. (2001). Cell cycle-dependent degradation of the *Saccharomyces cerevisiae* spindle motor Cin8p requires APC(Cdh1) and a bipartite destruction sequence. Mol Biol Cell *12*, 3402–3416.

Hisamoto, N., Sugimoto, K., and Matsumoto, K. (1994). The Glc7 type 1 protein phosphatase of *Saccharomyces cerevisiae* is required for cell cycle progression in G_2/M. Mol Cell Biol *14*, 3158-3165.

Hsu, J.-Y., Sun, Z.-W., Li, X., Reuben, M., Tatchell, K., Bishop, D. K., Grushcow, J. M., Brame, C. J., Caldwell, J. A., Hunt, D. F.*, et al.* (2000). Mitotic phosporylation of histone H3 is governed by Ipl1/aurora kinase and Glc7/PP1 phosphatase in budding yeast and nematodes. Cell *102*, 279-291.

Huang, J., Brito, I. L., Villén, J., Gygi, S. P., and Amon, A. (2006). Inhibition of homologous recombination by a cohesin-associated clamp complex recruited to the rDNA recombination enhancer. Genes Dev *20*, 2887-2901.

Indjeian, V. B., Stern, B. M., and Murray, A. W. (2005). The centromeric protein Sgo1 is required to sense lack of tension on mitotic chromosomes. Science *307*, 130–133.

Inoue, H., Nojima, H., and Okayama, H. (1990). High efficiency transformation of *Escherichia coli* with plasmids. Gene *96*, 23-28.

Janke, C., Ortiz, J., Lechner, J., Shevchenko, A., Shevchenko, A., Magiera, M. M., Schramm, C., and Schiebel, E. (2001). The budding yeast proteins Spc24p and Spc25p interacts with Ndc80p and Nuf2p at the kinetochore and are important for kinetochore clustering and checkpoint control. EMBO J *20*, 777–791.

Janke, C., Ortiz, J., Tanaka, T. U., Lechner, J., and Schiebel, E. (2002). Four new subunits of the Dam1–Duo1 complex reveal novel functions in sister kinetochore biorientation. EMBO J. *21*, 181–193.

Jensen, S., Segal, M., Clarke, D. J., and Reed, S. I. (2001). A novel role of the budding

yeast separin Esp1 in anaphase spindle elongation: evidence that proper spindle association of Esp1 is regulated by Pds1, J Cell Biol *152*, 27-40.

Jiang, W., K. Middleton, H.-J. Yoon, C. Fouquet, and J. Carbon. 1993. An essential yeast protein, CBF5p, binds *in vitro* to centromeres and microtubules. Mol. Cell. Biol 13:4884-4893.

Jin, Q. W., Fuchs, J., and Loidl, J. (2000). Centromere clustering is a major determinant of yeast interphase nuclear organization. J Cell Sci *113*, 1903–1912.

Jones, M. H., He, X., Giddings, T. H., and Winey, M. (2001). Yeast Dam1p has a role at the kinetochore in assembly of the mitotic spindle. Proc Natl Acad Sci USA *98*, 13675 13680.

Kang, J.-s., Cheeseman, I. M., Kallstrom, G., Velmurugan, S., Barnes, G., and Chan, C. S.-M. (2001). Functional cooperation of Dam1, Ipl1, and the inner centromere protein (INCENP)-related protein Sli15 during chromosome segregation. J Cell Biol *155*, 763-774.

Kapitein, L. C., Peterman, E. J. G., Kwok, B. H., Kim, J. H., Kapoor, T. M., and Schmidt, C. F. (2005). The bipolar mitotic kinesin Eg5 moves on both microtubules that it crosslinks. Nature *435*,114–118.

Kenna, M. A., and Skibbens, R. V. (2003). Mechanical link between cohesion establishment and DNA replication, Ctf7p/Eco1p, a cohesion establishment factor, associates with three different replication factor C complexes. Mol Cell Biol *23*, 2999–3007.

Killian, A., Le Meur, N., Sesboue, R., Bourguignon, J., Bougeard, G., Gautherot, J., Bastard, C., Frebourg, T., and Flaman, J. M. (2004). Inactivation of the RRB1-Pescadillo pathway involved in ribosome biogenesis induces chromosomal instability. Oncogene *11*, 8597-602.

King, E. M. J., Rachidi, N., Morrice, N., Hardwick, K. G., and Stark, M. J. R. (2007). Ipl1p-dependent phosphorylation of Mad3p is required for the spindle checkpont response to lack of tension aat kinetochores. Genes Dev *21*, 1163-1168.

Kitajima, T. S., Kawashima, S. A., and Watanabe, Y. (2004). The conserved kinetochore protein shugoshin protects centromeric cohesion during meiosis. Nature *427*, 510–517.

Kitajima, T. S., Hauf, S., Ohsugi, M., Yamamoto, T., and Watanabe, Y. (2005). Human Bub1 defines the persistent cohesion site along the mitotic chromosome by affecting shugoshin localization. Curr Biol *15*, 353–359.

Kitajima, T. S., Sakuno, T., Ishiguro, K., Iemura, S., and Natsume, T. *et al* (2006). Shugoshin collaborates with protein phosphatase 2A to protect cohesin. Nature *441*, 46–52.

Kim, J.-H., Kang, J.-S., and Chan, C. S. M. (1999). Sli15 associates with the Ipl1 protein kinase to promote proper chromosome segregation in *Saccharomyces cerevisiae*. J Cell Biol *145*, 1381-1394.

King, E. M. J., Rachidi, N., Morrice, N., Hardwick, K. G., and Stark, M. J. R. (2007). Ipl1p-dependent phosphorylation of Mad3p is required for the spindle checkpont response to lack of tension aat kinetochores. Genes Dev *21*, 1163-1168.

Kosco, K. A., Pearson, C. G., Maddox, P. S., Wang, P. J., Adams, I.R., Salmon, E. D., Bloom, K., and Huffaker, T. C. (2001). Control of microtubule dynamics by Stu2p is essential for spindle orientation and metaphase chromosome alignment in yeast. Mol Biol Cell *12*, 2870–2880.

Krause, S. A., Loupart, M. L., Vass, S., Schoenfelder, S., Harrison, S., and Heck, M. M. (2001). Loss of cell cycle checkpoint control in *Drosophila* Rfc4 mutants. Mol Cell Biol *21*, 5156–516.

Kranz, J. E., and Holm, C. (1990). Cloning by function, an alternative approach for identifying yeast homologs of genes from other organisms. Proc Natl Acad Sci USA *87*, 6629-6633.

Krogan, N. J., Cagney, G., Yu, H., Zhong, G., Guo, X., Ignatchenko, A., Li1, J., Pu, S., Datta, N., Tikuisis, A. P. *et al.* (2006). Global landscape of protein complexes in the yeast *Saccharomyces cerevisiae*. Nature *440*, 637-643.

Lafontaine, D. L. J., Bousquet-Antonelli, C., Henry, Y., Caizergues-Ferrer, M., and Tollervey. D. (1998). The box H + ACA snoRNAs carry Cbf5p, the putative rRNA pseudouridine synthase. Genes Dev *12*, 527-537.

Lampson, M. A., Renduchitala, K., Khodjakov, A., and Kapoor, T. M. (2004). Correcting improper chromosome–spindle attachments during cell division. Nature Cell Biol *6*, 232–237.

Lavoie, B. D., Hogan, E., and Koshland, D. (2004). *In vivo* requirements for rDNA chromosome condensation reveal two cell-cycle-regulated pathways for mitotic chromosome folding. Genes Dev *18*, 76-87.

Lechner, J., and Carbon, J. (1991). A 240 kd multisubunit protein complex, CBF3, is a major component of the budding yeast centromere. Cell *64*, 717–725.

Lengronne, A., Katou, Y., Mori, S., Yokobayashi, S., Kelly, G. P., Itoh, T., Watanabe, Y., Shirahige, K., and Uhlmann, F. (2004). Cohesin relocation from sites of chromosomal loading to places of convergent transcription. Nature *430*, 573–578.

Lengauer, C., Kinzler, K. W., and Vogelstein, B. (1998). Genetic instabilities in human cancers. Nature *396*, 643-649.

Li, R., and Murray, A. W. (1991). Feedback control of mitosis in budding yeast. Cell *66*, 519–531.

Li, Y., Bachant, J., Alcasabas, A. A., Wang, Y., Qin, J., and Elledge, S. J. (2002). The mitotic spindle is required for loading of the DASH complex onto the kinetochore. Genes Dev *16*, 183–917.

Lim, H. H., Goh, P. Y., and Surana, U. (1996). Spindle pole body separation in *Saccharomyces cerevisiae* requires dephosphorylation of the tyrosine 19 residue of Cdc28. Mol. Cell Biol *16*, 6385–6397.

Lin, X., and Momany, M. (2003). The *Aspergillus nidulans swoC1* Mutant Shows Defects in Growth and Development. Genetics *165*, 543-554.

McCarroll, R. M., and Fangman, W. L. (1988). Time of replication of yeast centromeres and telomeres. Cell *54*, 505–513.

Machín, F., Torres-Rosell, J., Jarmuz, A., and Aragón, L. (2005). Spindle-independent condensation-mediated segregation of yeast ribosomal DNA in late anaphase. J Cell Biol *168*, 209-219.

Majka, J., and Burgers, P. M. (2004). The PCNA-RFC families of DNA clamps and clamp loaders. Prog Nucleic Acid Res Mol Biol *78*, 227–260.

Mayer, M. L., Pot, I., Chang, M., Xu, H., Aneliunas, V., Kwok, T., Newitt, R., Aebersold, R., Boone, C., Brown, G. W., and Hieter, P. (2004). Identification of protein complexes required for efficient sister chromatid cohesion. Mol Biol Cell *15*,1736–1745.

McAinsh, A. D., Tytell, J. D., and Sorger, P. K. (2003). Structure, function, and regulation of budding yeast kinetochores. Annu Rev Cell Dev Biol *19*, 519-539.

McGuinness, B, Hirota, T., Kudo, N.R., Peters, J. M., Nasmyth, K. (2005). Shugoshin prevents dissociation of cohesin from centromeres during mitosis in vertebrate cells. PLoS Biol *3*, e86.

Meluh, P. B., and Koshland, D. (1995). Evidence that the MIF2 gene of *Saccharomyces cerevisiae* encodes a centromere protein with homology to the mammalian centromere

protein CENP-C. Mol Biol Cell *6*, 793–807.

Meluh, P. B., and Koshland, D. (1997). Budding yeast centromere composition and assembly as revealed by *in vivo* cross-linking. Genes Dev *11*, 3401–312.

Measday, V., Hailey, D. W., Pot, I., Givan, S. A., Hyland, K. M., Cagney, G., Fields, S., Davis, T. N., and Hieter, P. (2002). Ctf3p, the Mis6 budding yeast homolog, interacts Ctf3p, the Mis6 budding yeast homolog, interacts with Mcm22p and Mcm16p at the yeast outer kinetochore. Genes Dev *16*, 101–113.

Monje-Casas, F., Prabhu, V. R., Lee, B. H., Boselli, M., and Amon, A. (2007). Kineetochore orientation during meiosis is controlled by Aurora B and the monopolin complex. Cell *128*, 477-490.

Muhlrad, D., Hunter, R., and Parker, R. (1992). A rapid method for localized mutagenesis of yeast genes. Yeast *8*, 79-82.

Murnion, M. E., Adams, R. R., Callister, D. M., David Allis, C., Earnshaw, W. C., and Swedlow, J. R. (2001). Chromatin-associated Protein Phosphatase 1 Regulates Aurora-B and Histone H3 Phosphorylation. J Biol Chem *276*, 26656-26665.

Nekrasov, V. S., Smith, M. A., Peak-Chew, S., and Kilmartin, J. V. (2003). Interactions between centromere complexes in *Saccharomyces cerevisiae*. Mol Biol Cell *14*,4931 4946.

Nasmyth, K. (2002). Segregating sister genomes: the molecular biology of chromosome separation. Science *297*, 559-565.

Nelson, K. K., Holmer, M., and Lemmon, S. K. (1996). *SCD5*, a suppressor of clathrin deficiency, encodes a novel protein with a late secretory function in yeast. Mol Biol Cell *7*, 245-260.

Nicklas, R. B. (1997). How cells get the right chromosomes. Science *275*,632–637.

Norden, C., Mendoza, M., Dobbelaere, J., Kotwaliwale, C. V., Biggins, S., and Barral, Y. (2006). The NoCut pathway links completion of cytokinesis to spindle midzone function to prevent chromosome breakage. Cell *125*, 85-98.

Ortiz, J., Stemmann, O., Rank, S., and Lechner, J. (1999). A putative protein complex consisting of Ctf19, Mcm21, and Okp1 represents a missing link in the budding yeast kinetochore. Genes Dev *13*, 1140–1155.

Pearson, C. G., Maddox, P. S., Salmon, E. D., and Bloom, K. (2001). Budding yeast chromosome structure and dynamics during mitosis. J Cell Biol *152*, 1255-1266.

Pearson, C. G., Yeh, E., Gardner, M., Odde, D., Salmon, E. D., and Bloom, K. (2004). Stable kinetochore–microtubule attachment constrains centromere positioning in metaphase. Curr Biol 14, 1962–1967.

Pedelini, L., Marquina, M., Ariño, J., Casamayor, A., Sanz, L., Bollen, M., Sanz, P., and Garcia-Gimeno, M. A. (2007). YPI1 and SDS22 proteins regulate the nuclear localization and function of yeast type 1 phosphatase Glc7. J Biol Chem *282*, 3282-3292.

Peggie, M. W., MacKelvie, S. H., Bloecher, A., Knatko, E. V., Tatchell, K., and Stark, M. J. R. (2002). Essential functions of Sds22p in chromosome stability and nuclear localization of PP1. J Cell Sci *115*, 195-206.

Pereira, G., and Schiebel, E. (2003). Separase regulates INCENP–Aurora B anaphase spindle function through Cdc14. Science *302*, 2120-2124.

Pereira, G., Tanaka, T. U., Nasmyth, K., and Schiebel, E. (2001). Modes of spindle pole body inheritance and segregation of the Bfa1p-Bub2p checkpoint protein complex. EMBO J *20*, 6359-6370.

Pereira, G., Höfken, T., Grindlay, J., Manson, C., and Schiebel, E. (2000). The Bub2p spindle checkpoint links nuclear migration with mitotic exit. Mol Cell *6*,1–10.

Petronczki, M., Chwalla, B., Siomos, M. F., Yokobayashi, S., Helmhart, W., Deutschbauer, A. M., Davis, R. W., Watanabe, Y., and Nasmyth, K. (2004). Sister chromatid cohesion mediated by the alternative RF-CCtf18/Dcc1/Ctf8, the helicase Chl1 and the polymerase-alpha-associated protein Ctf4 is essential for chromatid disjunction during meiosis II. J Cell Sci *117*, 3547–3559.

Pinsky, B. A., Tatsutani, S. Y., Collins, K. A., and Biggins, S. (2003). An Mtw1 complex promotes kinetochore biorientation that is monitored by the Ipl1/Aurora protein kinase. Dev Cell 5, 735–745.

Pinsky, B. A., Kotwaliwale, C. V., Tatsutani, S. Y., Breed, C. A., and Biggins, S. (2006a). Glc7/protein phosphatase 1 regulatory subunits can oppose the Ipl1/Aurora protein kinase by redistributing Glc7. Mol Cell Biol *26*, 2648-2660.

Pinsky, B. A., Kung, C., Shokat, K. M., and Biggins, S. (2006b). The Ipl1-Aurora kinase activates the spindle checkpoint by creating unattached kinetochores. Nat Cell Biol *8*, 78-83.

Pringle, J. R., Preston, R. A., Adams, A., Stearns, T., Drubin, D., Haarer, B. K., and Jones, E. (1989). Fluorescence microscopy methods for yeast. Methods Cell Biol *31*, 357-435.

Queralt, E., Lehane, C., Novak, B., and Uhlmann, F. (2006). Downregulation of $PP2A^{Cdc55}$ phosphatase by separase initiate mitotic exit in budding yeast. Cell *125*, 719-732.

Rabitsch, K. P., Petronczki, M., Javerzat, J.-P., Genier, S., Chwalla, B., Schleiffer, A., Tanaka, T. U., and Nasmyth, K. (2003). Kinetochore recruitment of two nucleolar proteins is required for homolog segregation in meiosis I. Dev Cell *4*, 535-548.

Riedel, C. G., Katis, V. L., Katou, Y., Mori, S., Itoh, T., Helmhart, W., Gálová, M., Petronczki, M., Gregan, J., Cetin, B. *et al*. (2006). Protein phosphatase 2A protects centromeric sister chromatid cohesion during meiosis I. Nature *441*, 53–61.

Rieder, C. L., and Alexander, S. P. (1990). Kinetochores are transported poleward along a single astral microtubule during chromosome attachment to the spindle in newt lung cells. J Cell Biol *110*, 81–95.

Rivera, T., and Losada, A. (2006). Shugoshin and PP2A, shared duties at the centromere. BioEssays *28*, 775-779.

Rose, M. D., Winston, F., and Hieter, P. (1990). Methods in Yeast Genetics (Cold Spring Harbor, NY, Cold Spring Harbor Laboratory Press).

Ruggero, D., and Pandolfi, P. P. (2003). Does the ribosome translate cancer? Nat. Rev. Cancer *3*, 179-192

Sakita-Suto, S., Kanda, A., suzuki, F., Sato, S., Takata, T., and Tatsuka, M. (2007). Aurora-B regulates RNA methyltransferase NSUN2. Mol. Biol. Cell *18*, 1107-1117.

Salic, A., Waters, J. C., and Mitchison, T. J. (2004). Vertebrate shugoshin links sister centromere cohesion and kinetochore microtubule stability in mitosis. Cell *118*,567–578.

Sandall, S., Severin, F., McLeod, I. X., Yates III, J. R., Oegema, K., Hyman, A., and Desai, A. (2006). A Bir1-Sli15 complex connects centromeres to microtubules and is required to sense kinetochore tension. Cell *127*, 1179-1191.

Sassoon, I., Severin, F. F., Andrews, P. D., Taba, M. R., Kaplan, K. B., Ashford, A. J., Stark, M. J., Sorger, P. K., and Hyman, A. A**.** (1999). Regulation of *Saccharomyces cerevisiae* kinetochores by the type 1 phosphatase Glc7p. Genes Dev *13*, 545–555.

Schäfer, T., Straub, D., Petfalski, E., Tollervey, D., and Hurt, E. (2003). The path from nucleolar 90S to cytoplasmic 40S pre-ribosomes. EMBO J *22*, 1370-1380.

Severin, F., Habermann, B. , Huffaker, T., and Hyman, T. (2001). Stu2 promotes mitotic spindle elongation in anaphase. J Cell Biol *153*,435–442.

Sharon, G., and Simchen, G. (1990). Centromeric regions control autonomous segregation tendencies in single-division meiosis of *Saccharomyces cerevisiae*. Genetics *125*, 487-494.

Sharp, J. A., Franco, A. A., Osley, M. A., and Kaufman, P. D. (2002). Chromatin assembly factor I and Hir proteins contribute to building functional kinetochores in *S. cerevisiae*. Genes Dev *16*, 85–100.

Shaw, P., and Doonan, J. (2005). The nucleolus, playing by different rules? Cell Cycle *4*, 102-105.

Shou, W., and Deshaies, R. J. (2002). Multiple *telophase arrest bypassed* (*tab*) mutants alleviate the essential requirement for Cdc15 in exit from mitosis in *S. cerevisiae*. BMC Genet *3*, 4-15.

Shou, W., Seol, J. H., Shevchenko, A., Baskerville, C., Moazed, D., Chen, Z. W. S., Jang, J., Shevchenko, A., Charbonneau, H., and Deshaies, R. J. (1999). Exit from mitosis is triggered by Tem1-dependent release of the protein phosphatase Cdc14 from nucleolar RENT complex. Cell *97*, 233-244.

Skibbens, R. V., Corson, L. B., Koshland, D., and Hieter, P. (1999). Ctf7p is essential for sister chromatid cohesion and links mitotic chromosome structure to the DNA replication machinery. Genes Dev *13*, 307–319.

Simanis, V. (2003). Events at the end of mitosis in the budding and fission yeasts. J Cell Sci *116*, 4263-4275.

Sorger, P. K., Severin, F. F., and Hyman, A. A. (1994). Factors required for the binding of reassembled yeast kinetochores to microtubules *in vitro*. J Cell Biol *127*, 995–1008.

Spencer, F., Gerring, S. L., Connelly, C., and Hieter, P. (1990). Mitotic chromosome transmission fidelity mutants in *Saccharomyces cerevisiae.* Genetics *124***,** 237-249.

Stearns, T., and Botstein, D. (1988). Unlinked noncomplementation: Isolation of new conditional-lethal mutations in each of the tubulin genes of *Saccharomyces cerevisiae*. Genetics *119*, 249-260.

Stegmeier, F., and Amon, A. (2004). Closing mitosis, the functions of the Cdc14 phosphatase and its regulation. Annu Rev Genet *38*, 203-232.

Stoepel, J., Ottey, M. A., Kurischko, C., Hieter, P., and Luca, F. C. (2005). The mitotic exit network Mob1p-Dbf2p kinase complex localizes to the nucleus and regulates passenger protein localization. Mol Biol Cell *16*, 5465-5479.

Straight, A. F., Marshall, W. F., Sedat, J. W., and Murray, A. W. (1997). Mitosis in living budding yeast, anaphase A but no metaphase plate. Science *277*, 574-578.

Straight, A. F., Shou, W., Dowd, G. J., Turck, C. W., Deshaies, R. J., Johnson, A. D., and Moazed, D. (1999). Net1, a Sir2-associated nucleolar protein required for rDNA silencing and nucleolar integrity. Cell *97*, 245-256.

Sugiyama, K., Sugiura, K., Hara, T., Sugimoto, K., Shima, H., Honda, K., Furukawa, K., Yamashita, S., and Urano, T. (2002). Aurora-B associated protein phosphatases as negative regulators of kinase activation. Oncegene *21*, 3103-3111.

Sullivan, M., Higuchi, T., Katis, V. L., and Uhlmann, F. (2004). Cdc14 phosphatase induces rDNA condensation and resolves cohesin-independent cohesion during budding yeast anaphase. Cell *117*, 471-482.

Takahashi, T. S., Yiu, P., Chou, M. F., Gygi, S., and Walter, J. C. (2004). Recruitment of *Xenopus* Scc2 and cohesin to chromatin requires the pre-replication complex. Nature Cell Biol *6*, 991–996.

Tanaka, T., Fuchs, J., Loidl, J., and Nasmyth, K. (2000). Cohesin ensures bipolar attachment of microtubules to sister centromeres and resists their precocious separation. Nat Cell Biol *2*, 492-499.

Tanaka, T. U., Rachidi, N., Janke, C., Pereira, G., Galova, M., Schiebel, E., Stark, M. J. R., and Nasmyth, K. (2002). Evidence that the Ipl1-Sli15 (Aurora kinase-INCENP) complex promotes chromosome-bi-orientation by altering kinetochore-spindle pole connections. Cell *108*, 317-329.

Tanaka, T. U. (2005a). Chromosome bi-orientation on the mitotic spindle. Phil Trans R Soc Lond B *360*, 581–589.

Tanaka, K. et al. (2005b). Molecular mechanisms of kinetochore capture by spindle microtubules. Nature *434*, 987–994.

Tanaka, K., Stark, M. R., Tamaka, K. (2005c). Kinetochore capture and bi-orientation on the mitotic spindle. Nature Rev Mol Cell Biol *6*, 929-942.

Tang, Z., Sun, Y., Harley, E., Zou, H., and Yu, H. (2004). Human Bub1 protect centromeric sister-chromatid cohesion through Shugoshin during mitosis. Proc Natl Acad Sci USA *101*,18012–1817.

Tang, Z., Shu, H., Qi, W., Mahmood, N. A., Mumby, M. C., and Yu, H. (2006). PP2A is required for centromeric localization of Sgo1 and proper chromosome segregation. Dev Cell *10*,575–585.

Tirnauer, J. S., O'Toole, E., Berrueta, L. , Bierer, B. E., and Pellman, D. (1999). Yeast Bim1p promotes the G1-specific dynamics of microtubules. J Cell Biol *145*,993–1007.

Tomonaga, T., Nagao, K., Kawasaki, Y., Furuya, K., Murakami, A., Morishita, J., Yuasa, T., Sutani, T., Kearsey, S. E., and Uhlmann, F., *et al*. (2000). Characterization of fission yeast cohesin, essential anaphase proteolysis of Rad21 phosphorylated in the S phase. Genes Dev *14*, 2757–2770.

Toth, A., Ciosk, R., Uhlmann, F., Galova, M., Schleiffer, A., and Nasmyth, K. (1999). Yeast cohesin complex requires a conserved protein, Eco1p(Ctf7), to establish cohesion between sister chromatids during DNA replication. Genes Dev *13*,320–333.

Tu, J., and Carlson, M. (1994). The GLC7 type 1 protein phosphatase is required for glucose repression in *Saccharomyces cerevisiae*. Mol Cell Biol *14*, 6789-6796.

Tung, H. Y. L., Wang, W., and Chan, C. S. M. (1995). Regulation of chromosome segregation by Glc8p, a structural homolog of mammalian inhibitor 2 that functions as both an activator and an inhibitor of yeast protein phosphatase 1. Mol Cell Biol *15*, 6064-6074.

Uhlmann, F., and Nasmyth, K. (1998). Cohesion between sister chromatids must be established during DNA replication. Curr Biol *8*, 1095–1101.

Vader, G., Medema, R. H., and Lens, S. M. A. (2006). The chromosomal passenger complex, guiding Aurora-B through mitosis. J Cell Biol *173*, 833-837.

Vagnarelli, P., and Earnshaw, W. C. (2004). Chromosomal passengers, the 4-dimensional regulation of mitotic events. Chromosoma *113*, 211-222.

van Breugel, M., Drechsel, D., and Hyman, A. (2003). Stu2p, the budding yeast member of the conserved Dis1/XMAP215 family of microtubule-associated proteins is a plus end binding microtubule destabilizer. J Cell Biol *161*,359–369.

Visintin, R., Craig, K., Hwang, E. S., Prinz, S., Tyers, M., and Amon, A. (1998). The phosphatase Cdc14 triggers mitotic exit by reversal of Cdk-dependent phosphorylation. Mol Cell *2*, 709-718.

Visintin, R., Hwang, E. S., and Amon, A. (1999). Cfi1 prevents premature exit from mitosis by anchoring Cdc14 phosphatase in the nucleus. Nature *398*, 818-823.

Wang, P. J., and Huffaker, T. C. (1997). Stu2p, A microtubule-binding protein that is an essential component of the yeast spindle pole body. J Cell Biol *139*,1271–1280.

Wang, Z., Castano, I. B., De Las Penas, A., Adams, C., and Christman, M. F. (2000.) Pol kappa, a DNA polymerase required for sister chromatid cohesion. Science *289*,774–779.

Warner, J. R. (1999). The economics of ribosome biosynthesis in yeast. Trends Biochem Sci *24*, 437-440.

Warren, C.D., Eckley, D. M., Lee, M. S., Hanna, J. S., Hughes, A., Peyser, B., Jie, C., Irizarry, R., and Spencer, F. (2004). S-phase checkpoint genes safeguard high-fidelity sister chromatid cohesion. Mol Biol Cell *15*,1724–1735.

Weitzer, S., Lehane, C., and Uhlmann, F. (2003). A model for ATP hydrolysis-dependent binding of cohesin to DNA. Curr Biol *13*,1930–1940.

Welch, M. D., Vinh, D. B. N., Okamura, H. H., and Drubin, D. G. (1993). Screens for extragenic mutations that fail to complement *act1* alleles identify genes that are important for actin function in *Saccharomyces cerevisiae*. Genetics *135*, 265-274.

Westermann, S., Cheeseman, I. M., Anderson, S., Yates, III, J. R., Drubin, D. G., and Barnes, G. (2003). Architecture of the budding yeast kinetochore reveals a conserved molecular core. J Cell Biol 163, 215–222.

Westermann, S., Drubin, D. G., and Barnes, G. (2007). Structures and functions of yeast kinetochore complexes. Annu Rev Biochem *76*, 563-591.

Widlund, P. O., Lyssand, J. S., Anderson, S., Niessen, S., Yates III, J. R., and Davis, T. N. (2006). Phosphorylation of the chromosomal passenger protein Bir1 is required for localization of Ndc10 to the spindle during anaphase and full spindle elongation. Mol Biol Cell *17*, 1065-1074.

Wigge, P. A., and Kilmartin, J. V. (2001). The Ndc80p complex from *Saccharomyces cerevisiae* contains conserved centromere components and has a function in chromosome segregation. J Cell Biol *152*, 349–360.

Wilde, A., Lizarraga, S. B., Zhang, L., Wiese, C., Gliksman, N. R., Walczak, C. E., and Zheng, Y. (2001). Ran stimulates spindle assembly by altering microtubule dynamics and the balance of motor activities. Nature Cell Biol *3*, 221–227.

Winey, M., and O'Toole, E. T. (2001). The spindle cycle in budding yeast. Nature Cell Biol *3*,E23–E27.

Wong, L. H., Brettingham-Moore, K. H., Chan, L., Quach, J. M., Anderson, M. A., Northrop, E. L., Hannan, R., Saffery, R., Shaw, M. L., Williams, E., and Choo K. H. A. (2007). Centromere RNA is a key component for the assembly of nucleoproteins at the nucleolus and centromere. Genome Res *17*, 1146-1160.

Woodbury, E. L., and Morgan, D. O. (2007). Cdk and APC activities limit the spindle-stabilizing function of Fin1 to anaphase. Nat Cell Biol *9*, 106-112.

Xu, H., Boone, C., and Klein, H. L. (2004). Mrc1p is required for sister chromatid cohesion to aid in recombination repair of spontaneous damage. Mol Cell Biol *24*,7082–7090.

Yin, H., You, L., Pasqualone, D., Kopski, K. M., and Huffaker, T. C. (2002). Stu1p is physically associated with -tubulin and is required for structural integrity of the mitotic spindle. Mol. Biol. Cell *13*,1881–1892.

Yoder, T. J., Pearson, C. G., Bloom, K., and Davis, T. N. (2003). The *Saccharomyces cerevisiae* spindle pole body is a dynamic structure. Mol Biol Cell *14*, 3494-3505.

Yoon, H.-J., and Carbon, J. (1999). Participation of Bir1p, a member of the inhibitor of apoptosis family, in yeast chromosome segregation events. Proc Natl Acad Sci USA *96*, 13208-13213.

Zebarjadian, Y., King, T., Fournier, M. J., Clarke, L., and Carbon, J. (1999). Point Mutations in Yeast *CBF5* Can Abolish In Vivo Pseudouridylation of rRNA. Mol Cell Biol *19*, 7461-7472.

Zhang, T., Lim, H. H., Cheng, C. S., and Surana, U. (2006). Deficiency of centromere-associated protein Slk19 causes premature nuclear migration and loss of centromeric elasticity. J Cell Sci *116*, 519-531.

Zhang, Y., Yu, Z., Fu, X., and Liang, C. (2002). Noc3p, a bHLH protein, plays an integral role in the initiation of DNA replication in budding yeast. Cell *109*, 849-860.

VITA

Miri Jwa was born in Jeju, Korea on July 23, 1971, the daughter of Moon Cheol Jwa and Oksun Oh. She received her Bachelor of Science degree in Biology from Kyung Hee University, Seoul, Korea in 1995 followed by a Master of Science degree in Biochemistry from Yonsei University, Seoul, Korea in 1999. Thereafter, she worked as a research associate in Kiwon Song's laboratory in Yonsei University until August 2000, when she entered the Cellular and Molecular Biology Program of the University of Texas at Austin.

Permanent address: 7131, Wood hollow DR APT 143, Austin, Tx, 78731